Doctoral Dissertation

Effect of Pre- and Post-compaction Curing Conditions on Properties of Clayey Soils Treated with Paper Sludge ash-based Stabilizers

ペーパースラッジ灰系改質材で改質した粘性土の特性に締固め前後の養生が及ぼす影響

by

NAVILA TABASSUM

ナビラ タバスム

A dissertation submitted to
Graduate School of Urban Innovation
of
Yokohama National University
in partial fulfillment of the requirements for the award of the degree of

Doctor of Philosophy in Engineering

Academic Supervisor

Professor KIMITOSHI HAYANO

Yokohama National University

Yokohama, Japan

August,2023

YOKOHAMA NATIONAL UNIVERSITY

GRADUATE SCHOOL OF URBAN INNOVATION

This dissertation, written by Ms. Navila Tabassum, has been accepted by her supervisor and dissertation committee members. It is submitted to the Graduate School of Urban Innovation – Yokohama National University – Japan in partial fulfillment of the requirements for the award of the degree of Doctor of Philosophy in Engineering.

Committee members:

Prof. Kimitoshi HAYANO, Chair

Faculty of Urban Innovation – Yokohama National University

Prof. Mamoru KIKUMOTO

Faculty of Urban Innovation – Yokohama National University

Prof. Takayuki SUZUKI

Faculty of Urban Innovation – Yokohama National University

Assoc. Prof. Satoshi KOMATSU

Faculty of Urban Innovation – Yokohama National University

Assoc. Prof. Ying CUI

Faculty of Urban Innovation – Yokohama National University

ABSTRACT

Soils generated in construction sites have long been seen as a potential source for recycling in geotechnical engineering. However, their high water content and liquid limit prevent direct reuse without remediation. The absence of waste management innovations and concerns about ecological footprint and costs of construction have hindered their utilization. Usual methods of treatment, like cement solidification and sun drying, also come with cost and environmental issues. To address these problems, studies on eco-friendly substitute resources from different industries have been explored.

Soil stabilization using paper sludge ash-based stabilizers (PSASs) has also been developed. PSASs can be produced by insolubilizing heavy metals in original paper sludge (PS) ash particles, i.e., the wastes generated by the incineration of the PS discharged from paper mills. The surface shape of a PS ash particle has a porous structure with many complex irregularities and voids. The capillary action on these open micropores physically rapidly absorbs the free water in the soil, and the meniscus strongly holds the water within the particles. Owing to this characteristic, PS ash can absorb and retain the excess water in soils. Owing to the reduction in the free water, a PSAS can simultaneously improve the stability of mud and sludge when it is mixed with them. Moreover, scholars have reported that the water absorption and retention performance of PSASs increases with curing. This is because a PSAS is expected to create a hydration reaction when combined with water, although the reaction is not as strong as that of cement.

The conventional flow of the laboratory mixture design for treating construction-generated soil with cement-based stabilizers shows, generally, if no compaction is performed during construction, the specimens are cured after being prepared by mixing the soil with the cement-based stabilizer. Consequently, mechanical tests such as cone index tests or unconfined compression tests are conducted on the specimens. However, if compaction is performed during construction, the pre-compaction curing is conducted on the soil–cement mixture, and subsequently, the mixture is crumbled. Thereafter, the crumbled mixture is immediately compacted followed by post-compaction curing. The compacted specimens are subjected to mechanical tests (such as cone index tests) after the second curing step. Previous studies have reported that the strength characteristics of construction-generated soils treated with cement or lime are strongly affected by the pre-compaction and post-compaction curing conditions. These findings suggest that the strengths of PSAS-treated soils will also be affected by these conditions. However, this problem has not been investigated in detail.

In addition, the “crumbling” in the mixture design flow is considered a disturbance to the treated soils. Such disturbances are known to reduce the strengths of the treated soils Therefore, it has been empirically recommended that the pre-compaction curing of cement- or lime-treated soils should be as short as possible, followed by crumbling and prompt compaction for solidification during post-compaction curing. Meanwhile, PSAS-treated soils do not always solidify; hence, they can be compacted in granular states, such as while sand or gravel. Therefore,

the effects of crumbling on PSAS-treated soils may differ from those on cement- or lime-treated soils. However, this problem has also not been investigated in detail.

At first, this research aimed to investigate the effects of the pre-compaction curing conditions and subsequent crumbling on the physical, compaction, and strength characteristics of PSAS-treated soils, using two types of PSASs with different water absorption and retention performances. For comparison, the same investigation was conducted on soils treated with blast furnace cement type B (BFCB). The experimental results revealed that after crumbling, the PSAS-treated samples produced sand and gravel-like granules, regardless of whether in sealed or air pre-compaction curing conditions. In addition, the lower the water content at crumbling, the smaller the particle size. This was also true for the BFCB-treated samples. Consequently, the compaction test results demonstrated that in one of the two types of PSASs, the dry densities of the PSAS-treated samples with sealed pre-compaction curing were almost the same as those without pre-compaction curing. The same trend was observed for the BFCB-treated samples. However, for the other type of PSAS, the dry densities of the PSAS-treated samples with the sealed pre-compaction curing were lower than those without pre-compaction curing. This could be owing to the difference in the degree of disturbance caused by the crumbling depending on the type of PSAS where initial strength development is different. The rapid formation of hydrates in one type of PSAS may have significantly disturbed the treated samples owing to the crumbling, resulting in a decrease in the dry density. Finally, after secondary curing in a soaked environment, cone index tests were conducted on the PSAS- and BFCB-treated samples. The results indicated that the cone indexes of the PSAS-treated samples with pre-compaction curing were higher or lower than those of the samples without pre-compaction curing depending on the pre-compaction curing environment, the number of curing days, and the initial strength of PSAS. The different trends depending on the conditions were considered to be caused by the combined effects of the “strength reduction owing to crumbling,” and “strength increase owing to water content reduction at compaction.” These mechanisms suggest that for PSAS-treated soils with early strength development, the strength reduction caused by crumbling must be considered. However, for PSAS-treated soils with slow strength development, adjusting the water content of the treated soils through pre-compaction curing before compaction is an effective approach. Moreover, we suggest setting curing conditions in the laboratory mixture design to reflect the field conditions and minimize the discrepancies between the field and laboratory observations for the PSAS treatment.

The second part of the study assesses the durability of clays treated with PSASs in wet-dry or dry-wet environments using various evaluation tests. Initially, particle size distributions (PSDs) were assessed on the treated clays that had undergone various pretreatments. Unconfined compression tests were also performed on treated clays that had undergone dry and wet curing cycles, with the specimens demolded. Finally, cone index tests were carried out on the treated clays that had undergone cycles of dry and wet conditions while the samples were constrained in molds. Based on the test results, the durability assessment of clays treated with PSAS was discussed, considering the specifics of each evaluation test and contrasting the findings with those obtained for clays treated with BFCB. The obtained PSDs contained more fine particles as the time spent washing the samples prior to sieving increased. These findings indicate that the PSAS-treated clays eventually become muddy, even though it is unlikely that the treated clays would be

subjected to washing with water while being stirred after the construction. Unconfined compression test results also demonstrated that after several dry-wet cycles, the strength was reduced for the PSAS-treated specimens. The results indicated that clays treated with PSAS might be less resistant to dry-wet curing cycles than those treated with BFCB. However, the examination of PSAS-treated samples using unconfined compression test specimens is still under debate because the strength development mechanisms for PSAS and BFCB are not similar. To solve this issue, a series of cone index tests were conducted on samples treated with PSASs to examine the change in strength caused by the dry-wet curing process. This observation is different from that inferred from the results of the unconfined compression test. The cone index test results revealed that the samples must be constrained in the assessment tests to assess the durability of PSAS-treated soils subjected to dry-wet curing. In addition, we propose that the idea of maturity would apply to PSAS-treated soils with a range of curing temperatures and curing times as long as the soils are constrained in the assessment tests.

Keywords: construction-generated soil; construction-generated soil treatment; sustainable materials; paper sludge ash (PS); paper sludge ash-based stabilizer (PSAS); laboratory mixture design flow; compaction; pre-compaction curing; sealed curing; air curing; post-compaction curing; crumbling; water absorption and retention; cone index tests; durability; dry-wet environments; Unconfined compression tests; confinement of sample; maturity index

ACKNOWLEDGEMENTS

I want to express my deepest respect and appreciation to Professor Kimitoshi Hayano, my supervisor, for his exceptional guidance, unwavering motivation, significant suggestions, and understanding mentorship throughout the research project. His boundless enthusiasm and attentive support were indispensable in bringing this dissertation to completion.

I extend my heartfelt gratitude to Dr. Hiromoto Yamauchi from DOMI Environmental Solutions, whose profound insights and detailed deliberations during regular sessions and through the articles I published have greatly enlightened me on the ultimate goals of this study.

I am deeply grateful to Professor Mamoru Kikumoto and Associate Professor Cui Ying, my co-supervisors, for sharing their invaluable assistance as well as insightful counsel during this research. Additionally, I extend my thanks to Professor Takayuki Suzuki from the Estuarine and Coastal Laboratory and Associate Professor Satoshi Komatsu from the Concrete Engineering Laboratory for their valuable recommendations, encouraging feedback, and considerate assessment of my dissertation. I am thankful for Dr. Hiroto Higa's enthusiastic backing in laser diffraction during particle size analysis experiments.

I would like to express my heartfelt appreciation to the staff as well as students at the Graduate School of Urban Innovation for their warm and amiable demeanor, helpfulness, considerate encouragement, and positive outlook, all of which greatly enhanced my academic experience and life in Japan. I extend my sincere thanks to Ms. Hiromi Goto for her exceptional support and invaluable contributions to my research.

I am also grateful to the Department of urban innovation for allowing me to work as a research assistant at the Geotechnical engineering laboratory. I am grateful to Mitsubishi Corporation for granting the Mitsubishi Corporation International Scholarship. It provided me with the opportunity to engage in my study more passionately.

I want to use this opportunity to show my sincere appreciation to Dr. Hisashi Taniyama and the other professors from the Master's program in Civil and Environmental Engineering at Saitama University, Japan, for their consistent encouragement and emotional support both before and during the course of my doctoral studies. Without their generous assistance and support, the possibilities of advancing my academic career and enrolling in a doctoral program in Japan are impossible.

In conclusion, I'd want to share my sincere gratitude to everyone in my cherished family for dedicating this research work to them. I owe them a debt of gratitude for their heartfelt encouragement and constant moral support throughout the years I spent studying in Japan. Their unending affection is the primary force that drives me to finish this work.

Yokohama, April 2023

Tabassum Navila

PUBLICATION LIST

Throughout the research process, the following papers, subject to peer review, have been either published or submitted for publication

International Journals:

1. **Tabassum, N**., Taichi, H., Binh, N.,P., Kimitoshi, H., Hiromoto, Y., 2022. Effects of Primary Curing Conditions and Subsequent Crumbling on the Properties of Compacted Soils Treated with Paper Sludge Ash-Based Stabilizers. *Soils and Foundations,2022, 62 (5),* pp 101183, October 2022.
2. **Tabassum, N**., Kimitoshi, H., Hiromoto, Y., Some insights to durability assessment for compacted soils treated with paper sludge ash-based stabilizers. *Soils and Foundations* (under revision after 1st review)

International Conferences :

1. **Tabassum, N.,** Kimitoshi, H., Hiromoto, Y., 2023. Assessment of strength and compaction properties of clays treated with paper sludge-based stabilizers from laboratory mixture tests. *5th International Conference on Geotechnics for Sustainable Infrastructure Development,* December 14-15, 2023 - Hanoi, Vietnam. (submitted).

2. **Tabassum, N**., Kimitoshi, H., Hiromoto, Y., 2023. Some Insight into Effects of Primary Curing Conditions on the Strength Development of Soils Treated with Paper Sludge Ash-based Stabilizer. *2nd International Conference on Construction Resources for Environmentally Sustainable Technologies,* November 20-22, 2023 - Fukuoka, Japan. (accepted)

3. **Tabassum, N**., Kimitoshi, H., Hiromoto, Y., 2023. Effect of dry and wet cycles on the strength development of clay treated with paper sludge ash-based stabilizer. *Proceedings of the 17th Danube European Conference on Geotechnical Engineering,* pp 296-302, June 2023.

4. **Tabassum, N.,** Hayano, K. and Yamauchi, H., Strength Development Mechanism in Different Type of Paper Sludge Ash-Based Stabilizers Treated Soil Due to Two-Stage Curing Method, *The Proceedings of the 24th JSCE International Summer Symposium* , PP 33-34, September 2022.

5. **Tabassum, N.,** Hayano, K. and Yamauchi, H., Effect of curing conditions after compaction on the strength development of soils treated with paper sludge ash-based stabilizer, *The Proceedings of the 75th Canadian Geotechnical Conference* (GeoCalgary,2022). https://geocalgary2022.ca/wp-content/uploads/papers/143.pdf October 2022.

6. **Tabassum, N.,** Hayano, K. and Yamauchi, H., Estimation of Strength Development in Paper Sludge Ash treated soil due to Two-Stage Curing Method, *The Proceedings of the 23rd JSCE International Summer Symposium* , pp 55-56, September 2021

7. **Tabassum, N.,** Hayano, K. and Yamauchi, H., Estimation of Strength Development in Paper Sludge Ash treated soil due to Two-Stage Curing Method and Curing Environment, *The Proceedings of the 56th Annual Meeting of the Japan National Conference on Geotechnical Engineering.,* pp 12-1-3-05, July 2021.

Table of contents

List of Figures

List of Tables

CHAPTER 1

RESEARCH FRAMEWORK

1.1 GENERAL

The Sustainable Development Goals (SDGs) were established during the United Nations Summit in September 2015, highlighting the importance of sustainable development across environmental, social, and economic domains. This global initiative prompted the construction industry to incorporate SDGs and strive for a sustainable future. Consequently, the construction sector began recognizing the environmental consequences associated with specific waste types. In response, the construction industry has implemented technical measures to address waste management in line with SDG objectives. Construction-related waste, including concrete, timber, metals, plastics, and soils, has emerged as a focal area for improvement due to its significant environmental impact. Construction companies are also actively promoting the recycling and reuse of construction waste materials. Advanced sorting and separation technologies are utilized on construction sites and recycling facilities to effectively segregate different waste types, enabling the recovery of valuable resources for reintroduction into construction processes. This reduces the dependency on virgin materials and minimizes the environmental impact associated with extraction and production. By aligning with the SDGs and implementing these technical measures, the construction industry is making significant progress toward achieving sustainability. The adoption of waste management practices that prioritize waste reduction, recycling, and circularity not only mitigates environmental impacts but also contributes to the social and economic goals outlined in the SDGs. (Amrutha and Geetha, 2020; Lu and Yuan, 2011; Lu and Tam, 2013).

Construction and demolition waste management have gained significant traction as a prominent subject of scholarly discourse within the academic community (Yuan and Shen, 2011). Extensive research has been conducted by numerous experts, both in Japan (Yamamura, 1983; Gotoh, 1987) and internationally (Lu and Yuan, 2011; Yuan and Shen, 2011; Gao, 2008; Aslam et al., 2020; Blengini et al., 2010; Yuan et al., 2012; Coelho et al., 2012; MLIT,2014) to investigate and advance the understanding of construction waste management practices.

The construction industry has witnessed a significant surge in the adoption of recycling practices for construction resources, including materials such as asphalt and concrete lumps generated during construction activities. This trend is driven by the recognition of the "Responsibility to create" and "Responsibility to use" elements outlined in Sustainable Development Goal 11 (SDG 11). Based on the survey findings reported in MLIT,2014, which specifically focused on construction by-products, it was observed that all by-products, with the exception of construction-generated soil, have successfully met the predefined target values as indicated in Table 1.1. The inherent characteristics of construction-generated soil pose significant challenges to its widespread reuse, both within Japan and on a global scale. These challenges stem from various technical factors that hinder its effective utilization in construction practices. However, construction-generated soils often have negative characteristics for use as geomaterials in construction projects, such as (1) high fine particle contents, (2) high water contents, and (3) difficulty in compaction. Ongoing deliberations and discourse regarding the optimal utilization of construction-generated

soil are currently underway within the academic and industry domains, demonstrating active engagement and interest in addressing this topic at a technical level.

Table 1.1 FY 2018 Survey Results on Construction By-Products by the Ministry of Land, Infrastructure, Transport and Tourism

Waste Generated from construction	**Data Recorded (%)**		**Change (%) from 2012 to 2018**	**2018 Target Value as per Construction Recycling Promotion Plan 2014**	**Target Value Compliance Status**
	2012	**2018**			
Recycling rate of asphalt and concrete lumps	99.50	99.50	0.00	Above 99	Achieved
Recycling rate of concrete mass	99.30	99.30	0.00	Above 99	Achieved
Percentage of construction generated wood recycled/reduced	94.40	96.20	1.80	Above 95	Achieved
Construction sludge recycling rate/reduction rate	85.00	94.60	9.60	Above 90	Achieved
Recycling and reduction rate of mixed construction waste	58.20	63.20	5.00	Above 60	Achieved
Percentage of mixed construction waste generated	3.90	3.10	−0.80	Under 3.5	Achieved
Construction waste recycling rate/reduction rate	96.00	97.20	1.20	Above 96	Achieved
Effective utilization rate of construction soil	77.80	79.80	2.00	Above 80	Not achieved

1.2 BACKGROUND CONTEXT

1.2.1 Application Potential of Construction-Generated Soil

On-site treatment of construction generated soil is usually conducted. Figure 1.1 shows the typical process for treating construction generated soil.

Initially, the soil undergoes a thorough examination to identify any foreign substances mixed with it, which would classify it as construction waste sludge. In Japan, this soil is regulated as industrial waste. Subsequently, stabilization processes are implemented, involving the incorporation of binders or stabilizers into the soil to enhance its stability. Throughout the on-site treatment process, rigorous monitoring and testing of treated soil samples are conducted to ensure treatment efficacy and adherence to regulatory standards. Numerous factors influence soil strength, necessitating careful monitoring and testing, including compaction, moisture content, temperature, and the dry-wet effect. These factors will be further elaborated in Chapter 2. The suitability of the treated soil

for reuse on-site or in nearby areas is assessed. If the treated soil meets the necessary criteria, it can be reused for activities such as backfilling, landscaping, or erosion control. Figure 1.2 shows an example of recycling construction-generated soil on site. In cases where reuse is not feasible, the treated soil may be transported to an appropriate off-site facility for disposal or used as cover material in nearby landfills.

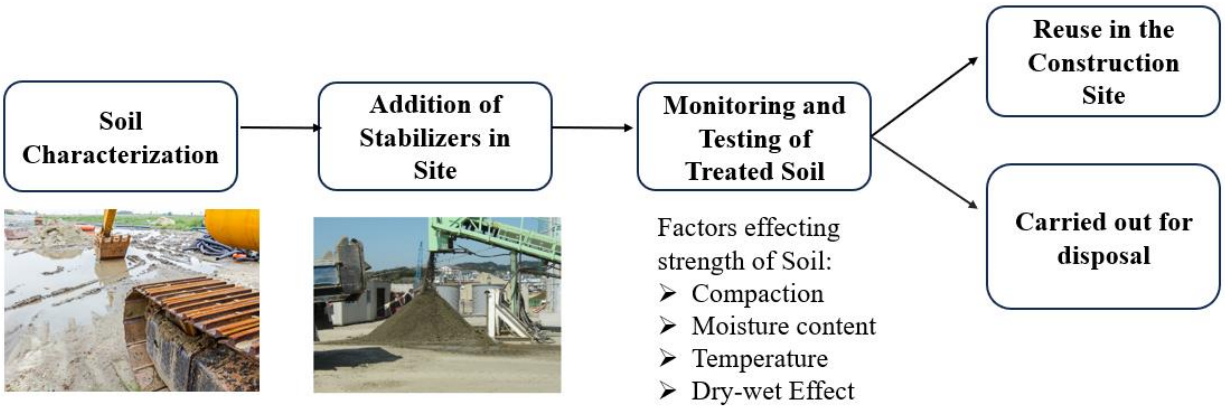

Figure 1.1 Typical process for treating construction-generated soil

Figure 1.2 Example of recycling construction-generated soil on site

On a global scale, an enormous volume of construction-generated soil, amounting to hundreds of millions of cubic meters annually, is disposed of. The predominant method of disposal involves storing these soils in landfills. The costs associated with this disposal practice are substantial. Furthermore, both landfilling and dumping of construction-generated soils give rise to a multitude of environmental challenges, such as the deterioration of groundwater quality, the degradation of surrounding habitats, and the disruption of ecosystems, among other adverse impacts. The escalating implementation of stringent environmental regulations has exacerbated the social, economic, and environmental issues stemming from the large quantities of construction-generated

soils in various nations. In contrast, construction activities in coastal areas often require significant volumes of high-quality soil for purposes such as reclamation, backfilling, and foundation bases. However, the extensive excavation of soils from mountainous regions presents several unfavourable environmental consequences and becomes impractical when the excavation site is located far away from the construction site, resulting in a significant increase in construction expenses. As per the data presented by MLIT in 2014 (Fig 1.3), there is a notable disparity between the total amount of soil transported off-site for disposal and the quantity of soil reused on-site. This emphasizes the significance of on-site treatment; however, it also highlights a substantial volume of soil being sent for disposal instead of being reused. This situation calls for an enhanced focus on maximizing the reuse potential of soil to minimize waste generation. Taking advantage of on-site treatment and implementing effective soil management strategies can significantly contribute to reducing the amount of soil requiring off-site disposal, leading to improved resource utilization and reduced environmental impacts.

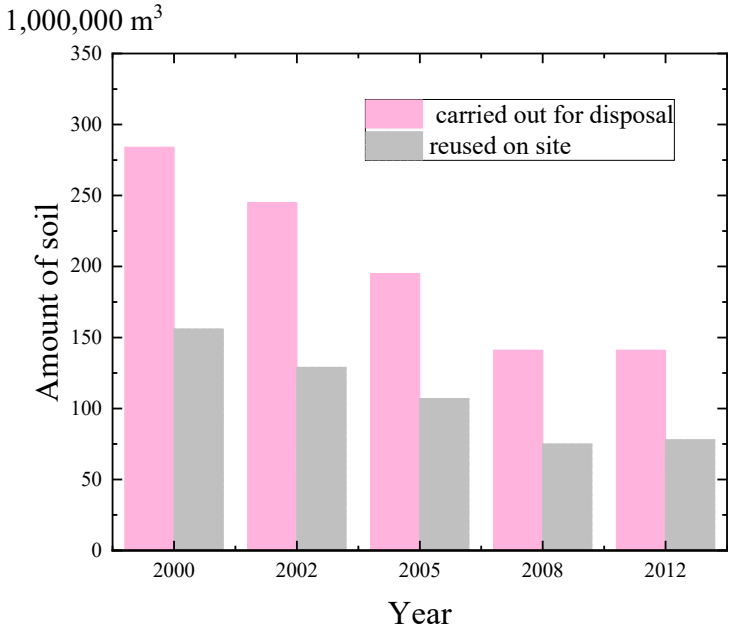

Figure 1.3 Construction-generated soils management in Japan (MLIT, 2014).

1.2.2 Example of On-site Treatment of Construction-Generated Soil

On-site treatment of construction-generated soil is a widely adopted practice. Figure 1.4 illustrates an exemplification of on-site treatment, showcasing the utilization of a cement-based stabilizer, which is the most commonly employed stabilizer. The objective is to utilize muddy construction-generated soil as the widening material for an embankment. To achieve this, the mud content within the construction-generated soil undergoes a transformation into treated soil through a systematic treatment process. The treatment commences by incorporating a stabilizer into the muddy soil, ensuring proper mixing to achieve homogeneity. The stabilizer, often cement-based, imparts crucial engineering properties to the soil, such as increased strength, improved load-bearing capacity, and enhanced durability. Following the addition of the stabilizer, pre-compaction curing is implemented, allowing for the development of early-stage strength and stabilization

within the treated soil. Subsequently, the treated soil undergoes a meticulous process known as crumbling, which involves breaking down the compacted soil into smaller pieces. This

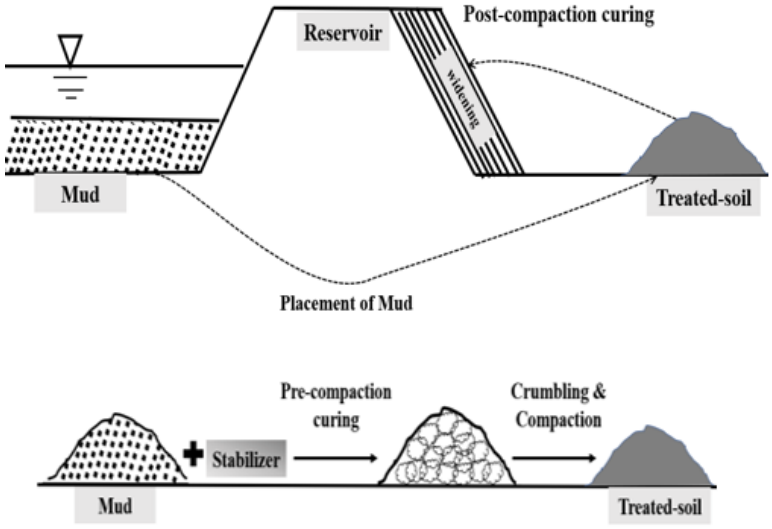

Figure 1.4 Example of construction-generated soil treatment on-site using cement-based stabilizer

crumbling step aids in improving the workability of the treated soil and facilitating subsequent compaction. The final stage entails compacting the treated soil, thereby achieving the desired density and strength required for its application as the widening material for the embankment. The compacted treated soil exhibits enhanced stability, reducing the risk of settlement or deformation over time. Considering the embankment's susceptibility to changes in the water table, the durability of the structure becomes a paramount concern. In this context, the effects of both pre-and post-compaction curing become crucial for the successful utilization of cement-treated construction-generated soil.

Through a comprehensive examination of pre- and post-compaction curing methods, coupled with an in-depth analysis of the impact of crumbling, many research endeavors have been conducted to contribute a deeper understanding of the behavior and characteristics of cement-treated construction-generated soil. Ultimately, the findings have informed practitioners and engineers regarding the most effective strategies for the successful application of cement-treated soil as a widening material for embankments, considering the vital role played by pre- and post-compaction curing in conjunction with the crumbling process.

1.2.3 Conventional Flow of Laboratory Mixture Design

Based on the situation explained in the previous section, a conventional flow of laboratory mixture design was proposed. According to the findings published by the Public Works Research Institute in 2013, Fig 1.5 illustrates the conventional flow of the laboratory mixture design process used to treat construction-generated soil with cement-based stabilizers. The procedure involves preparing specimens by mixing the soil with the cement-based stabilizer, followed by curing, regardless of

whether compaction is performed during the construction process. Subsequently, mechanical tests, such as cone index tests or unconfined compression tests, are conducted on these specimens. Alternatively, if the soil and cement mixture undergo compaction during the construction phase, a pre-compaction curing process is carried out on the combination. However, this pre-compaction curing often causes the mixture to crumble. In order to address this, the crumbled mixture is subjected to quick compaction, followed by post-compaction curing. Once the second curing step is completed, the compacted specimens are subjected to various mechanical tests, such as cone index tests.

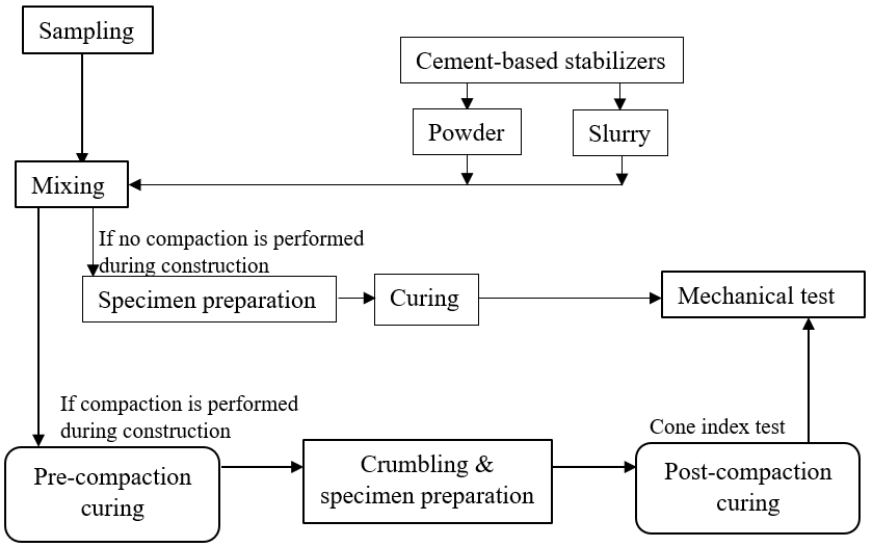

Figure 1.5. The conventional flow of laboratory mixture design for treating construction-generated soil with cement-based stabilizers (revised from Public Works Research Institute, 2013)

Previous research has indicated that both the pre-compaction and post-compaction curing conditions significantly influence the strength properties of construction-generated soils treated with cement or lime (Miyashita et al., 2019). Moreover, the "crumbling" phenomenon observed in Fig 1.5 is considered as disturbance to the treated soils. It is well-established that such disturbances weaken the treated soils (Tani et al., 2006; Huang et al., 2011; Makino et al., 2015; Cikmit et al., 2021; Sato and Hatakeyama, 2021). Considering these factors, empirical research suggests that the pre-compaction curing period for soils treated with cement or lime should be as short as possible. This is followed by intentional crumbling and rapid compaction to achieve solidification during the subsequent post-compaction curing period. This approach aims to mitigate the weakening effects caused by disturbances and enhance the overall strength properties of the treated soils.

1.3 RESEARCH RATIONAL

1.3.1 Problems Associated with Cement-Based Stabilizers

In light of our previous discussion, it is evident that construction-generated soils often exhibit a water content exceeding their liquid limit. Consequently, conventional methodologies employed for the treatment and recycling of these soils primarily encompass cement solidification or water

content reduction via sun-drying or the utilization of water-absorbing materials. Although cement employment stands as the prevailing and uncomplicated approach, it is not bereft of certain technical drawbacks concerning cost and environmental ramifications.

Cement, as a treatment agent, entails considerable financial implications due to its relatively high cost. The procurement, transportation, and application of cement in large-scale soil treatment projects impose significant expenses, thereby rendering cement solidification economically unviable or presenting budgetary constraints. Cement production entails notable environmental consequences. The manufacturing process involves substantial carbon dioxide (CO_2) emissions, contributing to the amplification of greenhouse gas levels and exacerbation of climate change. Furthermore, cement production necessitates the extraction of raw materials such as limestone, leading to habitat degradation and biodiversity loss. The transportation of cement further contributes to carbon emissions, further exacerbating the environmental footprint associated with its use. Moreover, the sun-drying method does not contribute to environmental issues, but it does slow construction progress. From this perspective, methods for utilizing water-absorbing materials instead of cement have been developed.

1.3.2 Paper Sludge Ash as an Alternative to Cement

Artificial water absorption materials are typically expensive, whereas natural absorption materials or waste products frequently can not fulfill the specified amount as well as characteristics. Therefore, numerous researches have been conducted regarding eco-friendly alternative approaches for reusing construction-generated soils such as the use of fly ash, biomass ash, and bio sludge. However, the majority of alternative treatment methods have not been extensively implemented due to a lack of production capacity and associated technical issues. Many researchers have studied the effective use of ash from paper sludge incineration for treating construction-generated soil because of its

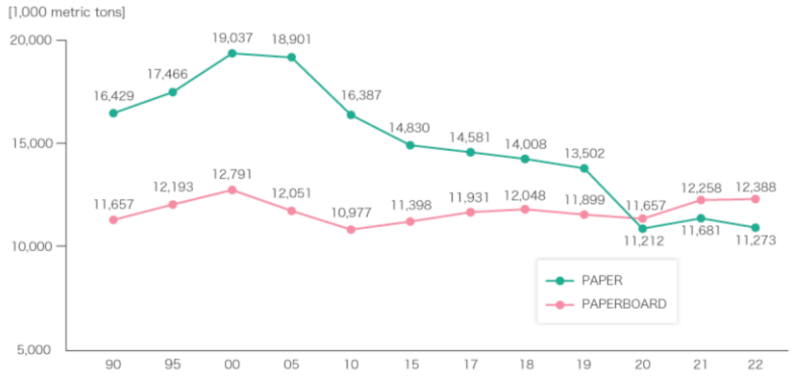

Figure 1.6 Manufacturing of paper and paperboard (Japan Paper Association homepage)

water absorption capacity which is different from cement . Moreover, paper sludge ash doesnot solidify as rapidly as cement when mixed in construction generated soil.In this study, we employ paper sludge ash as a prominent water absorbing material, given the significant annual production of paper waste in Japan (Fig 1.6) and the challenges associated with achieving complete recycling of paper produced every year.

Paper sludge ash (PS ash), a residue resulting from the pyrolysis of paper sludge, a byproduct of paper manufacturers, represents a sustainable and viable material option. Given the consistent production levels in the paper industry over the years, the potential utilization of PS ash is significant. Historically, PS ash has mostly been either disposed of in landfills or utilized as a constituent in concrete (Amit and Islam, 2016; Mochizuki, 2019). The porous surface structure of PS ash particles, characterized by numerous irregularities and voids, enables it to absorb and retain excess water in soft soil. As a result, the demand for PS ash has been on the rise for stabilizing mud in construction projects such as dredging in harbors, lakes, and rivers or excavating underground chambers and underground pits (Kawasaki and Ishimito, 1992; Mochizuki et al., 2003).

In order to utilize PS ash in construction engineering on a large scale, it must comply with environmental standards. Therefore, a PS ash-based stabilizer (PSAS) has been developed to immobilize the heavy metals present in the original PS ash. This process exclusively targets the removal of heavy metals, leaving the properties of PSAS, such as its chemical compositions and water absorption capacity, unchanged when compared to the original PS ash. Previous researches suggest for waste-derived materials that care must be taken to avoid leaching of heavy metals and other substances (Leelarungroj et al., 2018, Dontriros, 2020). In consideration of this point, PSASs are safe to use.

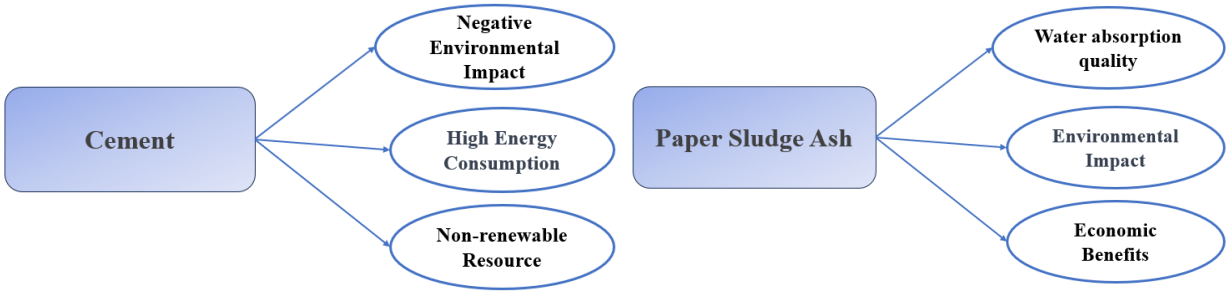

Figure 1.7 Paper sludge ash as an alternative material for cement

1.4 PURPOSE OF RESEARCH

1.4.1 Research-gap in Existing Research

The previous section provided insights into the traditional laboratory mixture design process employed for treating construction-generated soil using cement-based stabilizers. However, the use of cement presents environmental and economic challenges. In light of these concerns, there has been growing interest in exploring alternative water-absorbing materials as substitutes for cement in soil stabilization. One such material that has garnered attention is PS ash, which exhibits promising properties as a stabilizer. By delving deeper into the technical aspects and elaborating on the environmental and economic issues associated with cement usage, researchers have directed their focus towards investigating the efficacy of PS ash within soil stabilization applications.

The process of stabilizing soil with stabilizers derived from paper sludge ash, known as PSASs, has been established. PSASs can be formed by insolubilizing heavy metals in the initial paper sludge (PS) ash particles, which are the wastes generated by the burning of the PS discharged from paper mills. This process is known as paper sludge ash solidification. A PS ash particle has the appearance of a porous structure on its surface, with many different kinds of complicated imperfections and spaces. The free water in the soil is physically and rapidly absorbed by the capillary action on these open micropores, and the meniscus keeps the water within the particles with a great deal of strength (Mochizuki et al., 2003). Because of this property, PS ash has the ability to absorb and keep the excess water that is found in soils. When combined with mud and sludge, a PSAS can simultaneously improve the stability of mud by the reduction in the amount of free water it contains. In addition, researchers have observed that curing increases the water absorption and retention performance of PSASs (Phan et al., 2021). This is due to the fact that a PSAS is anticipated to generate a hydration response when coupled with water, even though the reaction will not be as powerful as cement's hydration reaction. In light of this characteristic, Watanabe et al., 2021 conducted laboratory experiments using potential irrigation earth dam materials to demonstrate that the quantity of PSAS required to achieve a specified compaction degree could be reduced by curing the PSAS-treated soil prior to compaction. This was accomplished through the use of potential irrigation earth dam materials.

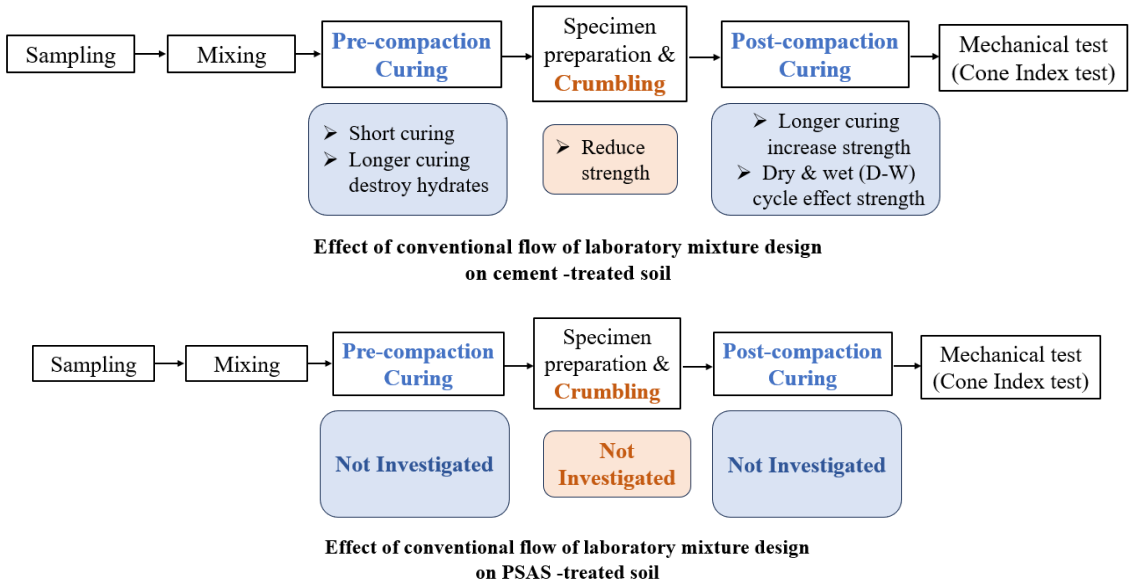

Figure 1.8 Research gap in the existing literature

The conventional flow of the laboratory mixture design is established for treating construction-generated soil with cement-based stabilizers. Previous research clearly indicates that pre-compaction curing conditions are expected to affect soil that has been treated with PSAS, according to a prediction. Moreover, crumbling after pre-compaction curing should have an impact on PSAS-treated soil. In addition, the curing process that occurs after compaction also affects the strength development mechanism for PSAS-treated soil. For instance, when PSAS-treated soil is used to construct irrigation earth dams (Watanabe et al., 2021), the soil may be subjected to dry and wet cycles, which may result in a change in the strength of PSAS-treated soils. These cycles

may also affect the stability of the soil. However, the effect of pre-compaction and post-compaction curing on soil that has been treated with PSAS is not characterized at present.

1.4.2 Objective of Research

The objective of this research is to establish a comprehensive and technically rigorous laboratory mixture design flow for treating construction-generated soil using PSAS-based stabilizers, which offer sustainable alternatives to traditional cement-based stabilizers. Given the distinct water absorption mechanisms exhibited by PSAS-based stabilizers compared to cement, there is a need to develop a specialized design approach that accounts for their unique properties and performance characteristics. This research aims to address this gap in knowledge and provide practical guidelines for optimizing the mixture design process when utilizing PSAS-based stabilizers for construction-generated soil treatment (Fig 1.9). Based on that the objective of this research is given below :

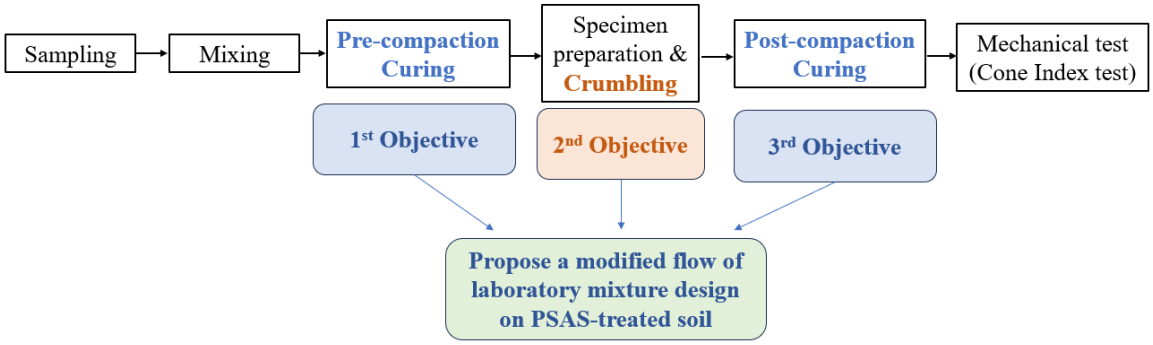

Figure 1.9 Objective of this research

- Firstly, in this work, the impacts of the pre-compaction curing conditions on the physical, compaction, and strength characteristics of PSAS-treated clays were explored using two different types of PSASs: PSAS-N and PSAS-R, that performed differently in terms of their water absorption and retention performances. In order to provide a comparison, the experiment was also carried out on soils that had been treated with blast furnace cement type B. (BFCB).
- Secondly, the effect of crumbling between pre-compaction and post-compaction curing conditions on laboratory mixture design flow for PSAS-treated clays was investigated in detail in this research using two different types of PSAS: PSAS-N and PSAS-R. This research was carried out to determine how PSAS-treated soil behaves when subjected to crumbling between pre-compaction and post-compaction curing conditions. The results were compared with those of clays that had previously been treated with blast furnace cement type B, just as they were with the first objective (BFCB).
- Thirdly, an investigation of the influence of post-compaction curing in the laboratory mixture design flow was carried out in order to gain a better understanding of the durability of PSAS-treated clays. Using a variety of various evaluation methods, the purpose of this study was to evaluate the durability of PSAS-treated clays that were placed in environments that alternated between wet and dry conditions. There will be discussions on the durability

evaluation of clays that have been treated with two different types of PSAS: PSAS-N and PSAS-R. These evaluations will take into consideration the characteristics of each evaluation test, and the results of these tests will be compared to the findings of BFCB-treated clays. Based on the test results a new method for testing the durability of PSAS-treated soil in the laboratory was proposed.

- Finally, Based on the effects of pre-compaction curing, crumbling & post-compaction curing on two types of PSAS-treated clay, a new laboratory mixture design flow is proposed for PSAS-treated construction-generated soil.

1.5 RESEARCH FLOW

Initially, an extensive literature review was undertaken to identify the research gap pertaining to the treatment of construction-generated soil using PSAS-based stabilizers with unique water absorption mechanisms distinct from conventional stabilizers such as cement. Subsequently, the selection of appropriate materials relied on their specific physical and chemical properties to facilitate the research investigation. Two types of clay were chosen, along with two distinct PSASs: PSAS-N and PSAS-R. To facilitate result comparison, identical tests were conducted using Blast furnace cement type B (BFCB), serving as a benchmark. A series of cone index tests were then carried out using the two types of PSASs and BFCB, employing different pre-compaction curing environments and curing durations to ascertain the impact of pre-compaction curing on PSAS-treated soil. The assessments also aimed to discern crumbling effects.

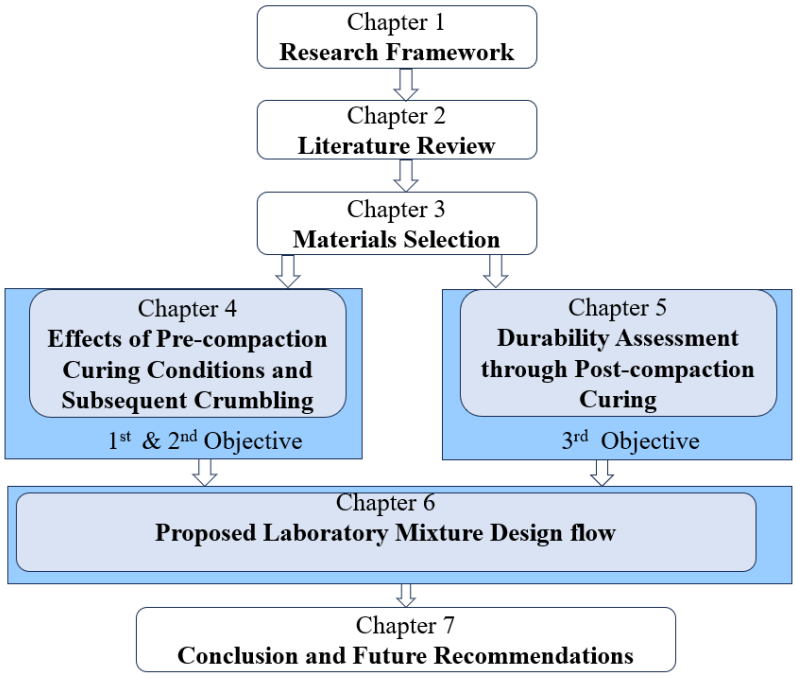

Figure 1.10 Methodological Framework Employed for the Execution of the Research Study

Moreover, the durability of the PSAS-treated soil was evaluated through unconfined compression tests, subjecting the samples to repeated dry and wet (D-W) cycles. Due to the failure of unconfined

compression test samples, a novel method was recommended to assess the durability of PSAS-treated soil. Accordingly, a range of experiments was conducted, considering various drying temperatures and periods. By considering the effects of pre-compaction curing, crumbling, and post-compaction factors on PSAS-treated soil, a new laboratory mixture design flow was proposed for the treatment of construction-generated soil using PSAS-based stabilizers. Figure 1.10 shows the methodological framework employed for the execution of this research study.

1.6 DISSERTATION STRUCTURE

The dissertation comprises 8 chapters in its arrangement.

Chapter 2 details construction-generated soil treatment procedures using cement and sustainable materials. Beginning with construction-generated soil compositions, the chapter explains its features. The chapter next discusses the compositions and drawbacks of typical stabilizers for treating these soils. This gives paper sludge ash soil stabilization research background. The benefits and qualities of paper sludge ash as a soil stabilizer are explored, along with past research. Additionally, past research related to sustainable materials is also explained in this chapter.

Chapter 3 introduces the objectives of the present research. The purpose of the research was to investigate the effects of pre-and post-compaction curing on the properties of laboratory-compacted specimens and to determine the optimal curing conditions for achieving the desired properties. By addressing this research gap, the study aimed to contribute to a better understanding of the factors that affect the behavior of laboratory-compacted specimens, and to provide practical guidance for the use of these materials in engineering applications.

Chapter 4 seeks to address the research gap by clarifying the effects of pre-compaction curing conditions and the ensuing effects of crumbling on PSAS-treated soil. The chapter provides a detailed description of the laboratory mixture design experiments conducted in the study and discusses the effects of different pre-compaction curing conditions on soil strength and the formation of hydrates. The chapter also examines the effects of crumbling on PSAS-treated soil and provides insights into the optimal conditions for stabilizing construction-generated soil with PSASs.

Chapter 5 presents an experimental study that investigates the effect of post-compaction curing on the durability of PSAS-treated soil. A new method for evaluating the durability of PSAS-treated soil is introduced, which takes into account the soil's response to wetting and drying cycles. The chapter also discusses the potential implications of the findings for the use of PSAS-treated soil in practical applications.

Chapter 6 suggests a modified laboratory mixture design flow for treating construction-generated soil with PSAS-based stabilizers based on pre-compaction curing effects, subsequent crumbling and post-compaction curing effects obtained from Chapter 4 and Chapter 5.

Chapter 7 In the final chapter, an overview of the research findings and outcomes is provided. Conclusions are drawn, and both constraints and suggestions for future investigations are presented.

References

Amit, S.K.S., Islam, M.R., 2016. Application of Paper Sludge Ash in Construction Industry-a review, in: Proceedings of the 3rd International Conference on Civil Engineering for Sustainable Development (ICCESD 2016). pp. 737–746.

Amrutha, V.N. and Geetha, S.N., 2020. A systematic review on green human resource management: Implications for social sustainability. Journal of Cleaner production, 247, p.119131.

Aslam, M.S., Huang, B. and Cui, L., 2020. Review of construction and demolition waste management in China and USA. Journal of Environmental Management, 264, p.110445.

Blengini, G.A. and Garbarino, E., 2010. Resources and waste management in Turin (Italy): the role of recycled aggregates in the sustainable supply mix. Journal of Cleaner Production, 18(10-11), pp.1021-1030.

Cikmit, A.A., Tsuchida, T., Takeyama, K., Hashimoto, R., Noguchi, T. and Kaya, K., 2021. Effects of primary curing and subsequent disturbances on strength development of steel slag-treated marine clay. Soils and Foundations, 61(5), pp.1287-1301.

Coelho, A. and De Brito, J., 2012. Influence of construction and demolition waste management on the environmental impact of buildings. Waste Management, 32(3), pp.532-541.

Dontriros, S., Likitlersuang, S., Janjaroen, D., 2020. Mechanisms of chloride and sulfate removal from municipal-solid-waste-incineration fly ash (MSWI FA): Effect of acid-base solutions. Waste Management, 101, pp. 44-53.

Gao, M.Z.A., 2008. Construction & demolition waste management: From Japan to Hong Kong. Griffin's view on international and comparative law, pp. 1-29.

Gotoh, S., 1987. Waste management and recycling trends in Japan. Resources and conservation, 14, pp.15-28.

Huang, Y., Zhu, W., Qian, X., Zhang, N. and Zhou, X., 2011. Change of mechanical behavior between solidified and remolded solidified dredged materials. Engineering Geology, 119(3-4), pp.112-119.

Japan Paper Association Homepage, https://www.jpa.gr.jp/en/industry/data02/

Kawasaki, K. and Ishimito, K., 1992. Technology of treatment and utilization of surplus soils in construction work-Improvement technology for sludge produced in shield tunneling work: PMF super additive for sludge produced using industrial waste effectively. Mon. J. Sewerage, 15, pp.81-84.

Leelarungroj, K., Likitlersuang, S., Chompoorat, T., Janjaroen, D., 2018. Leaching mechanisms of heavy metals from fly ash stabilised soils. Waste Management & Research, 36(7), pp. 616-623.

Lu, W. and Yuan, H., 2011. A framework for understanding waste management studies in construction. Waste management, 31(6), pp.1252-1260.

Lu, W. and Tam, V.W., 2013. Construction waste management policies and their effectiveness in Hong Kong: A longitudinal review. Renewable and sustainable energy reviews, 23, pp.214-223.

Mochizuki, Y., Yoshino, H., Saito, E., Ogata, T., 2003. Effects of soil improvement due to mixing with paper sludge ash, in: Proceeding of China-Japan Geotechnical Symposium.

Makino, M., Takeyama, T. and Kitazume, M., 2015. The influence of soil disturbance on material properties and micro-structure of cement-treated soil. Lowland Technology International, 17(3), pp.139-146.

Ministry of Land, Infrastructure, Transport and Tourism (MLIT), 2018. Results of the FY 2018 Survey on Actual Conditions of Construction By-Products, 1st ed.; Public Works Planning and Coordination Division, General Policy Bureau: Tokyo, pp. 1–5.

Miyashita, Y., Sanjeewani, D., Kuwano, R., 2019. Effect of curing conditions on long term mechanical property of improved surplus soils. E3S Web of Conferences. E3S Web conference 92. 92.

Mochizuki, Y., 2019. Evaluation of water absorption performance of various PS ashes produced with different incineration methods and its applicability for mud improvement. Journal of Japan Society of Civil Engineers, Ser. C (Geosphere Engineering), 75(2), pp.155-166.

Phan, N.B., Hayano, K., Mochizuki, Y. and Yamauchi, H., 2021. Mixture design concept and mechanical characteristics of PS ash–cement-treated clay based on the water absorption and retention performance of PS ash. Soils and Foundations, 61(3), pp.692-707.

Public Works Research Institute, 2013. Manual for utilization of soils from construction (4th edition). Public Works Research Center, 204.

Sato, A. and Hatakeyama, O., 2021. Influence of preparation conditions on solidified -crushed soil characteristics and strength. GEOMATE Journal, 20(79), pp.48-55.

Tani, S., Fukushima, S., Kitajima, A. and Nishimoto, K., 2006. Applicability of cement-stabilized mud soil as embankment material. ASTM International.

Watanabe, Y., Binh, P.N., Hayano, K. and Yamauchi, H., 2021. New mixture design approach to paper sludge ash-based stabilizers for treatment of potential irrigation earth dam materials with high water contents. Soils and Foundations, 61(5), pp.1370-1385.

Yamamura, K., 1983. Current status of waste management in Japan. Waste Management & Research, 1(1), pp.1-15.

Yuan, H., Chini, A.R., Lu, Y. and Shen, L., 2012. A dynamic model for assessing the effects of management strategies on the reduction of construction and demolition waste. Waste management, 32(3), pp.521-531.

Yuan, H. and Shen, L., 2011. Trend of the research on construction and demolition waste management. Waste management, 31(4), pp.670-679.

CHAPTER 2

LITERATURE REVIEW

2.1 SYNOPSIS

Chapter 2 provides an in-depth exploration of construction-generated soil and its reuse as a resource in other construction projects. It covers the classification of construction-generated soil and presents case studies of relevant projects where its reuse has been implemented. The chapter discusses the utilization of common stabilizers and sustainable materials for treating construction-generated soil, along with associated problems. Previous research on treating PSAS in construction-generated soil is also reviewed. The final part of the chapter examines the conventional flow for treating construction-generated soil and its impact on various stabilizers.

2.2 CONSTRUCTION GENERATED SOIL

Construction-generated soil is soil removed in construction projects. Especially, soil generated in excavation works during pile construction and tunnel construction is called construction-generated soil, in Japan. Construction-generated soil often exhibits mud-like properties. Construction waste sludge (which is regulated as industrial waste), is not considered as construction-generated soil in Japan according to Japanese Geotechnical Society, 2006.

Construction-generated soil presents numerous unfavorable characteristics, including a high content of fine particles and elevated water levels, making compaction challenging. The soil's inferior load-bearing capacity and poor geotechnical properties can lead to settlement issues and compromise the stability of foundations and structures. Furthermore, susceptibility to erosion and potential contamination risks further compound the challenges associated with this type of soil. To address these issues, comprehensive soil testing and engineering techniques are essential. Stabilization methods, such as the use of binders and compaction aids, should be employed to improve soil properties. Additionally, implementing proper drainage and erosion control measures becomes crucial to mitigate water-related problems. Effective management of construction-generated soil is vital to ensure the safety and longevity of construction projects (MLIT,2007)

Figure 2.1 Construction-generated soil during pile and tunnel construction

Table 2.1 depicts the classification of construction-generated soil according to its characteristics and the law governing waste disposal. Soil for construction has a cone index of at least 200 kN/m^2; anything less is considered mud. Mud with a cone index value of less than 200 kN/m^2 has the ability to flow such that it cannot be loaded onto a standard dump vehicle and cannot support the human weight (Nakao et al. 2023).

Figure 2.2 shows an image of a cone penetrometer, which is used to determine the cone index value. The cone index standardized by "JGS 0716" refers to the degree of resistance to penetration when a cone penetrometer is pushed into the soil and is an indicator of the soil's strength. In the cone index the average of the penetration resistance forces at penetrations of 5 cm, 7.5 cm and 10 cm, to obtain the average penetration resistance force. It is a kind of bearing capacity test where shear resistance is also considered. Though this test cannot directly measure friction angle and cohesion, it has a relationship with the unconfined compressive strength q_u. It is q_c = (5-10) q_u.

Table 2.1 Classification of construction-generated Soil

	Classification	Property, strength
Construction surplus soil	First grade construction generated soil	Sand, gravel and similar materials
	Second grade construction generated soil	Cone index q_c: 800kN/m^2 or more
	Third grade construction generated soil	Cone index q_c: 400kN/m^2 or more
	Fourth grade construction generated soil	Cone index q_c: 200kN/m^2 or more
	Mud	Cone index q_c: less than 200kN/m^2

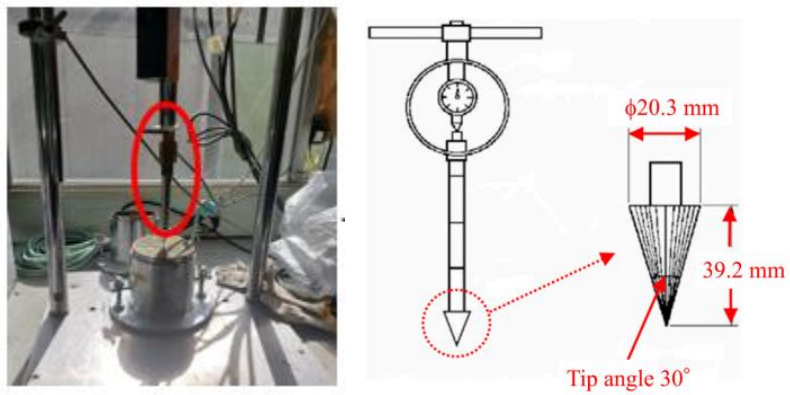

Figure 2.2 Cone index test

2.3 CONSTRUCTION GENERATED SOIL'S STRENGTH DEVELOPMENT

Construction-generated soil undergoes on-site treatment through the addition of stabilizers to enhance its engineering properties for construction purposes. This process involves rigorous and continuous monitoring and testing to ensure optimal stabilization. Various critical factors are regularly assessed to gauge the effectiveness of soil treatment. Chemical stabilization, which entails the introduction of additives like lime, cement, fly ash, or other stabilizing agents, is meticulously monitored. These additives react with the construction-generated soil's components, altering its properties and increasing its strength. Special emphasis is placed on monitoring the chemical reactions and ensuring proper distribution of stabilizers throughout the soil mass. To gauge the effectiveness of soil treatment, in-situ and laboratory testing are conducted on a routine basis. Various geotechnical tests, such as standard and modified Proctor compaction tests, California Bearing Ratio (CBR) tests, unconfined compressive strength tests, and direct shear tests, are performed to assess parameters like moisture content, density, shear strength, and compressibility. Moisture control is a critical aspect of soil treatment, as excessive moisture can lead to weakened soil properties. Therefore, monitoring and managing proper drainage systems are integral to preventing water accumulation and maintaining soil stability. Overall, the technical approach to treating construction-generated soil on site involves a systematic and comprehensive evaluation of numerous factors to achieve optimal soil strength and stability for safe and successful construction operations.

2.3.1 Compaction

In practical applications, the addition of a binder to construction-generated soil significantly influences its density. When construction-generated soil is stabilized with a binder, the maximum dry density is generally lower compared to unstabilized soil at the same level of compaction. The optimal moisture content tends to increase with higher binder proportions (Sherwood, 1993).

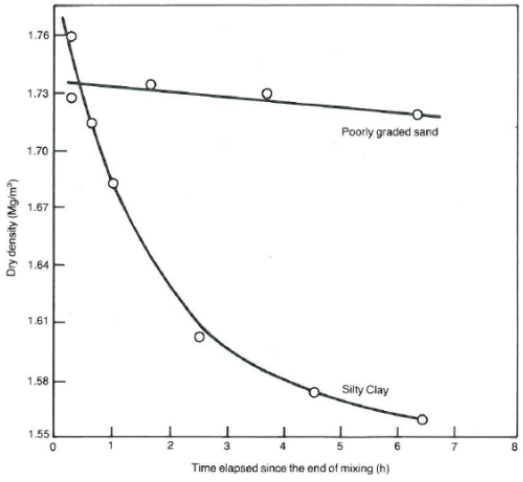

Figure 2.3 Dry density versus time elapsed since the end of mixing of two materials stabilized with 10% cement (Sherwood, 1993)

In the case of cement-stabilized soils, the hydration process starts immediately upon contact with water. To achieve the desired properties, it is crucial to compact the soil mix promptly. Delay in compaction can lead to premature hardening, necessitating extra compaction efforts to achieve the desired effect. This delay may result in bond breakage and a loss of strength, especially in clay soils, as the plasticity properties of clays are altered by stabilization (Figure 1) (Sherwood, 1993).

On the other hand, lime-stabilized soils may benefit from a mellowing period after stabilization. Allowing lime to diffuse through the soil during this period can maximize its effect on plasticity. After this mellowing period, the lime-stabilized soil can be remixed and compacted, resulting in notably improved strength compared to immediate compaction (Sherwood, 1993).

2.3.2 Moisture Content

Adequate moisture content is crucial in stabilized soils, serving not only to facilitate the hydration process but also to ensure efficient compaction. When cement is fully hydrated, it absorbs approximately 20% of its own weight of water from the surrounding environment (Sherwood, 1993). Similarly, quicklime (CaO) absorbs about 32% of its own weight of water from the surrounding environment (Roger et al., 1993; Sherwood, 1993). If the moisture content is insufficient, the binders will compete with the soil to gain the required amount of moisture. In soils with a high affinity for water, such as clay, peat, and organic soils, the hydration process may be delayed due to insufficient moisture content, ultimately impacting the final strength of the stabilized soil.

2.3.3 Temperature

The pozzolanic reaction is highly influenced by temperature variations. In practical construction settings, temperatures fluctuate throughout the day. Lower temperatures can slow down the pozzolanic reactions between binders and soil particles, leading to reduced strength in the stabilized material. For regions with cold climates, it is advisable to carry out soil stabilization during the warmer seasons to optimize the effectiveness of the process (Sherwood, 1993; Maher et al., 2003).

2.3.4 Freeze-Thaw and Dry-Wet Effect

Stabilized soils are vulnerable to damage caused by freeze-thaw cycles, necessitating the need for protection in the field (Maher et al., 2003; Al-tabbaa and Evans, 2005). The extent of shrinkage forces in stabilized soil depends on the chemical reactions of the binder used. Soil stabilized with cement is particularly susceptible to frequent dry-wet cycles due to temperature changes throughout the day, leading to internal stresses within the stabilized soil. As a result, measures should be taken to shield the stabilized soil from such effects (Sherwood, 1993; Maher et al., 2003).

2.4 PREVIOUS STUDIES FOR TREATING CONSTRUCTION GENERATED SOIL

In the study conducted by Tang et al. (2001), the focus is on addressing the issue of dredging waste in Japan and the critical need to minimize waste generation while promoting the reutilization of dredged soils. The researchers present compelling instances where improved dredging practices have been successfully employed in diverse marine construction endeavors. These examples encompass the reclamation of land for constructing airport runways, the establishment of breakwaters and seawalls, and the development of ports. To optimize the utilization of dredged materials, the study establishes an empirical relationship specifically tailored for cement-treated dredging. This relationship takes into account crucial factors like unconfined compressive strength, cement content, and water content of the dredged materials. The estimation of strength variance is a key aspect of the investigation. Based on their analysis, the researchers find that the estimated variance of unconfined compressive strength lies within the range of 0.29 to 0.38, considering variances of cement content and water content as 0.15 and 0.16, respectively. Furthermore, the study conducts a comparison between the aforementioned estimated strength variance and the actual strength variance observed in cement-treated dredging with normal strength uniformity. The observed strength variance in this case varies from 0.24 to 0.42. Additionally, the researchers assess strength variance using cone resistance as well, which yields smaller variance values ranging from 0.11 to 0.19. These findings hold significant implications for assessing the quality of recycled geomaterials, particularly cement-treated dredging, and are instrumental in cost reduction during reclamation projects.

Kitazume et al. (2003) address the growing challenge of securing sufficient soil for reclamation purposes and the associated difficulty in locating suitable waste subsoil or dredged soil disposal sites. Consequently, geotechnical engineers are increasingly resorting to the use of low-quality materials as fill materials, which contrasts with practices of the past few decades. The paper emphasizes the development of various soil admixture techniques aimed at enhancing the properties of these materials, leading to the production of high-quality fill materials. Particularly, the study focuses on the application of cement-treated soil mixtures, exemplified by the Pneumatic Flow Mixing Method, in the construction of man-made islands for diverse objectives. An essential aspect of the investigation involves the comprehensive analysis of the deformation and strength characteristics of cement-treated soils. These evaluations play a pivotal role in assessing the stability of structures adjacent to or buried within the treated ground. By delving into these technical details, the research underscores the efficacy of utilizing cement-treated soil mixes for engineered land reclamation projects, thus providing valuable insights for geotechnical engineering practices.

Siham et al. 2008 conducted a study to explore the potential utilization of Dunkirk marine dredged sediment as a novel resource for road construction, specifically in the foundation and base layers. The researchers assessed the mineralogical composition of the sediments through X-ray diffraction and microscopy analysis. After dewatering the sediments, they identified several suitable mixtures and proceeded to optimize them for cost-effective reuse.

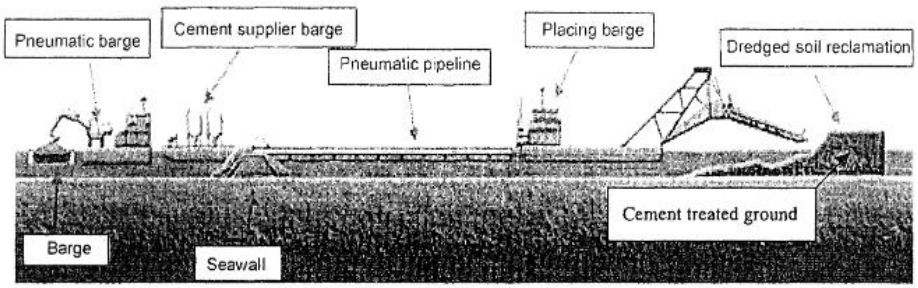

Figure 2.4 Schematic view of Pneumatic Flow Mixing Method (Kitazume and Sato, 2002)

A preliminary mixture indicated as "A" has been proposed, comprising dewatered sediment obtained through the Extract process, 4% of lime, dredged sand, 0/4 mm sand, and Portland cement termed as "cem1." The specific composition details of mixture "A" can be found in Table 2.2.

Table 2.2 Composition of mixture ‘‘A’’ (Siham et al. 2008)

	Dry content (%)
Dewatered sediment	27
Dredged sand	37
Boulogne sand	28
Portland cement ‘‘cem1’’	8

The experimental findings indicate that when mixture 'A' contains 11% water content, it falls under the S4 class. To evaluate the robustness of the mixture, a sensitivity analysis is performed on the water content, and the direct tensile strength and elastic modulus are measured at a lower water content (7.8%). Consequently, the mixture is now classified within the S2-S3 limits, which is sufficient for considering its use in base and foundation layers, as per Andriexu et al. 1998. This

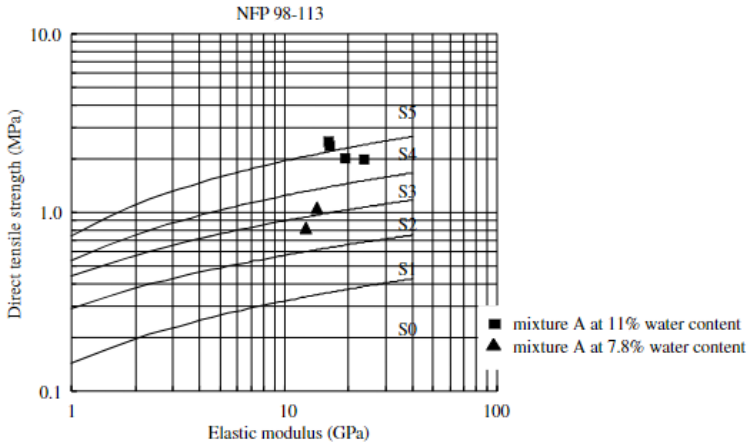

Figure 2.5 Structural classification of mixture ‘‘A’’ (Siham et al. 2008)

change in classification is attributed to the variation in water content, where the higher hydration degree of cement at 11% water content contributes to better mechanical strength (Fig. 2.5).

The results indicate that Dunkirk marine dredged sand and sediments can be successfully utilized as a new material for road construction. However, economically, mixture 'A' contains a relatively high cement content. To enhance competitiveness and reduce the risk of cracking, a new mixture 'B' is studied, employing only 6% of cement, a standard value for treated sand in road construction. Moreover, lower cement content also offers the advantage of reduced shrinkage in the mixture. To improve the workability of mixture 'B', a third mixture 'C' is proposed, which is similar in composition but uses a different type of cement, 'cem2', consisting of 67% slag and 12% limestone by mass. The use of 'cem2' is more practical for road construction due to its extended setting period of more than 13 hours, compared to 4.5 hours for cement 'cem1'. The composition of 'cem2' is detailed in Table 2.3, while the compositions of mixtures 'B' and 'C' are presented in Table 2.4.

Table 2.3 Composition of cement ‘‘cem2’’ (Siham et al. 2008)

	Composition in mass (%)
Clinker	21
Slag	67
Limestone	12
Anhydrite	5

The experimental findings demonstrate that both mixtures, 'B' and 'C,' exhibit favorable mechanical strength. Mixture 'B' with a water content of 9.9% and mixture 'C' with a water content of 11.5% fall within the S2 and S3 classification limits (Fig 2.6). From a geotechnical perspective, mixture 'B' is suitable for foundation layers and could also serve as a base layer if proper water content control is maintained. On the other hand, mixture 'C' is well-suited for foundation layers and offers added advantages for road construction, including those mentioned earlier.

Table 2.4 Composition of mixtures ‘‘B’’ and ‘‘C’’ (Siham et al. 2008)

Dry content (%)		Dry content (%)
Dewatered sediment	27	27
Dredged sand	39	39
Boulogne sand	28	28
Portland cement ‘‘cem1’’	6	-
Portland cement ‘‘cem2’’	-	6

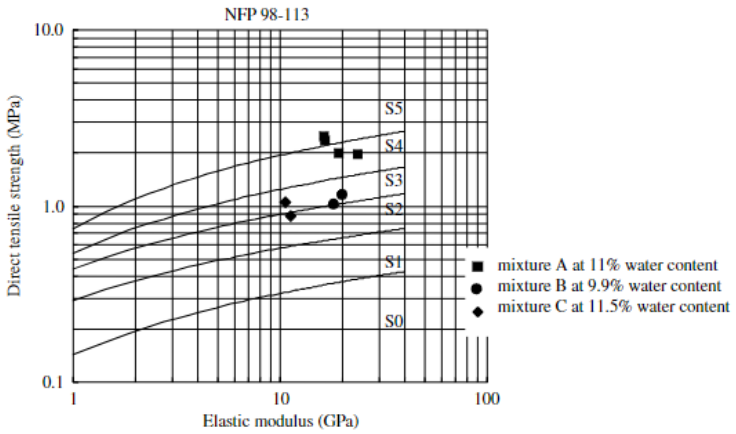

Figure 2.6 Structural classification of mixture ‘‘B’’ and ‘‘C’’ (Siham et al. 2008)

2.5 PROBLEMS RELATED WITH COMMON STABILIZERS

In the previous section, some research where construction-generated soil is reused is described. In all cases, construction-generated soil is stabilized with cement or lime. When cement is combined with construction-generated soil, a chemical reaction takes place, which causes the cement to become more rigid and form a solid mass. The result of this process, which is known as hydration, is a substance that is harder and more resistant to erosion than soil construction-generated soil.

(a) Cement (b) Lime

Figure 2.7 Common soil stabilization materials

There are challenges and considerations associated with cement stabilization. While cement stabilization may mitigate some environmental issues related to dredged materials, it may still have environmental impacts, such as carbon emissions during cement production and the potential leaching of trace elements from the cementitious mix. Additionally, the effectiveness of cement stabilization depends on the type and characteristics of the dredged materials. Moreover, not all dredged soils may be suitable for this treatment method. Also, proper engineering design and ongoing monitoring are essential to ensure the successful implementation of cement stabilization and its long-term effectiveness (Dong et al., 2011; Imai et al., 2020).

2.6 SUSTAINABLE MATERIALS

The term "sustainable material" refers to any material that is sourced, produced, utilized, and disposed of in a manner that is responsible to both the environment and society. These types of

materials are developed to have a lower impact not just on the natural world but also on human health, and they also support environmentally responsible activities over their whole life cycles. For a material to be considered sustainable, it must meet certain criteria, including being renewable, biodegradable, non-toxic, energy-efficient, and low in carbon emissions. The materials bamboo, cork, recycled plastic, organic cotton, and recycled paper are examples of sustainable materials. These materials are frequently used in eco-friendly products and industries. Promoting sustainable development, which attempts to strike a balance between economic, social, and environmental issues in the pursuit of a more fair and resilient future, one of the most significant aspects of which is the use of sustainable materials. We can help lessen the impact that we have on the earth and build a more sustainable future for ourselves and future generations by selecting materials that are made from sustainable sources. (Dong et al., 2011; Imai et al., 2020; Inasaka et al., 2021; Trung et al., 2021, 2022)

2.6.1 Common Sustainable Materials as a Soil Stabilizer

Usually cement and lime is used as soil stabilization material but they have a significant negative impact on the environment and economy. When we refer to "common sustainable materials," we are referring to materials that are utilized in a manner that is both environmentally friendly and beneficial to the environment regularly. These materials are often renewable, biodegradable, or recyclable, and they are utilized in the manufacturing of a wide variety of items. In several different fields, including building, the utilization of these materials is frequently considered as a means of reducing the impact on the environment and advancing the cause of sustainability. Coal ash, steel slag, concrete slag, biomass ash, sewage sludge ash and fly ash are some of the examples of common sustainable materials, use in construction engineering instead of cement or lime.

2.6.2 Sustainable Materials in Construction- generated Soil Treatment

Recently, there has been an increase in the utilization of sustainable materials that are produced by industries to recycle soil that is generated by construction to make society more environmentally friendly. In this section, several previous research on the treatment of construction-generated soil with sustainable materials will be explained. Kim et al., 2015 indicate that dredged soil is typically

Figure 2.8 Stabilizers from sustainable material

utilized as a filler material for land located near coastal areas, but that to improve its engineering features, it requires further treatments. Since these treatments require a significant amount of time and money, experts have been looking at other potential solutions to find a way around these challenges. The use of coal ash, a byproduct of the manufacture of thermal power, as a material for the reclamation of dredged soils is the topic of discussion in this study. According to the findings of the research, the incorporation of dredged soils and coal ash increased the ground's particle distribution as well as its cohesiveness and consolidation.

The difficulty of finding a sustainable application and suitable and useful use of dredged soils in Korea, which are generated in enormous amounts due to the construction of ports, the development of coastal areas, and the maintenance of water channel works, is discussed in Oh et al., 2015. Due to the fine-grained nature of dredged soils, they are not desirable as materials for earthwork or backfill unless they can be combined with additional cementitious materials to increase their strength. The purpose of this study is to evaluate the compressive strength characteristics of mixes of dredged soils with slag for applications in geotechnical engineering. According to the findings of the study, the compressive strength of the soil-slag mixture is affected by several parameters. These elements include the types of dredging soil (Fig 2.9), the types of slag (Fig 2.10), the mixing ratio of soil-to-slag, and the mixing water content (Fig 2.11).

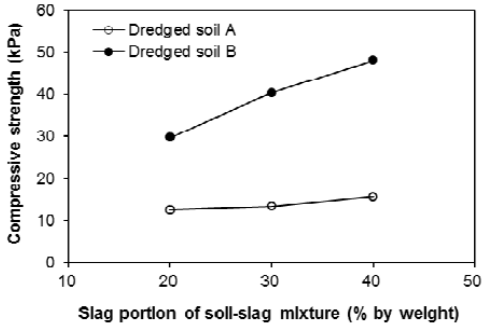

Figure 2.9 Compressive strength of dredged soils mixed with steelmaking slag (water content = 30%, curing time = 7 days) (Oh et al., 2015)

Nabeshima, 2016 discusses the 2011 Tohoku Earthquake, the strongest earthquake ever recorded in Japan. Three prefectures in Japan's north-eastern region, Miyagi, Iwate, and Fukushima, sustained substantial damage from the earthquake. The tsunami surges that followed the earthquake devastated the Pacific coast of Japan's northeastern district, causing the deaths and disappearances of approximately 19,000 individuals. The paper proposes a method for reusing tsunami sediment soil by combining it with stabilizers such as steel slug and concrete sludge to produce building materials for reconstruction in the afflicted areas. The addition of concrete sludge as an alkaline irritant can accelerate the hardening time of blast furnace slug (Fig 2.12), which is used for strengthening tsunami sediment soil.

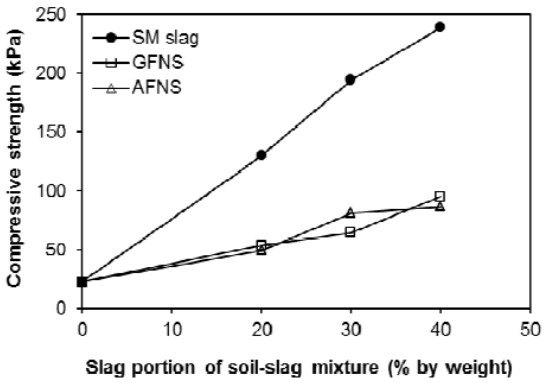

Figure 2.10 Compressive strength of dredged soil mixed with three different types of slag (water content = 22%) (Oh et al., 2015)

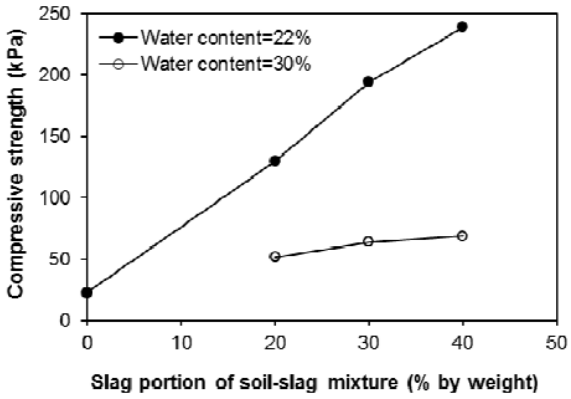

Figure 2.11 Effect of water content on compressive strength of dredged soil (Oh et al., 2015)

Vichan and Rachan, 2013 discuss the use of calcium carbide residue (CCR) and biomass ash (BA) as a chemical stabilizer for porous Bangkok clay soil. Low inherent shear strength and excessive water content can lead to soil settlement. The study investigates the efficacy of using CCR and BA to enhance the soil's strength and stability for infrastructure construction. In prior research, cement, quick lime, and calcium carbide were utilized for this purpose. The study investigates the efficacy of using CCR and BA to enhance the soil's strength and stability for infrastructure construction. In prior research, cement, quick lime, and calcium carbide were utilized for this purpose. Sewage sludge has been incorporated into building construction materials, such as replacing cement in concrete and clay in glaze tile production. Chen and Lin, 2009 discuss the use of incinerated sewage sludge ash (ISSA) combined with cement to strengthen porous, cohesive subgrade soil. The purpose of this paper is to investigate the potential geotechnical applications of ISSA/cement admixture. The study demonstrates that the addition of ISSA/cement enhances the unconfined compressive strength (Fig 2.13), and reduces the swelling behavior of soil samples (Fig 2.14).

Extensive research has been conducted on the effects of various factors, such as water content, cement content, curing condition, replacement ratio, and compaction energy, on the microstructure and engineering properties of cement-stabilized soils. Also extensively used to stabilize clayey

soils are lime and cement. Instead of cement, discusses the use of refuse materials such as fly ash for soil stabilization. Instead of cement, some researchers propose using refuse materials such as fly ash and calcium carbide residue for soil stabilization. (Lo and Wardani, 2002; Horpibulsuk et al., 2009)

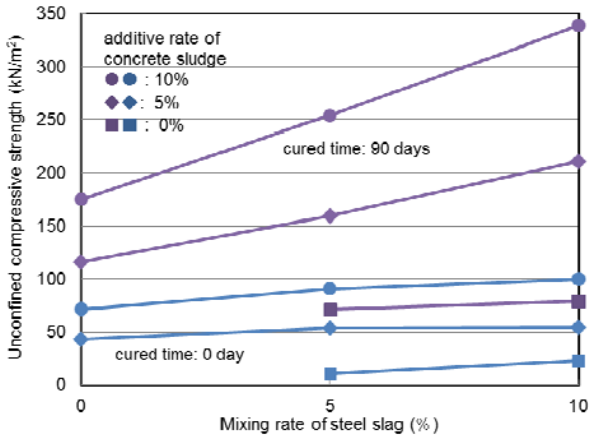

Figure 2.12 Unconfined compressive strength of muddy tsunami sediment with a mixing rate of steel slag (Nabeshima, 2016)

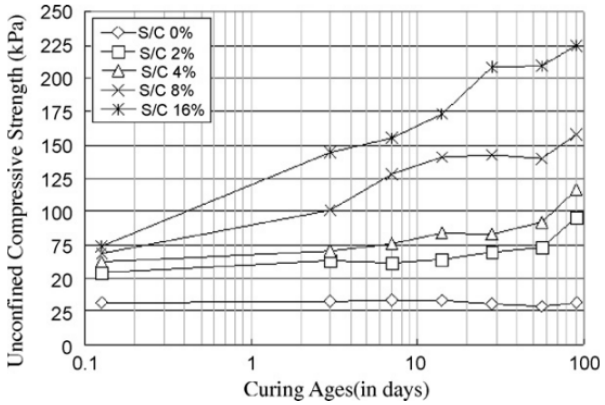

Figure 2.13 The relationship between ISSA/cement and the unconfined compressive strength of specimens at different curing ages. (Chen and Lin, 2009)

Horpibulsuk et al., 2009, investigate the strength characteristics of a mixture of calcium carbide residue and fly ash for soil stabilization. The study focuses on the role of fly ash in improving strength in the inert and deterioration zones.

While the disposal of paper sludge ash is a major concern, an increasing number of researchers have investigated whether or not the ash that is produced during the incineration of paper sludge can effectively be used to improve soil that has been generated through construction. Also, PSAS's

water absorption capacity attracts researchers to use it as a soil stabilization material. In the next section, a details discussion on paper sludge ash will be provided.

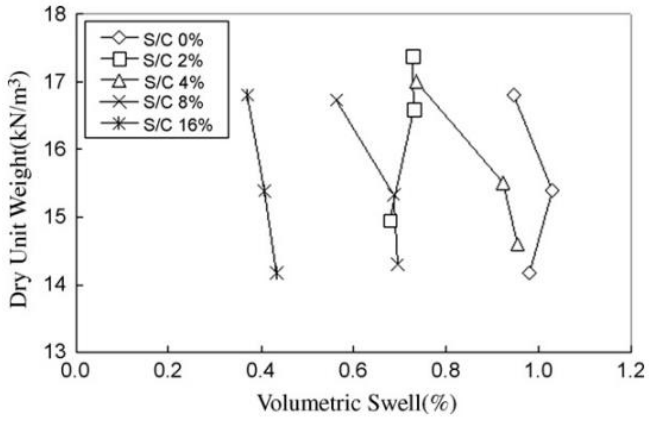

Figure 2.14 The relationship between volumetric swelling and dry unit weight for the ISSA/cement soil specimens. (Chen and Lin, 2009)

2.7 PS ASH AS SOIL STABILIZATION MATERIAL

Due to its high levels of calcium oxide (CaO) and silicon dioxide (SiO), paper sludge ash (PS ash) can be an effective soil stabilization material. These compounds have pozzolanic properties, which means they react with water to form a cement-like substance that can enhance the strength and stability of the soil. The use of ash from paper sludge as a soil stabilizer is also an environmentally beneficial practice, as it reduces waste and makes use of a byproduct that would otherwise be discarded. In addition, it may reduce the need for other stabilizing materials, such as cement, that may have negative environmental effects. In this section, characteristics, environmental benefits and previous research related to PSAS will be discussed.

2.7.1 Characteristics of PS Ash

Mineral fillers, microscopic cellulose fibres, water, inorganic salts, and organic compounds make up paper mill sludge. PS ash is produced by incinerating refuse paper sludge generated during the papermaking process. Mochizuki et al. (2003) determined that, depending on its composition, its pH ranges from nearly neutral to around 12; its particle density is between 2.2 and 2.9 g/cm^3; and its maximal dry density is between 0.65 and 0.95 g/cm^3. Corinaldesi et al. (2010) determined PS ash's water absorption capacity to be approximately 25%, in saturated surface-dried conditions, and its specific gravity to be 1.72 g/cm^3. Additionally, the percentage of PS ash that passes through a 75 m sieve is 80%. The PS ash has a bulk density of 1.2 g/cm^3 and is lighter than conventional sand (with a predictable range of 2.5 to 2.6 g/cm^3) and binders (2100 to 3100 kg/m^3) are typically used in the process of producing mortar. According to Ahmad et al. (2013), the specific gravity of paper slurry ash is 2.60. Table 2.3 contains particle density for PS ash and other materials. Lime, cement, and magnesium oxide demonstrate the ability to chemically absorb water and possess a

particle density of a minimum of 3 g/cm^3. The particle density of PS ash, which shows physical absorption of water as well, is equal to or lower than 2.8 g/cm^3.

Mochizuki (2019) investigated in depth the particle density of a variety of PS ash varieties. While the particle density of PS ash may differ based on the incinerator, it closely resembles soil values. Additionally, the variations in particle density within each PS ash sample are relatively small. Further, due to the porous nature of PS ash particles, they have low bulk density, affecting the moist and dry densities of the soil.

CaO and SiO_2 are the predominant constituents found in PS ash, alongside other significant elements like Al_2O_3, Fe_2O_4, MgO, SO_3, K_2O, etc. The expansion caused by the hydration of CaO to $Ca(OH)_2$ can lead to insufficiency if after setting it occurs, which is considered detrimental. Mochizuki (2019) discovered that the chemical composition of PS ash, notably high levels of CaO, SiO2, and Al2O3, is comparable to cement. However, because of modifications in the incineration process, the composition of these materials has undergone alterations as shown in Fig. 2.15.

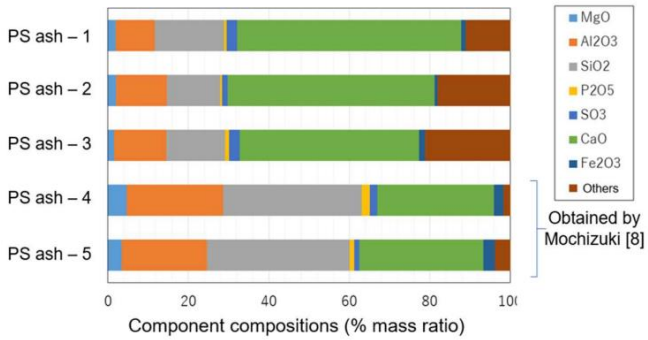

Figure 2.15 Main chemical components of different types of PS ash

PS ash-based stabilizer (PSAS) is a commercially available product produced by immobilizing heavy metals found in the original PS ash. As a result, PSAS exhibits similar water absorption characteristics to the initial PS ash. Its porous surface structure, with numerous intricate irregularities and voids, allows PSAS to effectively absorb and retain excess water in soft soil (Mochizuki et al. 2003). When combined with mud and sludge, PSAS significantly enhances their stability in a prompt manner. The swift water absorption during the mixing process with clay leads to a reduction in the water content within voids, resulting in decreased fluidity of the treated clay.

Kawai et al. (2018), who investigated the PSAS-A as part of their study, have determined that the PSAS-A's component composition is comparable to that of standard Portland cement. The amount of calcium oxide (CaO) in PSAS accounted for 40.6% of its total weight, which was similar to the findings of Rahmat and Kinuthia (2011) and Segui et al. (2012). Consequently, when PSAS is mixed with water, a hydration reaction occurs, as documented by Kawai et al. (2018). During curing, the porous structures of PSAS particles physically absorb excess water from the mud, followed by chemical absorption by the hydrated compound ettringite.

2.7.2 PSAS as a Water-Absorbing Material

From previous research, it was clear that PSAS has a high water absorption capacity because of its porous structure. To quantify the amount of water absorption and retention by PSAS, Kato et al. (2005) have proposed the cylinder method. This method was used by Kawai et al. (2018) to investigate the water absorption and retention performance of PSAS. As shown in Fig. 2.17, after 30 minutes, the water absorption and retention capacity of PSASs remained nearly unchanged. So current method showed no effect for long time curing periods. To overcome this problem, a new testing method is developed by Phan et al. (2021).

This study develops a new testing method that overcomes limitations to evaluate the water absorption and retention efficacy of PSAS named the sieving method. As depicted in Fig. 2.18, the method consists of applying vibration to a stainless steel net to separate PSAS particles that absorb and retain water from PSAS particles that do not absorb and retain water. Under the influence of vibration, these PSAS particles move closer together, while water that has not been absorbed or retained is expelled. These PSAS particles are then retained on the stainless steel net, while the unabsorbed and unretained water passes through the stainless net. Although there is still

Figure 2.16 Illustration depicting the testing procedure (Kawai et al. 2018)

a small amount of free water remaining in the voids of PSAS particles, most of the water content of the PSAS retained on the stainless net represents the amount of water absorbed and retained by PSAS. Based on the measurement, the water absorption and retention rate of PSAS over time can be evaluated as described in this section. The advantage of this method is that the PSAS solution is cured in a sealed soft plastic bag; therefore, the ability of PSAS to expand due to water absorption and retention is not limited. Moreover, most of the unabsorbed and unretained water is separated from the PSAS particles, thereby increasing the accuracy of the assessment. In addition, the vibration breaks down the weak hydration bond of the PSAS, resulting in the removal of most of the unabsorbed and unretained water trapped in voids between PSAS particles.

As shown in Fig. 2.18, a commercially available electromagnetic sieve shaker was used to generate vibrations to evaluate the water absorption and retention performance of PSAS. The mechanism shakes the sieves in three dimensions, including vertical, horizontal, and twisting movements. The width of the trembling ranges from 0 to 3 mm. As specified in Japan Industrial Standards (2019)

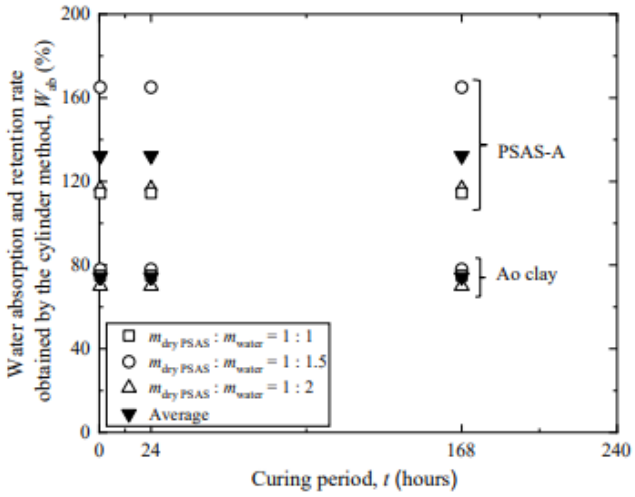

Figure 2.17 The water absorption and retention characteristics of PSAS-A and Ao clay obtained through the cylinder method. (Kawai et al., 2018).

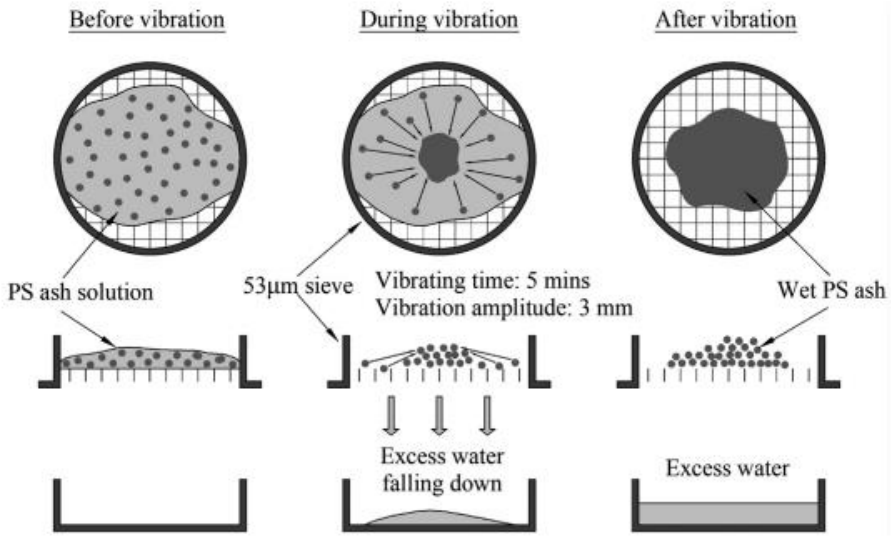

Figure 2.18 Experimental principle for determining water absorption and retention performance of PSAS (Phan et al., 2021).

and illustrated in Fig. 2.19, a 53 μm m sieve was chosen to minimize the quantity of PSAS passing through the sieve. In addition, the 53 μm sieve is the tiniest sieve for which surface tension effects do not prevent the passage of excess water. It was discovered that excess water splashes and adheres to the underside of the 53 μm sieve after passing through it during vibration, prohibiting excess water from passing through the sieve. To address this issue, a support sieve was positioned between the 53 μm sieve and the bottom tray. The support sieve was sufficiently large to not retain

water (greater than 4.75 mm). The duration and amplitude of the vibration were set to 5 minutes and 3 mm, respectively.

The test's specifics are depicted in Fig. 2.19. Before being transferred to a sieve, each variety of PSAS was first soaked in distilled water using a PSAS/water ratio of 0.25. After this, the PSAS was cured in conditions where it was sealed for predetermined amounts of time. The drying time ranged anywhere from 10 minutes to 72 hours. After that, a three-dimensional vibration was given to the PSAS in a stainless 53-m sieve using an electromagnetic sieve shaker to separate the PSAS particles that absorbed and retained water from the free water in the PSAS solution. This was done so that the PSAS particles that absorbed and retained water could be reused. The movement that occurred in all three dimensions was a circular motion that was superimposed on top of a vertical tossing action, and the amplitude was determined as the entire height at that the test sieve was lifted. The force of the vibration caused the PSAS particles to move closer to one another, and as a result, they were caught in the sieve. On the other hand, the free water was able to pass through. After that, the amount of water that was included in the PSAS particles that were retained on the stainless-steel sieve was determined.

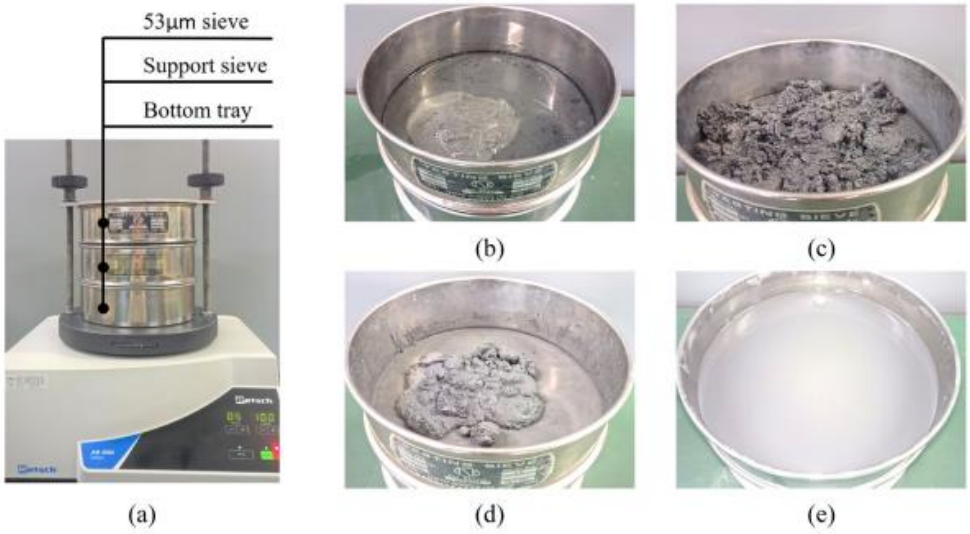

Figure 2.19 Test method to evaluate the water absorption and retention performance of PS ash : (a) overview of the experimental setup, (b) PS ash solution before vibration after 10 min curing in a sealed bag, (c) PS ash solution after 24 h curing in a sealed bag, (d) wet PS ash remaining on sieve after vibration, and (e) excess water with fine PS ash particles passing through the sieve. (Phan et al., 2021).

Fig. 2.20 depicts the time-dependent variation in the water content, w_{ab}, of PSAS, Ao clay, recycled glass sand, recycled ceramic sand, and glass pearls as determined by the newly developed method. For earth infill, recycled glass sand and recycled ceramic sand are used in place of natural gravel or sand. The particulate size of glass beads ranges from 38 to 53 μm, which is comparable to the D_{50}–D_{60} particle size range of PSAS. It was discovered that the water content, w_{ab}, of PSAS increased as curing time increased. PSAS's water content, w_{ab}, was 66% after 10 minutes of curing,

increasing to 112% and 131% after 24 and 72 hours, respectively. Results indicate that water is physically absorbed to fill the porous structure of PSAS particles during the initial stage. PSAS can undergo hydration to form silicate hydrate crystallizations such as ettringite (Kawai et al., 2018), thereby increasing the quantity of absorbed and retained water through chemical absorption. In consequence, the water absorption and retention performance of PSAS increased progressively over time.

The results of the experiment also revealed that the water content w_{ab} of recycled glass sand and recycled ceramic sand is constant at 19% and 22%, respectively, despite their inability to consume and retain water. Additionally, it was found that the moisture content of the glass bead sample remained steady at 24%, and the glass beads did not possess the capacity to soak up and retain water. Song et al. (2008) illustrated that when three-dimensional space is filled with identical spheres in a random manner, it occupies around 64% of the space, with the loosest filling taking up about 55%. The void ratio $e = 0.819$ and the degree of saturation $S_r = 58.0\%$ are estimated for the measured water content, $w_{ab} = 19\%$ and the specific gravity of the recycled glass sand particles $G_s = 2.5$ (obtained from the manufacturer's catalogue). This indicates that even under the influence of vibration, a certain amount of free water remained confined in the spaces between the recycled glass sand particles due to suction. In addition, According to Fig. 2.26, the water content (W_{ab}) of Ao clay is nearly 37%, surpassing the water content of recycled glass sand, recycled ceramic sand, and glass beads. The higher water content in Ao clay is attributed to its ability to absorb and retain water through the electrochemical bond between its particles, unlike other materials. The assumption made is that the 37% value includes both water retained through suction and electrochemical bonds.

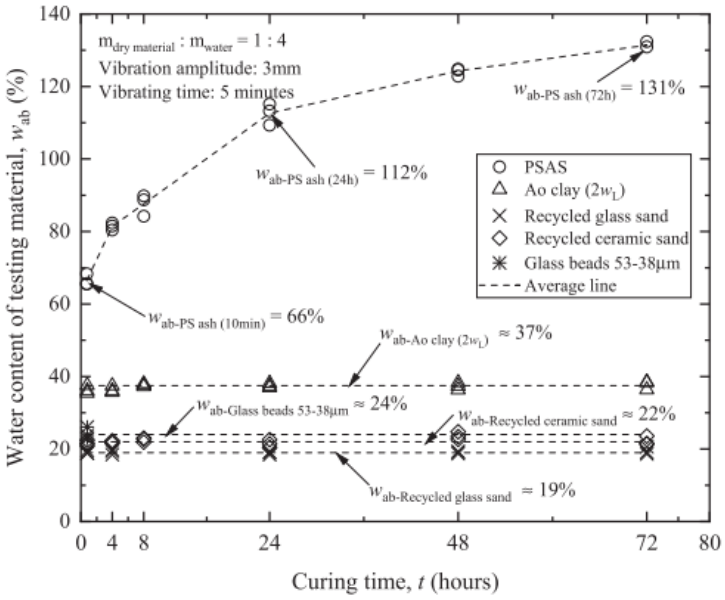

Figure 2.20 Change in water content of testing materials in water absorption and retention performance evaluation tests. (Phan et al., 2021).

PSAS material could be subject to a similar phenomenon. Consequently, the actual rate of water absorption and retention of PSAS, which is defined as W_{ab} , the ratio of the weight of absorbed and retained water to the dry weight of PS ash particles, should be less than that obtained in Fig. 2.20 by the quantity of water retained in the voids by suction. Although the particle size of the targeted material can influence the quantity of water that exists in the voids due to suction, the W_{ab} values of recycled glass sand, recycled ceramic sand, and glass beads are not significantly different.

In this study, the actual water absorption and retention rate W_{ab} of PS ash at a given time was determined by subtracting the average W_{ab} of recycled glass sand, recycled ceramic sand, and glass beads, which was 22%, from the corresponding W_{ab} of PS ash obtained from Fig. 2.20. W_{ab} (Wab after 10 minutes of curing) and Wab-24h (W_{ab} after 24 hours of curing) values for PS ash were 44% and 90%, respectively. The calculated W_{ab} for different types of PSASs after subtracting a value of 22% are shown in Fig. 4.21. Among all types of PSASs, PSAS-C has the highest water absorption capacity while PSAS-D has the lowest water absorption capacity. In this research, these two types of PSAS will be used. PSAS-C will be denoted as PSAS-R while PSAS-D will be denoted as PSAS-N.

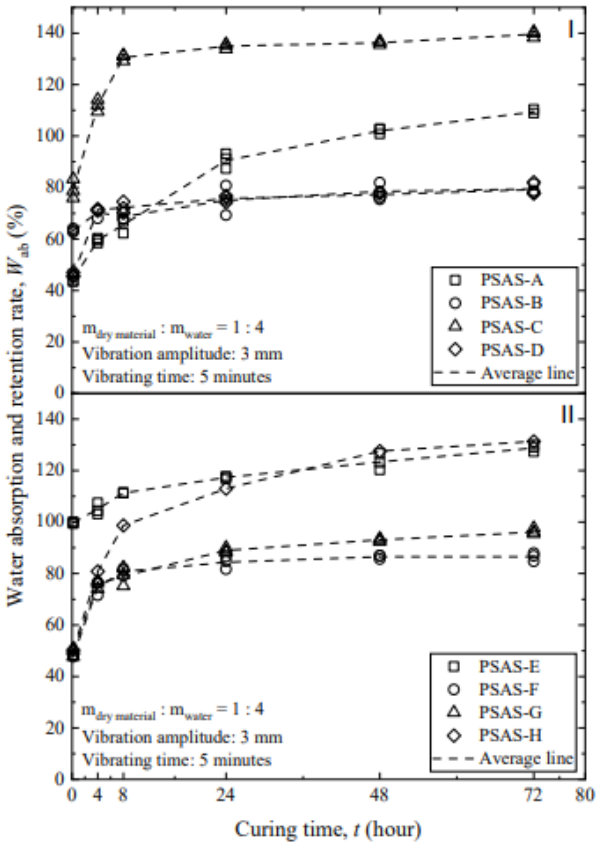

Figure 2.21 Estimated water absorption and retention rates of PSASs obtained using Sieving methods (Phan et al., 2021).

2.8 EFFECTS OF CONVENTIONAL FLOW FOR LABORATORY MIXTURES ON DIFFERENT MATERIAL

In Chapter 1, the conventional flow of laboratory mixture for treating construction-generated soil was described with cement-based stabilizers. The conventional flow consists of pre-compaction curing, crumbling and post-compaction curing. Previous studies show that this pre-compaction curing, crumbling and post-compaction curing have effects on cement or lime-treated soil. Besides cement or line, in recent years the use of sustainable materials has increased for treating construction-generated soil. The strength characteristics of construction-generated soil treated with sustainable materials are also impacted by the conventional flow of laboratory mixture. In this section, previous research on this topic will be discussed.

2.8.1 Effects of Pre-compaction Curing

Miyashita et al., 2019 described the effects of pre-compaction curing on cement or lime-treated soil. The research examines how environmental exposure conditions impact the long-term

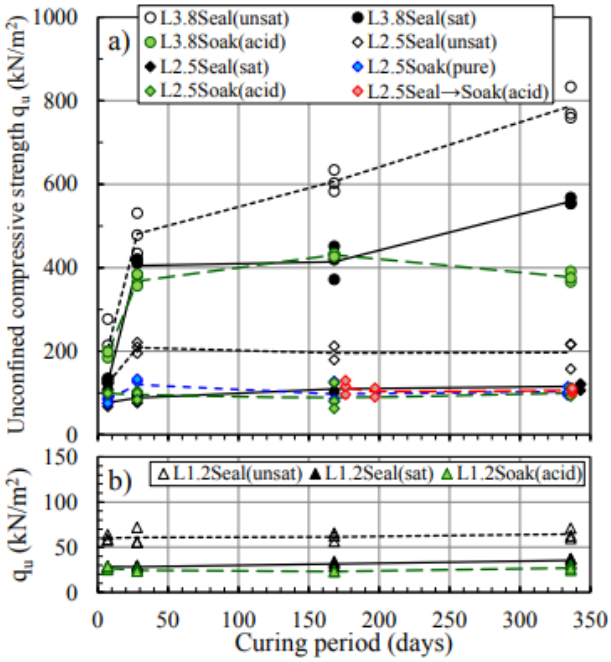

Figure 2.22 Relationships between unconfined compressive strength of lime-treated soils and the curing period (Miyashita et al., 2019)

mechanical properties of surplus soils treated with lime (Fig. 2.22) and cement (Fig. 2.23). Unconfined compression tests were conducted on specimens cured under various conditions. The findings revealed that the unconfined compressive strengths of the soaked specimens were the lowest, while those of the sealed specimens were the highest. The influence of soaking was particularly evident in the cement-treated soil, although its effect diminished with longer initial sealed curing durations. These variations in strengths were attributed to changes in physical

properties like the degree of saturation and chemical properties potentially caused by the leaching of hydration products during soaked curing.

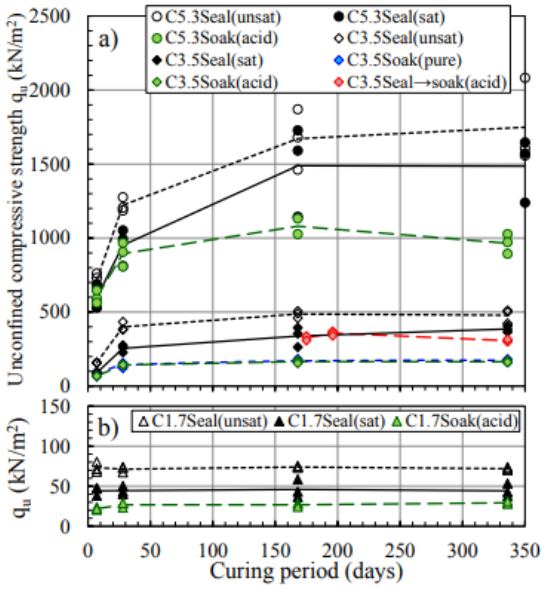

Figure 2.23 Relationships between unconfined compressive strength of cement-treated soils and the curing period (Miyashita et al., 2019)

Cikmit et al., 2021 report the effects of primary curing and subsequent disturbances on the strength development of steel slag-treated marine clay (SSTC), a novel geomaterial used for recycling steel slag. Here, the additional ratio of steel slag (R_{SS}) was 30% and 20%. As shown in Fig. 2.24 in both cases indicate that the initial strength of SSTC for maritime fill work can be improved by one to three days of pre-compaction curing (primary curing).

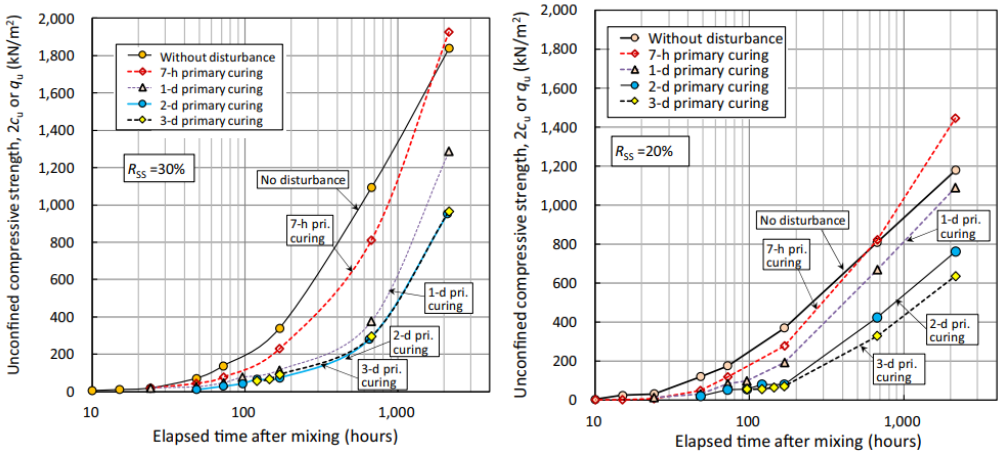

Figure 2.24 Strength development of SSTC with various primary curing times (Pre-compaction curing). (Cikmit et al., 2021)

2.8.2 Effects of Crumbling

Tani et al., 2006 described a method to repair embankments with crushed and compacted soil utilizing earth dam mud soil. The improved soil was produced by stabilizing the soil with cement, curing it for a few days, crushing, compacting, and re-stabilizing it. The mechanical tests for soil specimens prepared in a laboratory and obtained from actual embankments were used to obtain the curing times till crushing, and the strength and deformation characteristics of the crushed-compacted soil. Fig. 2.25 refers to a comparison of the unconfined compressive strength of two types of soil: initial stabilized soil and crushed-compacted soil. The comparison was made at different additive ratios of the stabilization material, ranging from 5% to 15%. The results of the comparison are shown in Fig 2.25, which indicates that the strength of the crushed-compacted soil was significantly lower than that of the initial stabilized soil. Specifically, the strength of the crushed-compacted soil was lowered to approximately half that of the initial stabilized soil at each additive ratio. This suggests that the process of crushing, compacting, and re-stabilizing the soil resulted in a significant reduction in its strength.

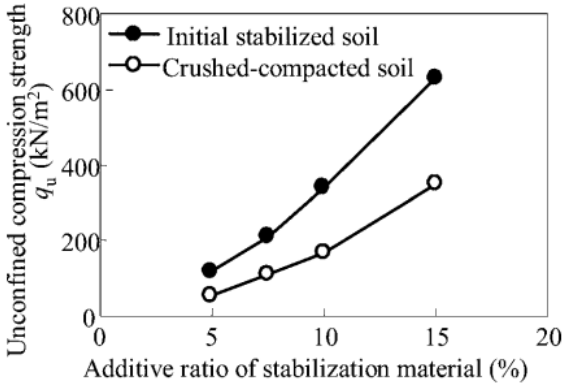

Figure 2.25 Effect of additive ratio of stabilization material to unconfined compression (Tani et al., 2006)

The research suggested a reduction in strength may be a trade-off for other benefits of the improved soil, such as its ability to resist cracking and its suitability as a core material for earth dam embankments.

Huang et al., 2011 investigate the mechanical behaviour of remolded solidified dredged material (RSDM) and compares it with intact solidified dredged material (SDM). The study finds that RSDM specimens show ductile behaviour, while SDM (Fig. 2.26) exhibits both ductile and brittle behaviours. The compressibility of RSDM (Fig. 2.27) is about three times higher than SDM at pre-yield, but less than SDM at post-yield. The yield stress of RSDM is about half that obtained for SDM. The strength of RSDM is much less than that of SDM, with the unconfined compressive strength of RSDM being about 20% to 40% when compared with the compressive strength of SDM. The strength difference between SDM and RSDM decreases as consolidation pressure

increases. The reasons for the mechanical differences may be attributed to the fact that SDM is a structured soil originating from strong cementation bonds, whereas, RSDM is not a structured soil.

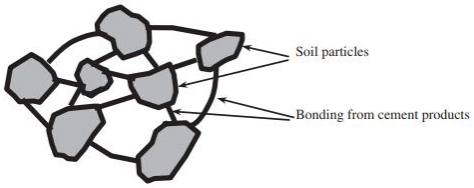

Figure 2.26 Schematic graph of bonding skeleton structure for SDM (Huang et al., 2011)

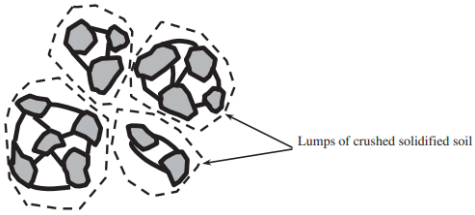

Figure 2.27 Schematic graph of crushed and compacted soil body for RSDM (Huang et al., 2011)

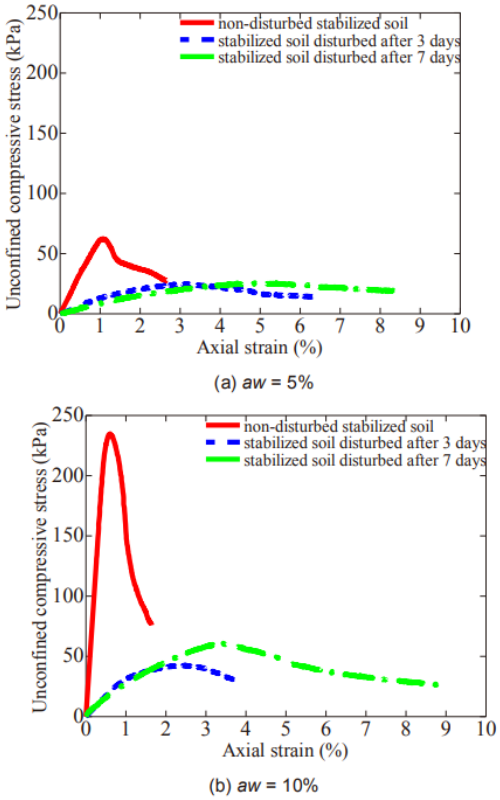

Figure 2.28 Stress-strain curves at the curing period of 28 days. (Makino et al., 2015)

Makino et al., 2015 discuss the effect of soil disturbance on the water content and stress-strain characteristics of cement-stabilized Kaolin clay in the unconfined compression test. The study provides insights into the effect of soil disturbance on the water content (*aw*) and stress-strain characteristics of cement-stabilized Kaolin clay as shown in Fig. 2.28. The findings of this research suggest crumbling reduced the unconfined compressive stress of the treated specimen. Cikmit et al., 2021 report the effects of subsequent crumbling on the strength development of steel slag-treated marine clay (SSTC) as shown in Fig. 2.23. With the additional ratio of steel slag (RSS) was 30% and 20%, in both cases the strength of treated soil was reduced due to crumbling. Sato and Hatakeyama, 2021 investigated the use of crushed solidified soil as a material whose strength development can be controlled even when a solidifier is added. The physical properties and strength of the crushed solidified soil were investigated, and two types of full-scale embankments were constructed on soft ground to compare their deformation characteristics. The results showed that the crushed solidified soil had lower strength than the solidified soil except when the solidifying material's mixing ratio was 5% (Fig.2.29).

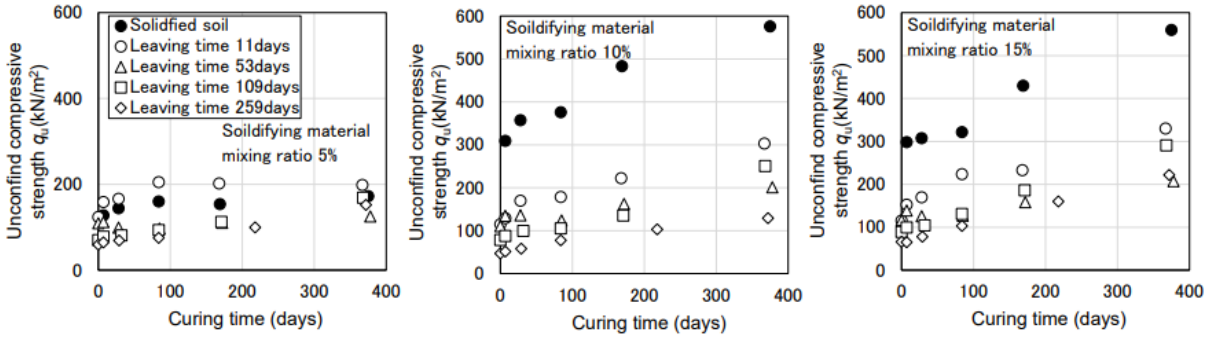

Figure 2.29 Relationship between curing time and unconfined compressive strength (Sato and Hatakeyama, 2021)

2.8.3 Effects of Post-compaction Curing

As mentioned above, the effects of pre-compaction curing conditions on the strength development of cement or lime-treated soils have been investigated to some extent. Also, the effects of post-compaction curing conditions on strength development are important to understand the durability . Beriha et al., 2018 demonstrated the effect of wet-dry cycles on the mechanical strength properties of cement-stabilized granular lateritic soil. The strength and stiffness of the soil were found to be increasing with the number of durability cycles, which contradicts the general assumption that the wet-dry process reduces the material integrity. The increase in unconfined compressive strength (UCS) (Fig. 2.30), flexural strength (FS) (Fig. 2.31), and flexural modulus (FM) (Fig. 2.32) were observed with the increase in the number of wet-dry cycles. The percentage increase in FM after 5, 10, and 15 wet-dry cycles were found to be 29%, 39%, and 53% approximately for 5% cement and 1%, 14%, and 17% for 9% cement compared to the specimens not subjected to wet-dry cycles. Similarly, the percentage increase in FS after 5, 10, and 15 wet-dry cycles were approximately 28%, 65%, 96% for 5% cement and 2%, 21%, and 29% for 9% cement from specimens not

subjected to wet-dry cycles. The percentage increase in UCS value for 7 days of cured specimens with 5% cement was 45%, 91%, and 102% after 5, 10, and 15 wet-dry cycles, respectively. For 28 days of cured specimens, this increase was 22%, 55%, and 68% respectively. Khoury and Zaman 2002, 2007; Zhang and Tao 2006 also show the effects of dry and wet cycles on soils stabilized with different materials.

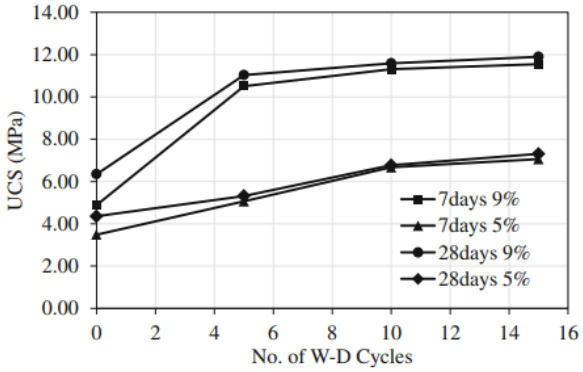

Figure 2.30 UCS values of 7-days- and 28-days-cured specimens subjected to W-D cycles (Beriha et al., 2018)

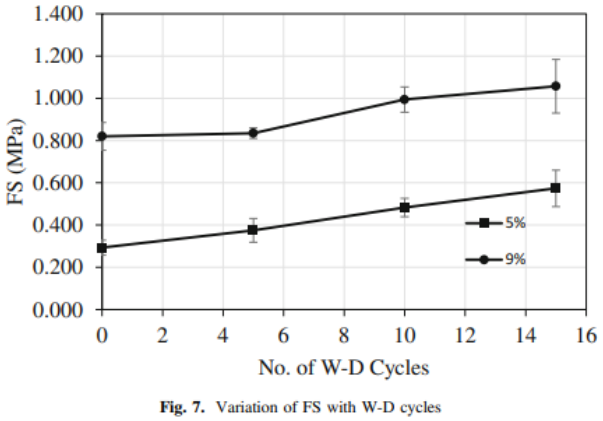

Fig. 7. Variation of FS with W-D cycles

Figure 2.31 Variation of FS with W-D cycles (Beriha et al., 2018)

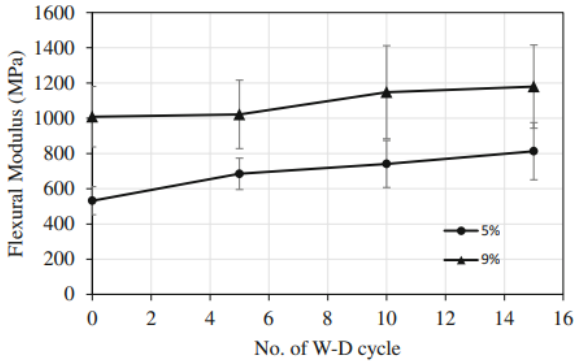

Figure 2.32 Variation of FM with W-D cycles (Beriha et al., 2018)

Ye et al., 2018 present experimental studies on the drying-wetting cycle characteristics of expansive soils improved by industrial wastes. The authors investigated the evolution of the unconfined compression strength and the Atterberg limits under drying-wetting cycling conditions for specimens treated by iron tailing sands and calcium carbide slag. The results showed that the unconfined compressive strength of the treated specimen initially increased and then decreased to reach a stable state with the continuous drying-wetting process (Fig 2.33). An exponential relationship was established to describe the evolution of the unconfined compressive strength with the drying-wetting cycle. The liquid limit and plastic index of the specimen increased initially followed by a decreasing trend, while a reverse trend was observed for that of the plastic limit during the drying-wetting process. The critical α_{CCS} of 10% was determined as the optimal value for the improvement of the expansive soils by mixing with the industrial wastes, which implies the minimum effect of drying-wetting cycles on the properties of the specimen.

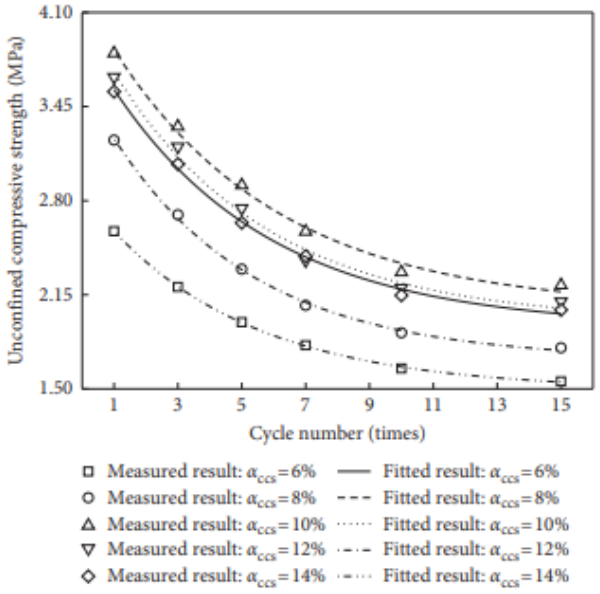

Figure 2.33 Relationships between the unconfined compressive strength and the number of drying-wetting cycles (Ye et al., 2018)

2.8.4 Effects of Conventional Flow for Laboratory Mixtures on PSAS-treated Soil

Like other soil stabilization materials PSAS-treated soil might have effects on pre-compaction curing, crumbling or post-compaction curing. Watanabe et al., 2021 proposed a new mixture design approach for paper sludge ash-based stabilizers (PSAS) to treat potential irrigation earth dam materials with high water contents. The study evaluated the effects of PSAS on the compaction and mechanical characteristics of coarse-grained soils to use them as materials for irrigation earth dams. The results showed that the modified optimum water content of the treated samples was almost equal to the untreated samples. A new mixture design approach was proposed based on the compaction characteristics, which successfully demonstrated that the range in the PSAS addition amount required to attain the targeted compaction degree for the curing period can

be estimated without conducting compaction tests on the treated samples. Also, PSAS-treated soils do not always solidify; hence, they can be compacted in granular states, such as sand or gravel (Trung et al., 2021; Watanabe et al., 2021). Therefore, the effects of crumbling on PSAS-treated soils may differ from those on cement- or lime-treated soils.

Insufficient literature exists to comprehensively grasp the impact of pre-compaction curing, crumbling, and post-compaction curing on soils treated with Partially Saturated Alkali-Activated Slag (PSAS). Consequently, this research aimed to investigate the effects of pre-compaction curing conditions, followed by crumbling and post-compaction curing, on the physical, compaction, and strength properties of PSAS-treated soils. The study employed two distinct types of PSASs, each with varying water absorption and retention capabilities.

2.9 SUMMARY

This chapter provides background regarding this research. Recycling construction-generated soil is an important issue not only in Japan but also all over the world. Cement on lime is a commonly used material for treating construction-generated soil but for making an eco-friendly society, the use of sustainable materials like paper sludge ash-based stabilizers has been increased day by day. From this chapter, we get an idea about the problems in the existing literature on using paper sludge ash-based stabilizers.

References

Ahmad, S., Iqbal Malik, M., Bashir Wani, M., Ahmad, R., 2013. Study of Concrete Involving Use of Waste Paper Sludge Ash as Partial Replacement of Cement. IOSR J. Eng. 3, 6–15.

Andriexu, P., Benaben, J., Colombier, G., Dac Chi, N., Kobisch, R., Lefort, M., Leroux S., Morel, G., Paute, J., Renault, Dand Seigneur, D., 1998. Assises de chaussees en graves non traitees et materiaux traits aux liants hydrauliques et pouzzolaniques-guide d'application des norms pour le reseau routier national.

Al-Tabbaa, A. and Perera, A.S., 2005. State of practice report, UK stabilization/solidification treatment and remediation, part I: binders and technologies-basic principles. In Proceedings of the international conference on stabilization/solidification treatment, Cambridge, Taylor and Francis, pp. 365-385.

Beriha, B., Biswal, D. R., Sahoo, U. C., 2018. Effect of wet-dry cycles on mechanical strength properties of cement stabilized granular lateritic soil. In: Springer, Cham, International Congress and Exhibition" Sustainable Civil Infrastructures: Innovative Infrastructure Geotechnology." pp. 112-121.

Chen, L., Lin, D.F., 2009. Stabilization treatment of soft subgrade soil by sewage sludge ash and cement. Journal of Hazardous Materials. 162(1), pp.321–327.

Cikmit, A.A., Tsuchida, T., Takeyama, K., Hashimoto, R., Noguchi, T. and Kaya, K., 2021. Effects of primary curing and subsequent disturbances on strength development of steel slag-treated marine clay. Soils and Foundations, 61(5), pp.1287-1301.

Corinaldesi, V., Fava, G., Ruello, M.L., 2010. Paper mill sludge ash as supplementary cementitious material, in: 2nd International Conference on Sustainable Construction Materials and Technologies.

Dong, P.H., Hayano, K., Kikuchi, Y., Takahashi, H. and Morikawa, Y., 2011. Deformation and crushing of particles of cement treat granulate soil. Soils and Foundations, 51(4), pp.611-624.

Horpibulsk, S., Rachan, R., Suddeepong, A., Chinkulkijniwat, A., 2011. Strength development in cement admixed bangkok clay: Laboratory and field investigations. Soils Found. 51, 239–251. Horpibulsuk, S., Phetchuay, C., Chinkulkijniwat, A., Cholaphatsorn, A., 2013. Strength development in silty clay stabilized with calcium carbide residue and fly ash. Soils Found. 53, pp. 477–486.

Huang, Y., Zhu, W., Qian, X., Zhang, N. and Zhou, X., 2011. Change of mechanical behavior between solidified and remolded solidified dredged materials. Engineering Geology, 119(3-4), pp.112-119.

Imai, K., Hayano, K. and Yamauchi, H., 2020. Fundamental study on the acceleration of the neutralization of alkaline construction sludge using a CO2 incubator. Soils and Foundations, 60(4), pp.800-810.

Inasaka, K., Trung, N. D., Hayano, K., & Yamauchi, H.,2021. Evaluation of CO2 captured in alkaline construction sludge associated with pH neutralization. Soils and Foundations. 61(6), pp.1699-1707.

Japanese Geotechnical Society, 2006, Technical term dictionary on geotechnical engineering, Maruzen, 661.

Kato, Y., Ohmukai, N., Mochizuki, Y., Saito, E., Yoshino, H., 2005. Study on improvement of liquid mud by use of paper sludge ash, in: The 40th Japan National Conference on Geotechnical Engineering. Hakodate, pp. 677-678 (in Japanese).

Kawai, S., Hayano, K., Yamauchi, H., 2018. Fundamental study on curing effect and its factor on the strength deformation characteristics of PS ash-based improved soil. J. JSCE (C Geotech. 74, 306-317 (in Japanese).

Khoury, N. N., & Zaman, M. M., 2002. Effect of wet-dry cycles on resilient modulus of class C coal fly ash-stabilized aggregate base. Transportation research record. 1787(1), pp.13-21.

Khoury, N. N., & Zaman, M. M., 2007. Durability of stabilized base courses subjected to wet–dry cycles. International Journal of Pavement Engineering. 8(4), pp.265-276.

Kim, K., Park, S.W., Shin, H., Kang, B., Kim, T., 2015. New Innovations and Sustainability. A study on the applicability of coal ash mixture to reclamation. In 15th Asian Regional Conference on Soil Mechanics and Geotechnical Engineering, ARC. Asian Regional Conference on Soil Mechanics and Geotechnical Engineering,pp. 2078–2081.

Kitazume, M. and Satoh, T., 2003. Development of a pneumatic flow mixing method and its application to Central Japan International Airport construction. Proceedings of the Institution of Civil Engineers-Ground Improvement, 7(3), pp.139-148.

Kitazume, M., Hayano, K. and Hashizume, H., 2003. , Seismic stability of cement treated ground by tilting and dynamic shaking table tests . Soils and foundations, 43(6), pp.125-140.

Kamon, M., Boutouil, M., Jeoung, J. and Inui, T., 2003. Microstructure and leaching characteristics of sludge treated with low alkalinity additives. Soils and foundations, 43(2), pp.105-114.

Lo, S-C & Wardani., Sri Prabandiyani., 2011. Strength and dilatancy of a silt stabilized by a cement and fly ash mixture. Canadian Geotechnical Journal. 39, pp.77-89.

Makino, M., Takeyama, T. and Kitazume, M., 2015. The influence of soil disturbance on material properties and micro-structure of cement-treated soil. Lowland Technology International, 17(3), pp.139-146.

Maher, A., Bennert, T., Jafari, F., Douglas, W.S. and Gucunski, N., 2004. Geotechnical properties of stabilized dredged material from New York-New Jersey Harbor. Transportation research record, 1874(1), pp.86-96.

Ministry of Land, Infrastructure, Transport and Tourism (MLIT). Standard for Utilization of Generated Soil, 1st ed, Committee for the Revision of Standard for Utilization of Generated Soil: Tokyo, Japan, 2007, pp. 2–3.

Miyashita, Y., Sanjeewani, D., Kuwano, R., 2019. Effect of curing conditions on long term mechanical property of improved surplus soils. E3S Web of Conferences. E3S Web conference 92. 92.

Mochizuki, Y., Yoshino, H., Saito, E., Ogata, T., 2003. Effects of soil improvement due to mixing with paper sludge ash. In Proceedings of China–Japan geotechnical symposium.

Mochizuki, Y., 2019. Evaluation of water absorption performance of various PS ashes produced with different incineration methods and its applicability for mud improvement. Journal of Japan Society of Civil Engineers, Ser. C (Geosphere Engineering), 75(2), pp.155-166.

Nabeshima, Y., 2015. New Innovations and Sustainability. Soil improvement of tsunami sediment soil by steel slug and concrete sludge. In 15th Asian Regional Conference on Soil Mechanics and Geotechnical Engineering, ARC. Asian Regional Conference on Soil Mechanics and Geotechnical Engineering, pp. 1884–1887.

Nakao, K., Shakya, S., Nozaki, T. and Inazumi, S., 2023. Neutralization Treatment for Recycling Construction-Generated Soils. Applied Sciences, 13(11), pp.6622.

Oh, M., Yoon, G.L., Yoon, Y.W., 2015. New Innovations and Sustainability. Evaluation on the compressive strength of dredged soil-steel slag. In 15th Asian Regional Conference on Soil Mechanics and Geotechnical Engineering, ARC. Asian Regional Conference on Soil Mechanics and Geotechnical Engineering, pp. 298–301.

Phan, N.B., Hayano, K., Mochizuki, Y., Yamauchi, H., 2021. Mixture design concept and mechanical characteristics of PS ash–cement-treated clay based on the water absorption and retention performance of PS ash. Soils and Foundations. 61(3), pp.692–707.

Rahmat, M.N., Kinuthia, J.M., 2011. Effects of mellowing sulfate-bearing clay soil stabilized with wastepaper sludge ash for road construction. Eng. Geol. 117, 170–179.

Rogers, C.D.F. and Glendinning, S.,1993. Modification of clay soils using lime. In C. a. Rogers (Ed.), Proceeding of the Seminar held at Loughborough University on Lime Stabilization ,pp. 99-114). London: Thomas Telford.

Sato, A., Hatakeyama, O., 2021. Influence of preparation conditions on solidified crushed soil characteristics and strength. International Journal of GEOMATE. 20(79), pp.48–55.

Segui, P., Aubert, J.E., Husson, B., Measson, M., 2012. Characterization of wastepaper sludge ash for its valorization as a component of hydraulic binders. Appl. Clay Sci. 57, pp.79–85.

Sherwood, P., 1993. Soil stabilization with cement and lime. State of the Art Review London: Transport Research Laboratory, HMSO.

Siham, K., Fabrice, B., Edine, A.N. and Patrick, D., 2008. Marine dredged sediments as new materials resource for road construction. Waste management, 28(5), pp.919-928.

Tani, S., Fukushima, S., Kitajima, A., Nishimoto, K., 2006. Applicability of cement-stabilized mud soil as embankment material. Journal of ASTM International. 3(7).

Tang, Y.X., Miyazaki, Y., Tsuchida, T., 2001. Practices of reused dredgings by cement treatment. Soils Found. 41, pp. 129–143.

Trung, N. D., Ogasawara, T., Hayano, K., & Yamauchi, H., 2021. Accelerated carbonation of alkaline construction sludge by paper sludge ash-based stabilizer and carbon dioxide. Soils and Foundations, 61(5), pp.1273-1286.

Trung, N. D., Ogasawara, T., Hayano, K., & Yamauchi, H., 2021. Accelerated carbonation of alkaline construction sludge by paper sludge ash-based stabilizer and carbon dioxide. Soils and Foundations, 61(5), pp. 1273-1286.

Vichan, S., Rachan, R., 2013. Chemical stabilization of soft Bangkok clay using the blend of calcium carbide residue and biomass ash. Soils and Foundations. 53(2), pp. 272–281.

Watanabe, Y., Nguyen Binh, P., Hayano, K., Yamauchi, H., 2021. New mixture design approach to paper sludge ash-based stabilizers for treatment of potential irrigation earth dam materials with high water contents. Soils and Foundations. 61(5), pp. 1370–1385.

Ye, H., Chu, C., Xu, L., Guo, K., Li, D., 2018. Experimental studies on drying-wetting cycle characteristics of expansive soils improved by industrial wastes, Advances in Civil Engineering 2018(3), pp.1-9.

Zhang, Z., Tao, M., 2006. Durability of cement stabilized low plastic soils. In: Transportation Research Board 2006 Annual Meeting, CD-ROM Publication, Transportation Research Board, National Research Council, Washington DC. 06-1255.Z.

CHAPTER 3

MATERIALS SELECTION

3.1 INTRODUCTION

This chapter presents a comprehensive analysis of the materials utilized in the study to investigate the properties of construction-generated soil. To prepare construction-generated soil-type material which contains high water content, clay was used, and two distinct types of clay were selected based on their liquid limit, as classified by the ASTM-D2487 (Unified soil classification system). These clay types are identified as Ao clay, characterized by a low liquid limit, and Kasaoka clay, which possesses a high liquid limit. For the purpose of stabilizing the clay, two variations of paper sludge ash-based stabilizers (PSASs) were introduced in the study based on their water absorption and retention rate. Alongside these PSASs, a familiar stabilizer widely used in soil stabilization, cement, was also included for comparison. The specific type of cement chosen for the treatment of clay is Blast furnace cement type B (BFCB).

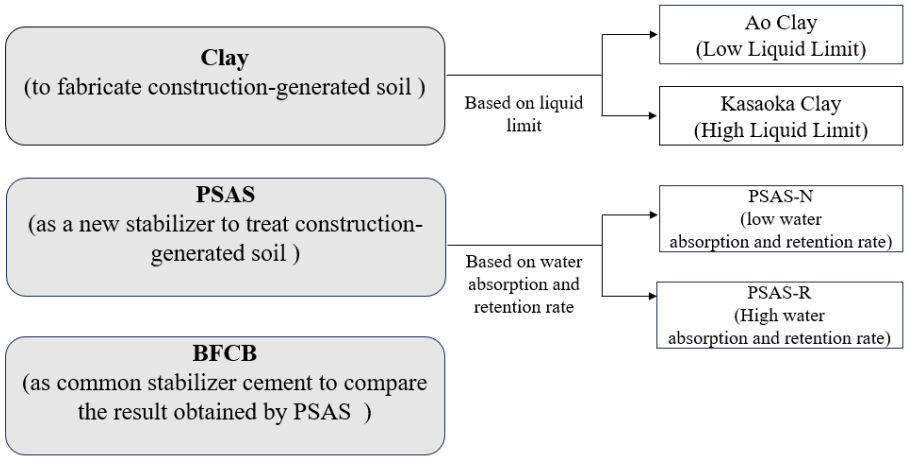

Figure 3.1 Materials for the study

Throughout this chapter, a detailed exposition of the material properties used in the research is presented, shedding light on the characteristics and potential applications of each stabilizer and clay type.

3.2 TYPES OF CLAY

3.2.1 Ao Clay

Ao clay, kind of clay that is frequently utilized in Japanese laboratories, was chosen for this study to examine the impact of pre-compaction curing conditions, subsequent crumbling and durability (post-compaction curing effects) on the properties of compacted soils stabilized with Paper sludge ash-based stabilizers. To prepare construction-generated soil Ao clay was used. Ao clay is a grey powder-like material consisting of 10.8% sand, 61.7% silt and 27.5% clay. Table 3.1 lists the chemical compositions of Ao clay. From the chemical component composition, it is found Ao clay contains 56.96% of SiO_2. The other main components are Fe_2O_4 (15.41%) & Al_2O_3 (15.27%).

Table 3.1 The chemical composition of Ao clay

SiO_2	Fe_2O_4	Al_2O_3	K_2O	CaO	TiO_2	MgO	P_2O_5	MnO	others
56.96	15.41	15.27	4.41	2.83	1.54	2.36	0.54	0.31	0.56

The Ao clay is classified as CL (clay (low liquid limit)) by the Unified Soil Classification System (ASTM-D2487). The Japanese Geotechnical Society standards (JGS 0131) were used to evaluate the Ao clay's PSD, which is depicted in Fig. 3.2.

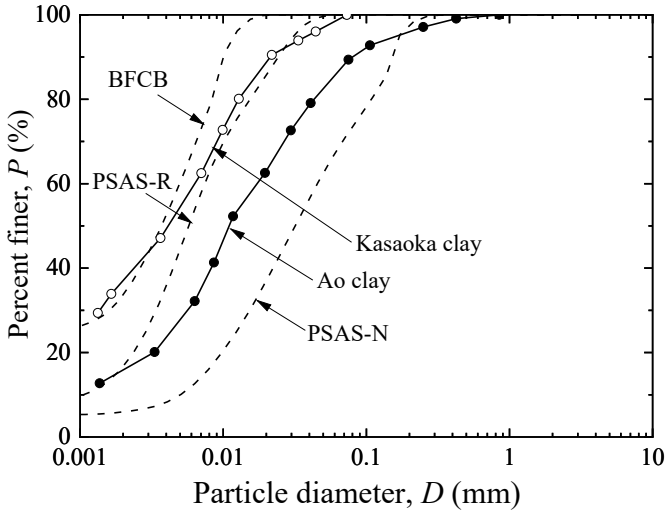

Figure 3.2 PSD of materials of this study

3.2.2 Kasaoka Clay

Another type of clay, Kasaoka clay, was chosen for this study to examine the impact of pre-compaction curing conditions, subsequent crumbling and durability (post-compaction curing) on the properties of compacted soils stabilized with Paper sludge ash-based stabilizers. Kasaka clay is a powder-like material. Compared with Ao clay, it is more finer as shown in Fig.3.2. Table 3.2 lists the chemical compositions of Kasaoka clay. From the chemical component composition, it is found Kasaoka clay contains 69.07 % of SiO_2. The other main components are Fe_2O_4 (5.46 %) & Al_2O_3 (20.22 %).

Table 3.2 Chemical Component Compositions of Kasaoka Clay

SiO_2	Fe_2O_3	Al_2O_3	K_2O	CaO	TiO_2	MgO	MnO	others
69.07	5.46	20.22	2.75	0.91	0.63	0.81	0.03	0.12

3.3 PAPER SLUDGE ASH BASED STABILIZERS (PSAS)

Soil stabilization using paper sludge ash-based stabilizers (PSASs) has also been developed, as a use of sustainable materials generated from industrial processes. PSASs can be produced by insolubilizing heavy metals in original paper sludge (PS) ash particles, i.e., the wastes generated by the incineration of the PS discharged from paper mills. The surface shape of a PS ash particle has a porous structure with many complex irregularities and voids, as described in previous chapter

2. The capillary action on these open micropores physically rapidly absorbs the free water in the soil, and the meniscus strongly holds the water within the particles. Owing to this characteristic, PS ash can absorb and retain the excess water in soils. Owing to the reduction in the free water, a PSAS can simultaneously improve the stability of mud and sludge when it is mixed with them.(Mochizuki et al., 2003; Shigematsu et al., 2010; Elias, 2015).

3.3.1 Different Types of PSAS

Paper sludge ash-based stabilizer (PSAS) which is used frequently in Japan was used to treat construction-generated soil specimens prepared with Ao clay or Kasaoka clay. Since PSAS is made by insolubilizing heavy metals in the original PS ash, it has properties resembling those of the initial PS ashes while being environmentally beneficial. The PSASs fall under the NP category (non-plastic). Based on the method of manufacturing, the properties of PSASs are not exactly identical. Especially, water absorption and retention rate differs based on their chemical properties. Based on a previous study by, Phan et al. (2021), in this study, two types of PSASs are used which have different water absorption and retention rate which will be discussed in the next section in detail. The two PSASs were denoted as PSAS-N and PSAS-R, and both were produced by insolubilizing heavy metals in the original PS ash particles. However, the type of original PS ash used differed between PSAS-N and PSAS-R. The ρ_s of PSAS-N and PSAS-R were 2.603 and 2.840 g/cm^3, respectively. The appearance of PSAS-N and PSAS-R is not the same. PSAS-N is a grey powder-like material whereas PSAS-R is a white powder-like material.

Table 3.3 Chemical Component Compositions of PSASs (PSAS-N & PSAS-R)

(a) PSAS-N

CaO	SiO_2	Al_2O_3	SO_3	Fe_2O_4	TiO_2	MgO	P_2O_5	others
63.89	13.55	6.89	6.06	3.27	2.99	1.31	0.95	1.09

(a) PSAS-R

CaO	SiO_2	Al_2O_3	SO_3	Fe_2O_4	TiO_2	MgO	P_2O_5	others
72.49	11.42	8.43	3.07	1.01	1.34	1.48	0.55	0.23

Table 3.3 shows the chemical component compositions PSAS-N and PSAS-R. For two of them, CaO is the main chemical component although for PSAS-R CaO is a little higher compared with PSAS-N. As CaO is present among both PSASs, the two PSASs were expected to undergo hydration reactions when combined with water, although the reactions were not the same as those of the cement commonly used for stabilizing construction-generated soil. This was because when the cement is mixed with the construction-generated soil, the strength development of the treated soils occurred through a hydration reaction, such as a pozzolanic reaction. In contrast, for the two PSASs, the excess water in the construction-generated soil was physically absorbed by the porous structures of the PS ash particles and subsequently chemically used to generate hydrates such as

ettringite during curing (Kawai et al., 2018). Both PSAS-N and PSAS-R are very fine clay-like materials. The PSD of the PSASs could not be obtained by the sieve analysis according to the JGS 0131. Owing to their hydration progress, the soil particle size test according to JGS 0131 was not conducted on PSAS-N and PSAS-R. Instead, the PSDs of the PSAS- N and PSAS-R were obtained using a laser diffraction-type PSD-measuring device that used ethanol as the solvent instead of an aqueous solution. The particle size of PSAS-R was smaller than that of PSAS-N as shown in figure 3.2.

3.3.2 Water Absorption and Retention Performances of PSAS

As described in the previous section, PSASs have recently attracted interest as mud stabilizers owing to their water absorption and retention performance. However, the water absorption and retention performances of PSASs differ owing to the differences in the particle size and chemical composition of each PSAS (Mochizuki et al., 2003). As in this study, the two types of PSAS used, PSAS-N & PSAS-R is different in particle size and chemical component composition, therefore, it is important to evaluate the water absorption and retention performance of each type of PSAS. Based on this, Phan et al. (2021) recently developed a new testing method for investigating the water absorption and retention performances of PSASs. In this study, the water absorption and retention performances of PSAS-N and PSAS-R were investigated using this method. The details for choosing this method are mentioned in Chapter 2.

The water absorption and retention evaluation test described above was conducted three times for the samples prepared under the same conditions. Figure 3.3 shows the test results for PSAS-N and PSAS-R. The results of three tests are shown for each case. As shown in the figure, there was little variation, with a maximum coefficient of variation of 3.67%.We observed that the water content of the two PSASs increased with the curing time. However, the rate of increase gradually decreased as the curing time increased. According to Phan et al. (2021), to eliminate the amount of free water in the voids trapped by the suction, the difference between the measured water content of the PSAS and that of sand or glass beads (= 22%) could be evaluated as the actual water absorption and retention ratio (W_{ab}) of the PSASs. Here, W_{ab} was defined as the ratio of the mass of the absorbed and retained water to the dry mass of the PSAS.

As shown in Table 3.4, the W_{ab} values were estimated for PSAS-N and PSAS-R after 45 min, 24 h, and 72 h of curing. The results shown in Table 3.4 indicate that PSAS-R had higher water absorption and retention performance from the early stage than PSAS-N. This may be attributed to the differences in the particle size and CaO content between PSAS-N and PSAS-R, as mentioned earlier. From Table 3.4, it was observed, for up to 24 hours, water absorption and retention quantity of both types of PSASs changed.

Phan et al. (2021), divided this water absorption and retention performance into two stages. Initially, water primarily underwent physical absorption, with limited chemical absorption. However, as the curing time progressed, PSAS particles expanded and continued physical absorption while sticking together, facilitated by the formation of the hydrated compound ettringite. This phenomenon bears similarities to the creation of ettringite in Portland cement concrete, where

sulfate compounds react with calcium aluminate upon mixing with water to generate ettringite within a few hours. Over time, absorption which was done physically decreased, while absorption

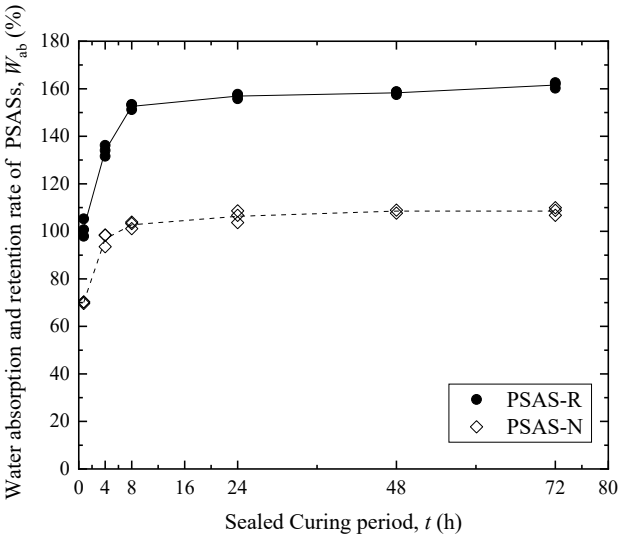

Figure 3.3 Change in water content of the PSAS-N and PSAS-R with the sealed curing period derived from water absorption and retention evaluation tests

Table 3.4 Estimated Water Absorption and Retention Ratio (W_{ab}) of the Two PSASs

Water absorption and retention ratio, W_{ab} (%)	Sealed curing period of the PSAS		
	45 min	24 h	72 h
PSAS-N	54.2	85.6	85.6
PSAS-R	86.4	137.1	137.3

due to chemical formation increased. The PSAS particles during hydration hardened and gradually stopped expanding volume to carry out physical absorption. Until the completion of hydration, chemical absorption was still functioning. Although it can be challenging to distinguish between physical and chemical absorption during the process, it can be assumed from experimental findings that PSAS's absorption and retention quantity was primarily influenced by its physical absorption during first few hours and primarily by chemical absorption during the longer curing period. To ensure the existence of ettringite in the following part SEM analysis was conducted.

3.4 BLAST FURNANCE CEMENT TYPE B (BFCB)

Blast furnace cement is also known as slag cement. It is one type of hydraulic cement which is manufactured by blending ground granulated blast furnace slag with Portland cement clinker. It is known as Type B cement in ASTM C595/C595M. This one is the standard specification for blended hydraulic cement. As it contains a hydraulic compound, it has some special chemical properties. It increases the strength of construction-generated soils because it contains hydraulic

compounds that react with water to form cementitious materials. It is one of the common materials to treat construction-generated soils. In this research, different properties of construction-generated soils were investigated by treating the soil with different types of PSASs. Then the result was compared with BFCB. The particle density, ρ_s for BFCB is 3.04 g/cm^3. Figure 3.2 shows the particle size distribution of BFCB. Compared with PSASs, BFCB contains finer particles. Like PSASs, due to hydration progress, the soil particle size test in accordance with JGS 0131 was not carried out for BFCB. In its alternative, a laser diffraction-type PSD-measuring system that used ethanol as the solvent rather than an aqueous solution was used to obtain the PSDs of the BFCB. Table 3.5 lists the chemical component composition of BFCB. Here, CaO is the major content for BFCB. The amount is 65.57% which is very close to the PSASs used for this research.

Table 3.5 Chemical Component Compositions of BFCB

CaO	SiO_2	Al_2O_3	SO_3	Fe_2O_4	MgO	TiO_2	MnO	P_2O_5	others
65.57	19.07	5.26	3.98	2.91	1.98	0.60	0.17	0.23	0.23

3.5 SEM IMAGE OF STABILIZERS

In the previous section, we showed how the water absorption and retention performance changes with different curing periods in the case of different PSASs (PSAS-N & PSAS-R). It is because, in the beginning, the majority of the water was absorbed via the physical process, whereas the chemical process did not work very well. Because of the development of hydrated compound ettringite, the PSAS particles expanded in volume as the curing period increased, which allowed them to continue their performance of physical absorption. To understand this two-stage water absorption mechanism more clearly, we further conducted SEM image analysis.

Figure 3.4 shows scanning electron microscope (SEM) images of the particles of each stabilizer used in this research (PSAS-N, PSAS-R, BFCB). In the case of PSAS-N and PSAS-R, we found porous structures. On the other hand, for BFCB no such kind of porous structures were observed. So at the beginning of the curing period, when water is added to PSASs, they are absorbed by these pores which are different from BFCB.

Meanwhile, as shown in Tables 3.3 and 3.5, the chemical component composition of PSASs and BFCB shows that all stabilizers contain an almost similar amount of CaO. We already know that, in the case of BFCB, when it is mixed with water, hydration reactions occur. It is anticipated, as PSASs contain CaO like BFCB when they are coupled with water, they will undergo similar types of hydration reactions. Figure 3.5 shows the SEM images of each stabilizer after curing in water. Crystals, including needle-like crystals that appeared to be ettringite, were observed in all types of stabilizers (PSASs & BFCB). This finding suggests that PSAS-N and PSAS-R are involved in the chemical absorption of water and the retention of that water in the soil through the creation of hydrates.

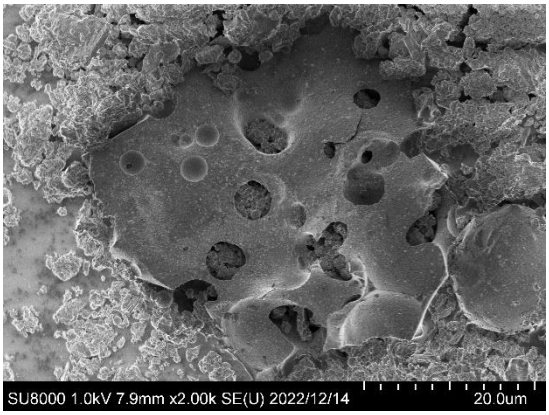

(a) PSAS-N

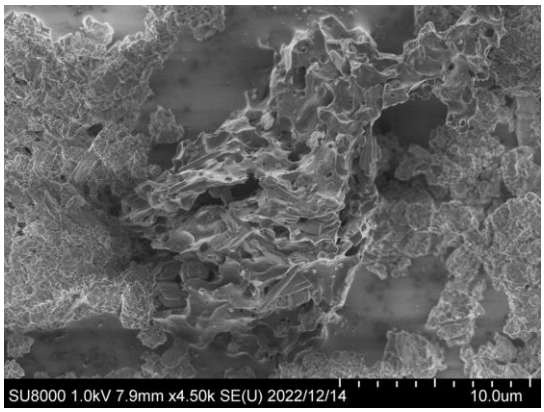

(b) PSAS-R

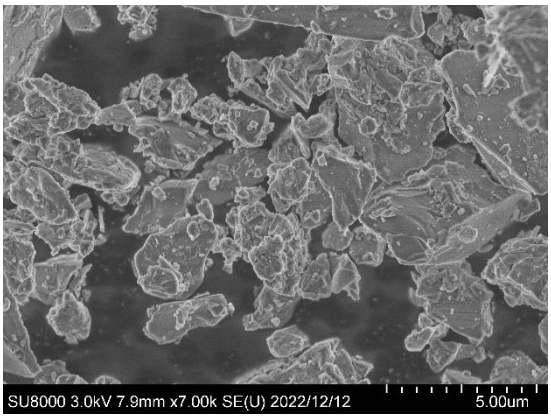

(c) BFCB

Figure 3.4 Examples of SEM images of particles of each type of stabilizer

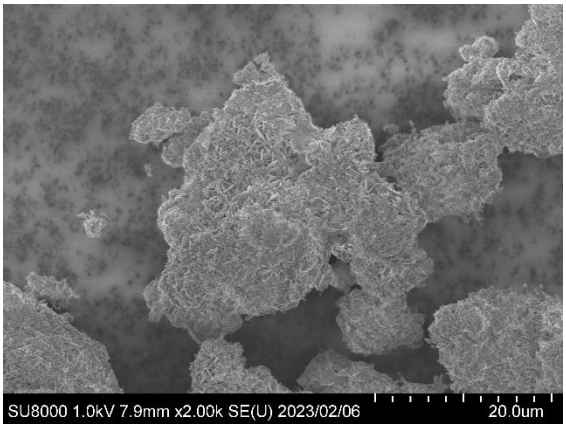

(a) PSAS-N

(b) PSAS-R

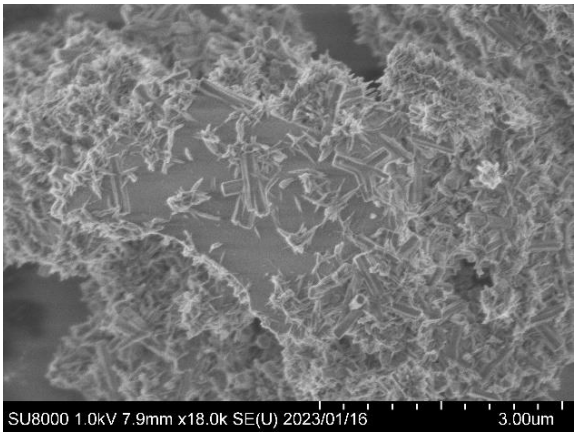

(c) BFCB

Figure 3.5 Examples of SEM images of hydrated particles of each type of stabilizer

3.6 SUMMARY

This chapter provides a description of the materials used in this research. Appearance, chemical component composition, different geotechnical properties and particle size distribution of Ao clay, Kasaoka clay, two types of PSASs and BFCB is included in this chapter. Further, this chapter clarifies the water absorption mechanism of PSASs, which are used in this research.

References

ASTM D2487-06.Standard Practice for Classification of Soils for Engineering Purposes (unified Soil Classification System)

Dong, P.H., Hayano, K., Kikuchi, Y., Takahashi, H. and Morikawa, Y., 2011. Deformation and crushing of particles of cement treat granulate soil. Soils and Foundations, 51(4), pp.611-624.

Elias, N., 2015. Strength development of soft soil stabilized with waste paper sludge. International Journal of Advanced Technology in Engineering and Science, 3(1), pp.141-149.

Japanese Geotechnical Society Standards, JGS 0131–2009: Test method for particle size distribution of soils. JGS, Tokyo, Japan.

Kawai, S., Hayano, K. and Yamauchi, H., 2018. Fundamental study on curing effect and its mechanism on the strength characteristics of PS ash-based improved soil. Journal of Japan Society of Civil Engineers, Ser. C (Geosphere Engineering), 74(3), pp.306-317.

Mochizuki, Y., Yoshino, H., Saito, E. and Ogata, T., 2003. Effects of soil improvement due to mixing with paper sludge ash. In Proceeding of China-Japan Geotechnical Symposium (pp. 1-8).

Nakase, A. and Kamei, T., 1986. Influence of strain rate on undrained shear characteristics of K0-consolidated cohesive soils. Soils and Foundations, 26(1), pp.85-95.

Phan, N.B., Hayano, K., Mochizuki, Y. and Yamauchi, H., 2021. Mixture design concept and mechanical characteristics of PS ash–cement-treated clay based on the water absorption and retention performance of PS ash. Soils and Foundations, 61(3), pp.692-707.

Shigematsu, H., Demura, Y., Otomo, M. and Fujiwara, Y., 2008. Stabilization of poor soil by paper sludge mixing. In Advances in Transportation Geotechnics (pp. 699-706). CRC Press.

CHAPTER 4

EFFECTS OF PRE-COMPACTION CURING CONDITIONS AND SUBSEQUENT CRUMBLING

4.1 INTRODUCTION

In Chapter 1, the conventional flow of laboratory mixture design for soils stabilized with cement-based materials is described. Pre-compaction curing in this flow is recommended to keep it as short as possible. A lengthy curing period prior to compaction inhibits the formation of hydrates during pre-compaction curing. Crumbling is regarded as a type of disturbance that weakens soil strength. No guideline for the conventional flow of laboratory mixture design experiments for treating construction-generated soil with PSAS-based stabilizers is provided in the existing literature. This chapter clarifies the effects of pre-compaction curing conditions and the ensuing effects of crumbling on PSAS-treated soil which are the first and second objectives of this research.

4.2 SAMPLE PREPARATION AND TESTING METHOD

To understand the effect of pre-compaction curing conditions and subsequent crumbling samples were prepared. The steps involved in the process of sample preparation are shown in Fig 4.1, beginning with sample preparation and progressing through primary curing, crumbling, compaction, and secondary curing before ending with cone index tests. The classification of construction-generated soil (mentioned in Chapter 2) is based on cone index strength. That's why, to understand the effect of pre-compaction curing conditions and subsequent crumbling on strength developments of treated samples, cone index tests were chosen. From the process of sample preparation flow, it is seen before the compaction, water content, w of all the samples were measured. Further, after the crumbling, sieve analysis was performed and also before sieve analysis samples water content, w of all the samples was measured. The entire procedure (Fig. 5.1) will be discussed in this section step by step for different types of samples.

Table 4.1 summarizes the mixture ratios of the treated samples used in this study. For making construction-generated soil in laboratory conditions, the initial water content of Ao clay should be set at w = 40.7%, which is equivalent to the liquid limit (w_L). After that, in order to prepare the PSAS-treated samples, either the PSAS-N or the PSAS-R with Ao clay at a dry mass ratio of 20% was combined. On the other hand, in order to prepare the BFCB-treated samples, the BFCB with Ao clay at a dry mass ratio of 6% was mixed. The ratio of PSASs and BFCB was chosen based on previous experiments. It needs to be mentioned the strength development mechanism due to the pre-compaction curing is not controlled by this % of dry mass ratio of the stabilizer.

Each sample was combined for ten minutes using a small kitchen mixer in a vessel Fig 4.2 (a). The dimensions of this vessel are 220 mm in diameter and 190 mm in depth. At a rate of 105 revolutions per minute, a paddle shown in Fig 4.2 (b) measuring 135 mm across and 115 mm in height was employed to agitate each sample. As appears in Fig 4.1, crumbling was not done to the samples when the condition of the sample stated that pre-compaction curing was not necessary. After the samples were prepared, the water content (w) was measured right away, and then the

uncrumbled samples were compacted into molds. For compaction, Japanese Geotechnical Society Standards JGS, 0716 was followed. Each sample was positioned in a mold, as shown in Fig 4.3 (a) with a diameter of 10 centimetres by first splitting the sample into three equal layers.

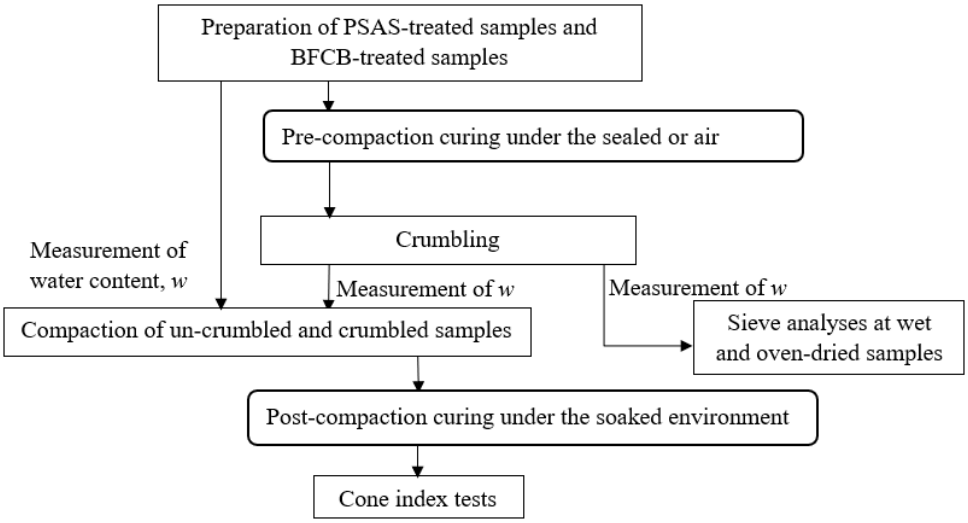

Figure 4.1 Flow of the process from sample preparation, pre-compaction curing, crumbling, compaction, and post-compaction curing to index tests

Table 4.1 Mixture ratios for PSAS-treated and BFCB-treated samples with Ao clay

Sample type	The water content of Ao clay, w (%)	Addition ratio of PSAS-N or PSAS-R, A_{PS} (%)	Addition ratio of BFCB, A_{BFCB} (%)
PSAS-treated samples (PSAS-N-treated samples, PSAS-R-treated samples)	40.7 ($w = w_L$)	20	0
BFCB-treated samples		0	6

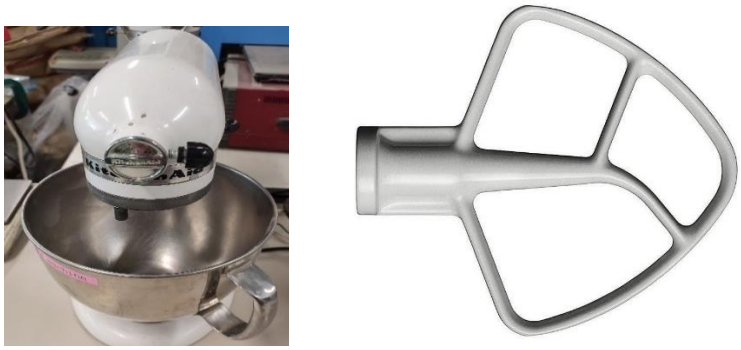

(a) (b)

Figure 4.2 Instruments used for sample mixing and crumbling

Subsequently, each layer was added to the mold in order and compressed 25 times using a hammer with a weight of 2.5 kilograms dropped from a height of 30 cm as shown in Fig 4.3. Water content, w was used to determine the dry density (ρ_d) of each compacted sample as well as the degree of saturation (Sr) of each sample. The experimental flow for the samples, where no pre-compaction curing was required is shown in Fig 4.4.

Figure 4.3 Instruments used for Compaction

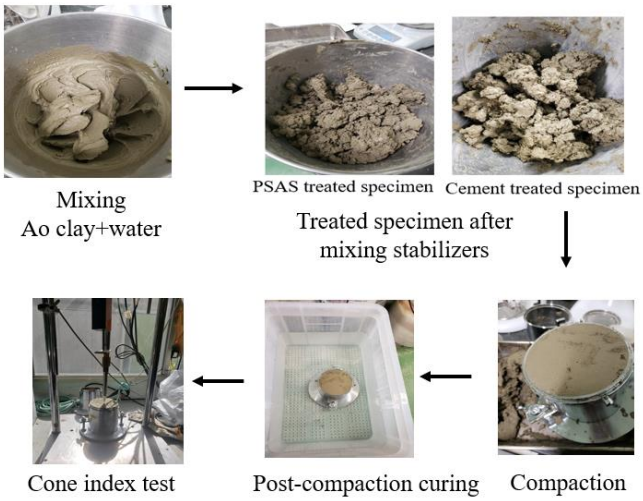

Figure 4.4 Sample preparation flow for samples with no pre-compaction curing

If, on the other hand, pre-compaction curing was required, the produced samples were cured for either one or three days before being crumbled. The pre-compaction curing was carried out in two distinct environments: a sealed environment and an air-cured environment. The result obtained from sealed curing showed the effects of crumbling while results obtained from air curing showed the effects of pre-compaction curing. The experimental flow for the samples, where pre-compaction curing was conducted in a sealed or air curing environment is shown in Fig 4.5 and 4.6. When the samples were ready, they were placed in zip-lock bags for the process of sealed curing (Fig. 4.5), whereas for air curing, they were placed in uncovered trays (Fig. 4.6). Both the air curing and the sealed curing were carried out at indoor temperature 20 ±1 °C. During the process of air-curing, there was no regulation of humidity control as humidity control is not required for the cone index test. But as all experiments were conducted in the summer season and room temperature is controlled by the air conditioner. By setting the air conditioner to a specific temperature and running it regularly, can effectively control the humidity levels in a room. After a predetermined amount of time had passed for the pre-compaction curing process (t_1), the samples

were crumbled. Using the compact kitchen mixer, the crumbling process took place for two minutes. In order to get the desired crumbling effect, the paddle was rotated at a rate of 78 times per minute. The process of crumbling the samples resulted in the treated soils, transforming into fragmented granules, which led to a change in the

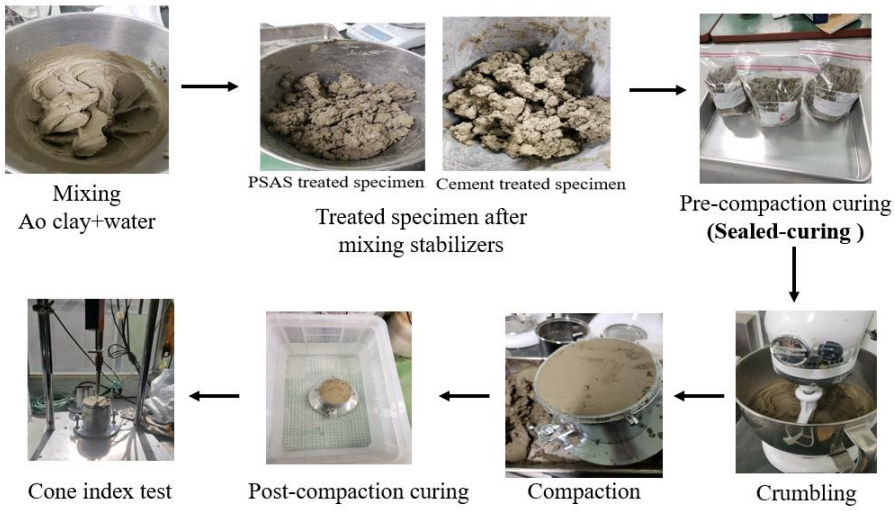

Figure 4.5 Sample preparation flow for samples with pre-compaction curing in a sealed environment

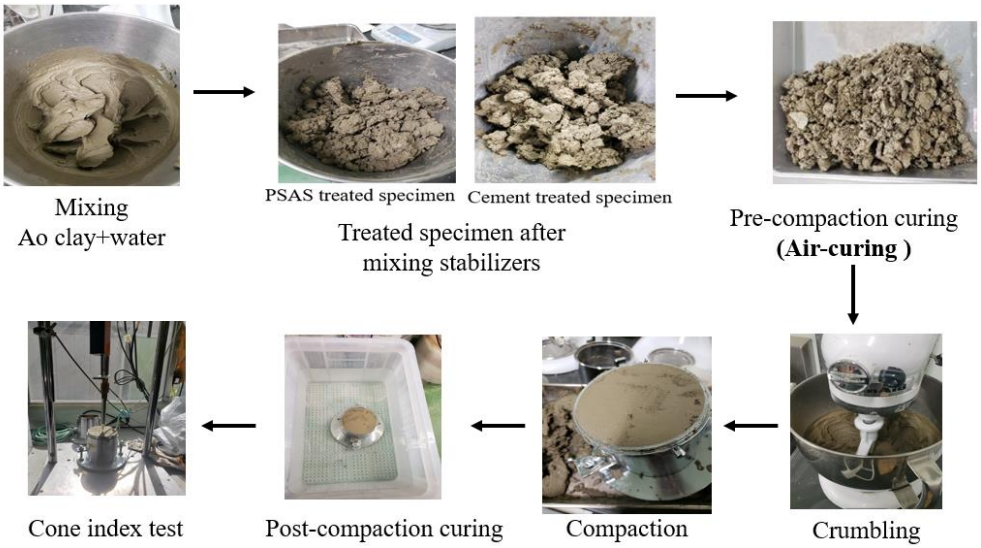

Figure 4.6 Sample preparation flow for samples with pre-compaction curing in the air environment

appearance of the samples. The variations in the appearance of the PSAS-N-treated and BFCB-treated samples that were predominantly cured for one day in either a sealed or air environment are depicted in Fig 4.7 and 4.8, respectively. Before they crumble, the samples that were treated

Before crumbling After crumbling

(a) Pre-compaction curing for 1-day sealed condition

Before crumbling After crumbling

(b) Pre-compaction curing for 1-day air condition

Figure 4.7 Change in the appearance of the PSAS-N-treated samples after crumbling after primary curing

Before crumbling After crumbling

(a) Pre-compaction curing for 1-day sealed condition

Before crumbling After crumbling

(b) Pre-compaction curing for 1-day air condition

Figure 4.8 Change in the appearance of the BFCB-treated samples after crumbling after primary curing

with BFCB are more solidified than the samples that were treated with PSAS-N. This is demonstrated in Fig 4.7 and 4.8. Regardless of whether the treated samples were first cured in the air or in a sealed environment, the crumbling process results in the production of granules that resemble sand and gravel. Granules are also produced by the samples that have been treated with PSAS-R.

The treated samples were compacted into molds according to JIS A 1210 as soon as they were crumbled, and the process was carried out under the same conditions as in the previous section for when no pre-compaction curing was conducted. Using the crumbled sample's water content (w) measured according to according to JGS 0122,calculations were made to determine each compacted sample's dry density (ρ_d) as well as its degree of saturation (S_r). Because the crumbling was followed immediately by the compaction, the water content that was recorded during the crumbling was identical to that which was measured after the compaction tremed as water content at compaction.

During the post-compaction curing, all molds that contained treated samples were soaked in water, regardless of whether the curing had been performed or not. After being completely submerged in water, the mold was then allowed to cure in such a way that the water was in direct touch with the top surface of the specimen. During the time of secondary curing t_2 that was mandated, cone index tests were carried out in accordance with Japanese Geotechnical Society Standards JGS, 0716. A variety of post-compaction curing periods, which are detailed in Table 4.2, were used. In Table 4.2, the titles of the test cases show the kind of stabilizer, the type of pre-compaction curing, the duration of pre-compaction curing (or zero if there is no pre-compaction curing), and the duration of post-compaction curing. For instance, PSN-0-7 is a PSAS-N treated sample with no pre-compaction curing and a post-compaction curing length of 7 days, whereas PSR-S1-27 is a PSAS-R treated sample with one day of sealed pre-compaction curing and a post-compaction curing period of 27 days. The cone index (q_c) that was obtained for the samples that were treated with PSAS-N and PSAS-R is summarized in Table 4.3, and the cone index (q_c) that was obtained for the samples that were treated with BFCB is summarized in Table 4.4, along with the properties of measured moisture content (w), calculated dry density (ρ_d), as well as degree of saturation (S_r) for each test scenario.

Table 4.2 Curing conditions for PSAS-N-treated, PSAS-R-treated, and BFCB-treated samples

Test scenario name			Pre- compaction curing period (t_1) and environment	Post-compaction curing period (t_2) under the soaked environment	Total curing period ($t=t_1+t_2$)
PSAS-N-treated samples	PSAS-R-treated samples	BFCB-treated samples			
PSN-0-1	PSR-0-1	BF-0-1	Not Implemented	1	1
PSN-0-3	PSR-0-3	BF-0-3		3	3
PSN-0-7	PSR-0-7	BF-0-7		7	7
PSN-0-14	PSR-0-14	BF-0-14		14	14
PSN-0-28	PSR-0-28	BF-0-28		28	28
PSN-S1-2	PSR-S1-2	BF-S1-2	1-day sealed curing	2	3
PSN-S1-6	PSR-S1-6	BF-S1-6		6	7
PSN-S1-13	PSR-S1-13	BF-S1-13		13	14
PSN-S1-27	PSR-S1-27	BF-S1-27		27	28
PSN-S3-4	PSR-S3-4	BF-S3-4	3-day sealed curing	4	7
PSN-S3-11	PSR-S3-11	BF-S3-11		11	14
PSN-S3-25	PSR-S3-25	BF-S3-25		25	28
PSN-A1-2	PSR-A1-2	BF-A1-2	1-day air curing	2	3
PSN-A1-6	PSR-A1-6	BF-A1-6		6	7
PSN-A1-13	PSR-A1-13	BF-A1-13		13	14
PSN-A1-27	PSR-A1-27	BF-A1-27		27	28
PSN-A3-4	PSR-A3-4	BF-A3-4	3-day air curing	4	7
PSN-A3-11	PSR-A3-11	BF-A3-11		11	14
PSN-A3-25	PSR-A3-25	BF-A3-25		25	28

Table 4.3 Properties of compacted PSAS-N-treated and PSAS-R-treated samples before secondary curing and the cone index obtained after secondary curing

PSAS-N-treated scenario	w (%)	ρ_d (g/cm^3)	S_r (%)	q_c (kN/m^2)	PSAS-R-treated scenario	w (%)	ρ_d (g/cm^3)	S_r (%)	q_c (kN/m^2)
PSN-0-1	36.7	1.29	89.9	1404.3	PSR-0-1	35.6	1.34	93.3	5784.1
PSN-0-3	35.6	1.29	87.5	2026.8	PSR-0-3	35.1	1.30	86.8	6350.3
PSN-0-7	38.1	1.28	91.9	2314.8	PSR-0-7	35.0	1.28	83.8	6685.5
PSN-0-14	36.1	1.32	92.0	4758.2	PSR-0-14	37.9	1.29	93.3	7007.4
PSN-0-28	37.9	1.31	91.8	5144.2	PSR-0-28	36.2	1.32	85.4	7407.4
PSN-S1-2	36.4	1.32	93.9	1646.1	PSR-S1-2	34.9	1.24	74.1	4718.7
PSN-S1-6	35.9	1.34	94.9	2191.4	PSR-S1-6	36.6	1.21	73.4	5219.6
PSN-S1-13	35.4	1.30	87.7	4691.4	PSR-S1-13	36.2	1.19	69.9	5249.0
PSN-S1-27	35.9	1.28	95.9	5080.4	PSR-S1-27	36.3	1.22	72.3	7307.4
PSN-S3-4	36.3	1.32	93.3	2067.9	PSR-S3-4	36.7	1.19	63.4	4024.0
PSN-S3-11	35.8	1.27	85.4	4372.4	PSR-S3-11	35.4	1.23	66.1	5249.7
PSN-S3-25	35.8	1.28	93.3	4867.9	PSR-S3-25	36.2	1.24	64.8	6198.6
PSN-A1-2	23.1	1.29	57.0	2417.7	PSR-A1-2	31.1	1.26	69.7	4114.6
PSN-A1-6	26.0	1.33	68.1	3112.1	PSR-A1-6	31.5	1.28	77.6	5160.7
PSN-A1-13	25.9	1.34	68.8	7407.4	PSR-A1-13	30.9	1.25	71.8	5661.7
PSN-A1-27	26.3	1.33	68.9	8127.9	PSR-A1-27	31.3	1.27	73.4	6275.72
PSN-A3-4	13.8	1.28	33.4	1903.3	PSR-A3-4	26.5	1.27	60.6	5594.6
PSN-A3-11	14.1	1.34	37.1	5761.3	PSR-A3-11	26.1	1.29	59.0	6640.5
PSN-A3-25	13.0	1.26	37.6	6327.4	PSR-A3-25	26.2	1.28	59.6	6678.9

w: Water content at the crumbling and/or the compaction
ρ_d: Dry density at compaction
S_r: Saturation degree at the compaction
q_c: Cone index of the compacted sample after the soaked curing

Table 4.4 Properties of compacted BFCB-treated samples before secondary curing and the cone index obtained after secondary curing

BFCB-treated scenario	w (%)	ρ_d (g/cm^3)	S_r (%)	q_c (kN/m^2)
BF-0-1	40.4	1.23	90.7	1882.7
BF-0-3	40.5	1.23	91.7	2777.8
BF-0-7	40.4	1.25	93.1	4912.6
BF-0-14	39.8	1.24	90.5	5812.8
BF-0-28	40.9	1.23	90.6	6790.1
BF-S1-2	39.8	1.27	94.4	2088.5
BF-S1-6	39.8	1.26	92.9	3580.3
BF-S1-13	38.5	1.29	95.4	5298.4
BF-S1-27	39.7	1.28	94.5	6145.8
BF-S3-4	40.3	1.21	88.2	3112.1
BF-S3-11	39.1	1.25	90.2	4516.5
BF-S3-25	39.5	1.24	89.3	5467.8
BF-A1-2	26.9	1.29	66.3	3600.8
BF-A1-6	28.3	1.37	78.0	6841.6
BF-A1-13	28.2	1.36	77.4	7407.4
BF-A1-27	27.1	1.37	76.1	8487.7
BF-A3-4	14.5	1.26	33.9	2572.0
BF-A3-11	17.1	1.26	40.1	5761.3
BF-A3-25	16.6	1.26	38.5	6454.3

w: Water content at the crumbling and/or the compaction
ρ_d: Dry density at compaction
S_r: Saturation degree at the compaction
q_c: Cone index of the compacted sample after the soaked curing

4.3 CHARACTERISTICS OF PSD OF TREATED SAMPLE

4.3.1 Relationship between Water Content (w) and Pre-compaction Curing Period (t_1)

During the process of compaction for each of the test scenarios, the amount of water that was present in each sample was measured and shown in Fig. 4.9. Based on the findings presented in Tables 4.3 and 4.4, Fig. 4.9 depicts the water content (w) of each sample plotted against pre-curing period(t_1). In the figures, the value of t_1 for the samples that did not undergo pre-compaction curing (also known as uncrumbled samples) has been set to zero. The water content (w) of all PSAS-N-treated, PSAS-R-treated, and BFCB-treated samples stays almost unchanged after pre-compaction curing in an air environment, but it drops after pre-compaction curing in a sealed environment. In addition, the water content (w) of the samples treated with PSAS-R does not decrease to the same substantial degree as the water content (w) of the samples treated with the other stabilizers. This is due to the fact that the samples that were treated with PSAS-R harden more quickly after being mixed in comparison to the samples that were treated with PSAS-N and BFCB, as will be explained in further detail below.

It is important to note that the measured liquid limit, (w_L) and plastic limit,(w_p) values of the samples that were treated with PSAS-N are respectively 66.0% and 40.3%, whereas the values of the samples that were treated with PSAS-R are respectively 69.8% and 40.1%, and the values of the samples that were treated with BFCB are respectively 60.0% and 39.8%. The liquid limit, (w_L) and plastic limit,(w_p) values were investigated using the samples one day after sealed primary curing with the mixture ratios listed in the previous section in Table 4.1. After one day of primary curing in an air or sealed environment, the consistency limits indicated that both PSAS-treated samples (PSAS-N-treated samples and PSAS-R-treated samples) and BFCB-treated samples could be in semi-solid or solid states, as long as the water content (w) was lower than the plastic limit (w_p).

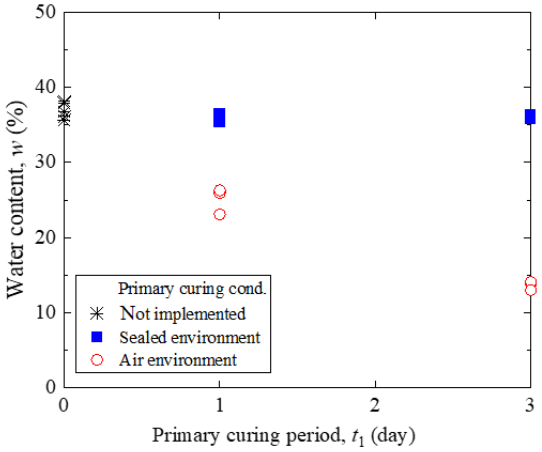

(a) PSAS-N-treated samples

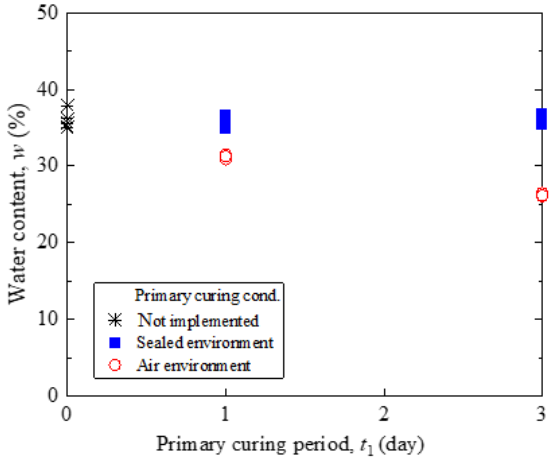

(b) PSAS-R-treated samples

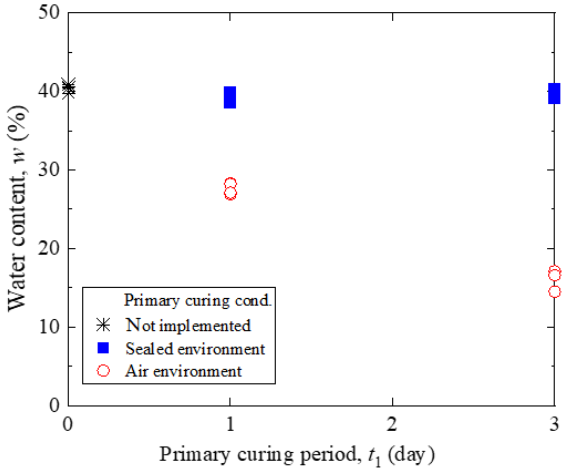

(c) BFCB-treated sample

Figure 4.9 Relationships between the water content (w) and primary curing period (t_1)

4.3.2 Particle Size Distributions of Treated Samples with Pre-compaction Curing

After crumbling to acquire the particle size distributions (PSDs), the samples that had been treated with PSAS and BFCB were put through sieve analysis. This process was explained in the previous section. In accordance with Japanese Geotechnical Society Standards JGS 0131, the sieve analysis was carried out utilizing sieves ranging from 0.075 mm to 75 mm in size; however, sedimentation analyses were not carried out. In the beginning, the sieve tests were carried out on the samples while they were still in their original states of water content (w). After that, the tests were carried out on dried samples that had originally been cleaned with water and dried in an oven. After crumbling, the particle size distributions of samples that were treated with PSAS-N, PSAS-R, and BFCB, respectively, are shown in Figures 4.10, 4.11, and 4.12, respectively. Also, the figures present the combined particle size distributions (PSDs) that were computed by taking into account the PSDs that were presented for each material in chapter 3 and the mixture ratio (Table 4.1). As shown in the figures, for the wet samples, granules of the same size range as sand and gravel can be seen in the PSAS-N and PSAS-R treated samples. These samples are constituted of granules. This is also the case for the samples that were treated with BFCB. During the pre-compaction curing process, the samples transform from plastic to being either semi-solid or solid, as was previously explained. Because of this change, crumbling might result in the production of granules that resemble sand and gravel (Figs. 4.7 and 4.8). As can be seen in Figs 4.10, 4.11, and 4.12, the particle size of the wet samples is reduced in proportion to the decrease in the sample's water content (w). However, there is a slight variation in this relationship. Also, we find that the samples treated with PSAS-R had slightly bit more granules that resemble sand in comparison to the samples treated with PSAS-N and BFCB.

In addition, the data presented in Figs 4.10, 4.11, and 4.12 demonstrate that the oven-dried samples, regardless of the type of stabilizer used, have greater proportions of fine contents. The wet samples, on the other hand, do not contain any fine contents. This is because the washing process with water and then drying in an oven allows the particles that have been clustered by the stabilizers to become smaller and finer. However, the PSDs of the oven-dried samples of all of the treated samples do not match those of the combined PSDs. This is the case for all of the treated samples. This gives the impression that the treated samples include particles that form chemical bonds with one another. When chemical water absorption (a hydration reaction) is involved, the PSD of the PSAS-treated soil does not necessarily follow that of the combined PSD. As a result of this, the PSAS-treated soil has a different PDS.

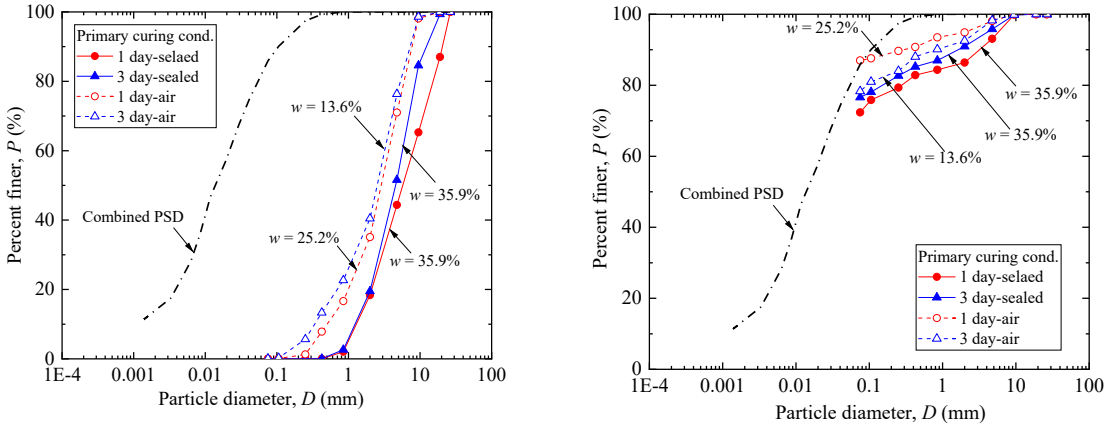

(a) Wet samples (b) Oven-dry samples

Figure 4.10 PSDs of the PSAS-N-treated samples with pre-compaction curing

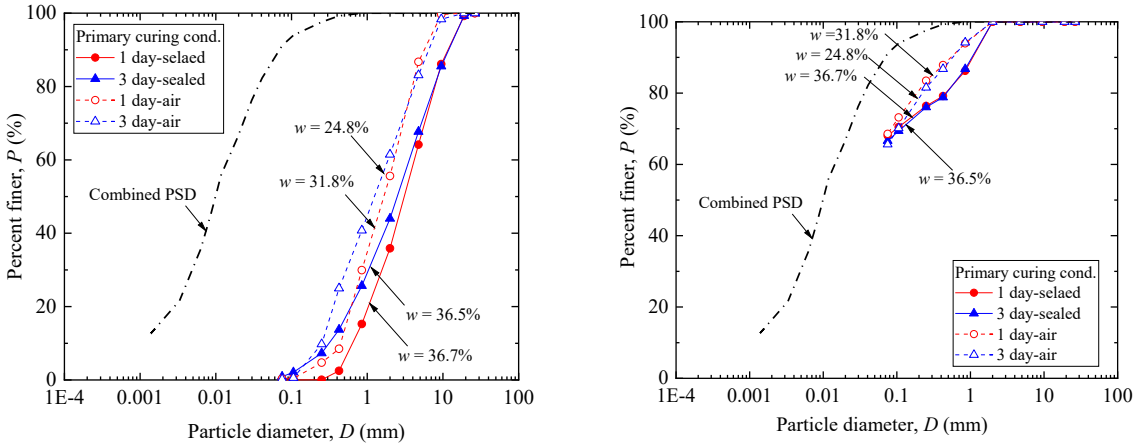

(a) Wet samples (b) Oven-dry samples

Figure 4.11 PSDs of the PSAS-R-treated samples with pre-compaction curing

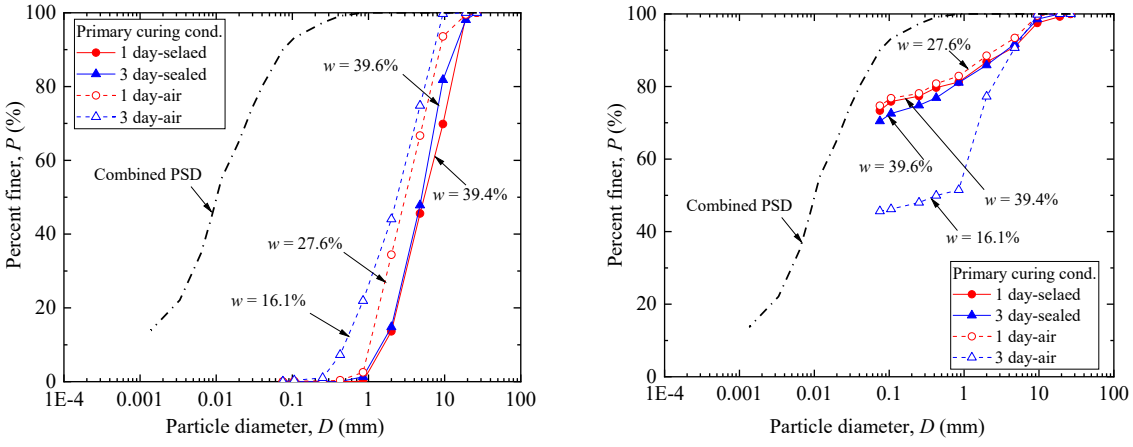

(a) Wet samples (b) Oven-dry samples

Figure 4.12 PSDs of the BFCB-treated samples with pre-compaction curing

4.4 CHARACTERISTICS OF COMPACTED SAMPLE DUE TO CRUMBLING

4.4.1 Relationship between Water Content (w) and Dry Density (ρ_d)

In the flow process of sample preparation, as shown in Fig. 4.1, we have seen that, for samples where no crumbling was conducted, water content (w) was measured immediately after sample preparation. For the samples, which went through sealed or air pre-compaction curing for 1 or 3 days, crumbling was conducted before compaction, and water content at crumbling was measured. With the measured water content (w), the dry density (ρ_d) for each of the samples was calculated. The dry density values obtained from the compaction of each sample were organized with respect to water content based on the results shown in Table 4.3. This was done so that we could explore the effects of the pre-compaction curing conditions and subsequent crumbling on the compaction characteristics of the PSAS-treated samples. The BFCB-treated samples (Table 4.4) went through the exact same process as mentioned for the PSAS-treated samples.

The compaction results for the samples that were treated with PSAS-N, PSAS-R, and BFCB are shown in Figs. 4.13(a), 4.13(b), and 4.13(c), respectively, along with the compaction curve for the Ao clay. As can be seen in Figures 4.13(a), (b), and (c), the dry density (ρ_d) values of the treated samples, regardless of whether they underwent pre-compaction curing or not, are lower than those of Ao clay. As can be seen in Figs 4.13(a), 4.13(b), and 4.13(c), the dry density (ρ_d) values of the treated samples, regardless of whether they underwent pre-compaction curing or not, are lower than those of Ao clay. From the previous studies, we can explain this matter. Clay particles have a tendency to cluster and form granules with small pores or gaps between the particles when specific stabilizers are introduced to a sample containing clay particles. Chemical substances called stabilizers are given to a system to prevent or minimize unfavorable reactions or changes. Stabilizers can aid in preventing the aggregation or clumping of clay particles, which could have an impact on the sample's characteristics. Some stabilizers, on the other hand, can also make the particles group and form granules, which may have tiny pores or gaps between the particles. These pores or gaps can alter the sample's surface area, permeability, or adsorption capacity, which can change how the sample behaves. For instance, the pores might enhance the sample's surface area, making it more responsive to specific substances or better able to absorb them. Alternately, the pores can make the sample more permeable and make it easier for some molecules to pass through. There is a relation between permeability and dry density (ρ_d). When the permeability increases, the dry density (ρ_d) decreases. This issue is explained in previous literature for granulated soil treated with cement. (Dong et al., 2012;Takahashi et al., 2010). Moreover, For paper sludge ash-treated soil, the same result was confirmed. (Hayano and Fujishima, 2013, and Hayano et al., 2016).

In addition, the dry density (ρ_d) values of the PSAS-N-treated samples with sealed pre-compaction curing are shown to be equal to those of the samples that were not subjected to pre-compaction curing in Fig. 4.13(a). The same trend is seen while observing the samples that were treated with BFCB (Fig. 4.13(c)). On the other hand, as can be shown in Fig. 4.13(b), the dry density (ρ_d) values of the PSAS-R-treated samples that were subjected to sealed pre-compaction curing are much

lower than those of the samples that were not subjected to pre-compaction curing. This may be explained by the fact that the type of PSAS makes a difference in the degree of disturbance that is generated when the crumbling occurs. The PSDs of the PSAS-N-treated samples after crumbling in Fig. 4.10(a) show that the mean particle diameter D_{50} of the one-day sealed curing sample is 6.0 mm and that the D_{50} of the three-day sealed curing sample is 4.9 mm. In contrast, the PSDs of the PSAS-R-treated samples after crumbling in Fig. 4.11(a) show that the D_{50} of the one-day sealed curing sample is 3.0 mm, and the D_{50} of the three-day sealed curing sample is 2.8 mm. Compared to the PSAS-N-treated samples, the PSAS-R-treated samples are more fragmented and have smaller particle sizes. The PSAS-R treated samples rapidly increased strength during the initial stage, as will be illustrated in the following section. It is likely that the PSAS-R-treated samples first lost more free water. It would appear from this phenomenon that the samples that were treated with PSAS-R were drier than the samples that were treated with PSAS-N. The term "free water" refers to water that is not bound to the sample and is therefore straightforward to extract. In light of this, it is probable that the curing process caused the water in the samples to evaporate, compared to the PSAS-N-treated sample. That’s why, the PSAS-R-treated sample had weaker plastic properties. The ability of a material to deform in response to applied stress and to maintain that shape after the stress is removed is referred to as plasticity. The PSAS-R-treated samples exhibited weaker plastic characteristics, which suggests that they were less able to maintain their shape when subjected to stress. The PSAS-R-treated samples were broken down into smaller pieces compared with PSAS-N-treated samples because of this free water loss and weaker plastic properties. It's possible that this breaking down into pieces changed the structure of the material. Therefore, the rapid formation of hydrates in the PSAS-R-treated samples may have caused large disturbances owing to crumbling, resulting in a decrease in dry density.

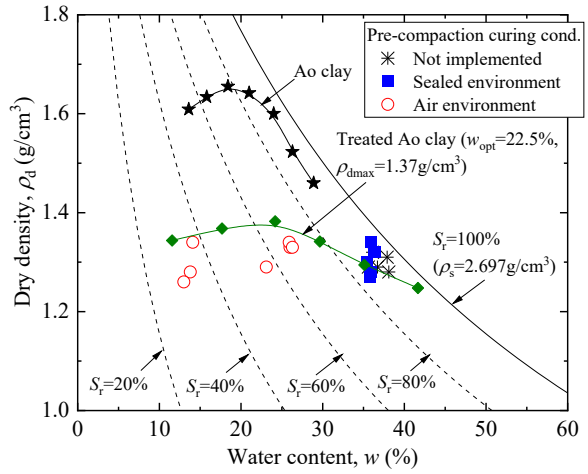

(a) PSAS-N-treated samples

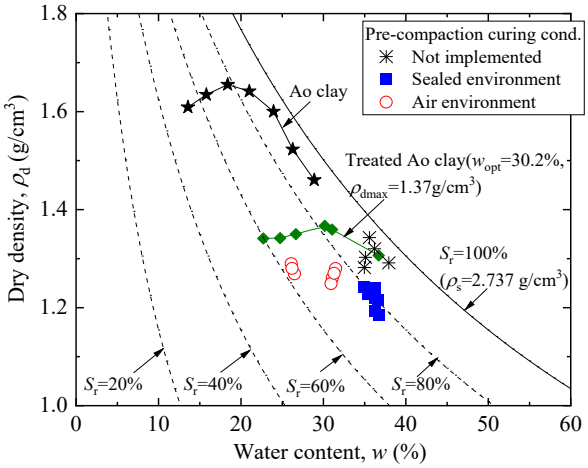

(b) PSAS-R-treated samples

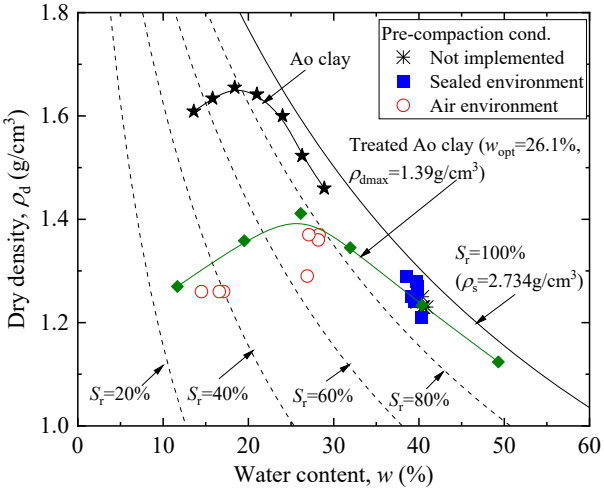

(c) BFCB-treated samples

Figure 4.13 Relationships between w and ρ_d

Figures 4.13(a), (b), and (c) also show the compaction curves of the Ao clay as treated with PSAS-N or PSAS-R with A_{PS} = 20% and that of the Ao clay treated with the BFCB with A_{BFCB} = 6%, respectively. The compaction curves are denoted as "Treated Ao clay" in each figure. Each of the three compaction curves was obtained by adding the respective stabilizers to Ao clay with different water contents (w) and then immediately compacting them. ρ_s was calculated according to the density of the constituent materials and mixture conditions to show the constant saturation degree curves using ρ_s in the figures. The maximum dry density (ρ_{dmax}) is the same; however, the optimum water content (w_{opt}) is higher in the PSAS-R treatment scenario than in the PSAS-N treatment scenario.

In addition to this, it can be seen in Figs. 4.13(a), 4.13(b), and 4.13(c) that the values of the dry density (ρ_s) of each type of sample that was treated with air pre-compaction curing are located below each of the three compaction curves. The dry density values of the samples that were treated without pre-compaction curing are practically identical across all three compaction curves. This is the case regardless of which curve was used. As discussed earlier, the disturbance caused by crumbling can reduce dry density for the air and sealed pre-compaction curing conditions. In addition, the differences in the initial water content of the Ao clay before stabilizers are added are considered to have induced this difference. For the samples subjected to air primary curing, each stabilizer was added to an Ao clay with a higher initial water content, and the water content of the treated samples decreased during the subsequent air curing. When the water content of the Ao clay at the time of stabilizer addition was high, there was sufficient free water for hydrate formation. Therefore, more hydrates were produced in the treated samples, and ρ_d could be lower than that of the treated Ao clay, which was obtained from clay with a lower initial water content. This may imply that PSAS-treated soil that has been primarily cured in an air environment and crumbled is less likely to be compacted than PSAS-treated soil to which PSAS has been added after the original soil is sun-dried.

4.4.2 Relationship between Water content (w) and Degree of Compaction (D_c)

Figure 4.14 illustrates the correlation between the degree of compaction (D_c), and the water content w, in each sample that was treated. As Fig. 4.14(a) shows, D_c is equal to 90% or higher for the PSAS-N-treated samples, regardless of whether the pre-compaction curing was conducted in air or sealed, the D_c values of the sealed pre-compaction cured samples are not significantly different from those of samples without pre-compaction curing. This trend is also observed for the BFCB-treated samples. However, for the PSAS-R-treated samples shown in Fig. 4.14(b), the D_c values of the samples with sealed pre-compaction-curing are lower than those of the samples without pre-compaction curing, and in many scenarios, the D_c value is 90% or lower. This could be owing to the difference in the degree of disturbance caused by crumbling depending on the PSAS type, as mentioned earlier. However, the D_c values of the PSAS-R-treated samples with air pre-compaction curing are significantly higher than those of the sealed pre-compaction samples; thus, air curing can be considered as one of the measures for improving D_c.

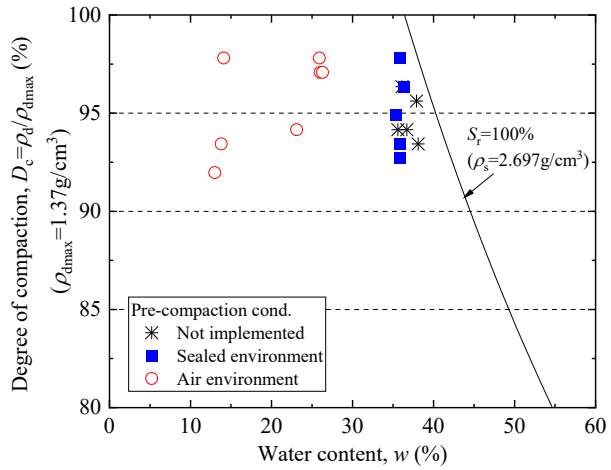

(a) PSAS-N-treated samples

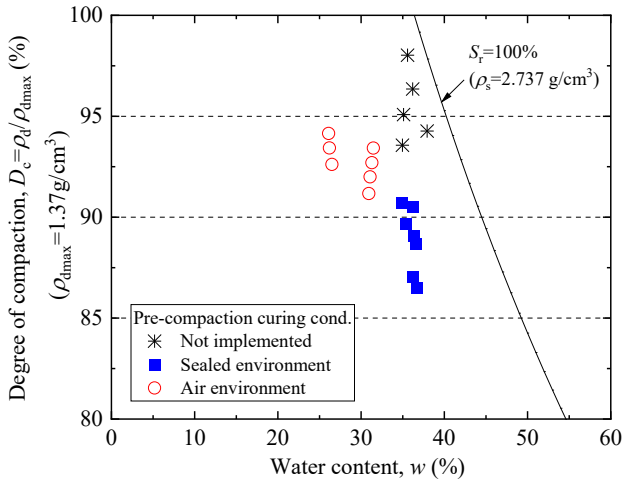

(b) PSAS-R-treated samples

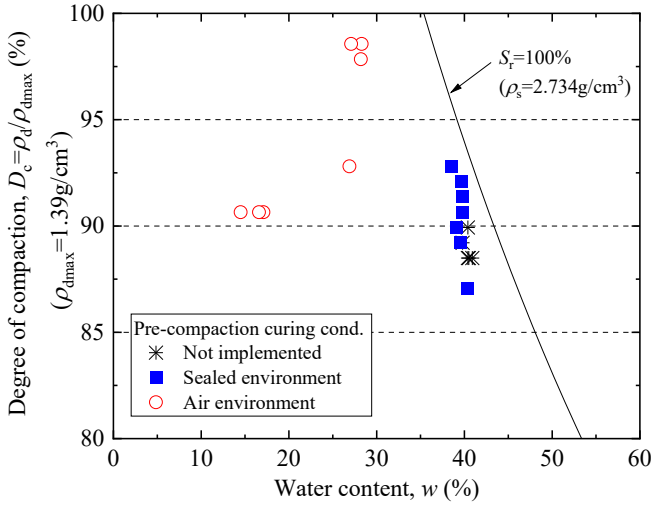

(c) BFCB-treated sample

Figure 4.14 Relationships between (w) and degree of compaction (D_c)

4.5 CHARACTERISTICS OF STRENGTH DEVELOPMENT (Ao Clay)

4.5.1 Cone Index Test Result

After post-compaction curing in a soaked environment, cone index tests were performed on the samples both with and without pre-compaction curing. This information was obtained from the sample preparation flow shown in Figure 4.1. The relationships between the cone index (q_c) and the total curing period (t) of samples treated with PSAS-N and PSAS-R, with and without pre-compaction curing, are shown in Fig. 4.15. The relationships between the samples that were treated with BFCB without pre-compaction curing are shown as well in the figure. The relationships between the PSAS-N-treated samples, the PSAS-R-treated samples, and the BFCB-treated samples are shown in Fig 4.15 (a), (b), and (c), respectively. Although the PSAS-R treated samples without pre-compaction curing demonstrate a large q_c from the early stage of curing, the PSAS-N treated samples without pre-compaction curing have relatively low strength in the early stage and progressively rise in strength. This is in contrast to the PSAS-R treated samples, which exhibit a large q_c from the early stage of curing. According to Table 3.4, the estimated water absorption and retention ratio (W_{ab}) of PSAS-R after 24 hours is greater than that of PSAS-N. The higher the W_{ab}, the more free water in the soil is constrained by the PSAS, and the stronger the treated samples are because of this phenomenon. Therefore, the difference in W_{ab} between PSAS-R and PSAS-N in Table 3.4 is qualitatively comparable with the difference in strength between the PSAS-R-treated samples and the PSAS-N-treated samples without primary curing in the initial stage of curing, as shown in Fig 4.15. The water absorption and retention performances of both PSAS-N and PSAS-R hardly increase after 24 hours, as shown in Fig. 3.3. On the other hand, as shown in Fig 4.15, the q_c of the treated samples increases after 24 hours. Even though more research needs to be done to determine the specifics of why this difference exists, it is possible that the reactions that take place between PSASs and Ao clay are a factor in the rise in q_c. In addition, Fig. 4.15 demonstrates that the strengths exhibited by the samples treated with BFCB are in between those exhibited by the samples treated with PSAS-R and those treated with PSAS-N. However, the addition ratio of BFCB (A_{BFCB}) was not the same as that of PSAS-R and PSAS-N (A_{PS}).

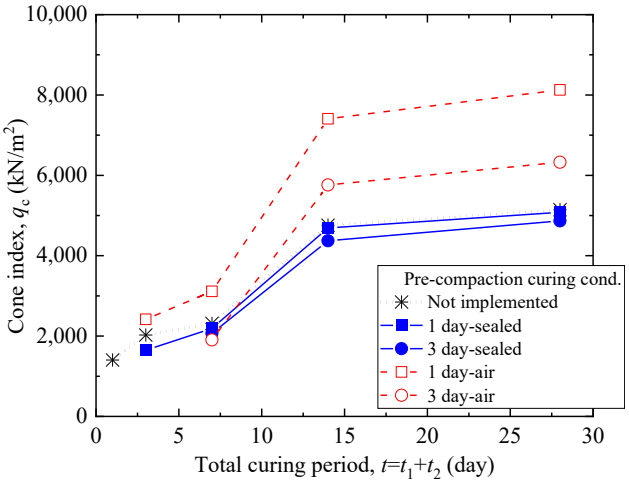

(a) PSAS-N-treated samples

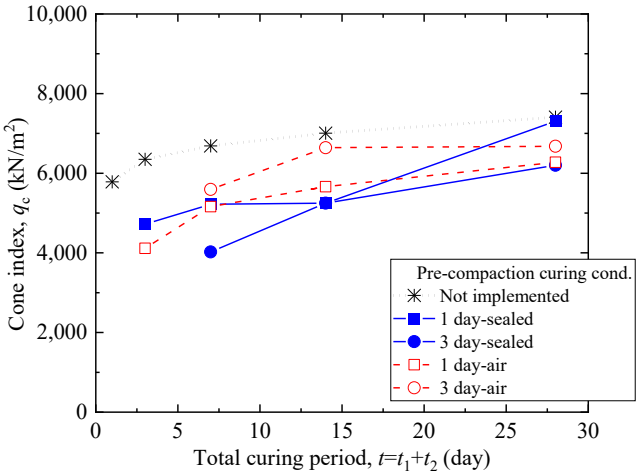

(b) PSAS-R-treated samples

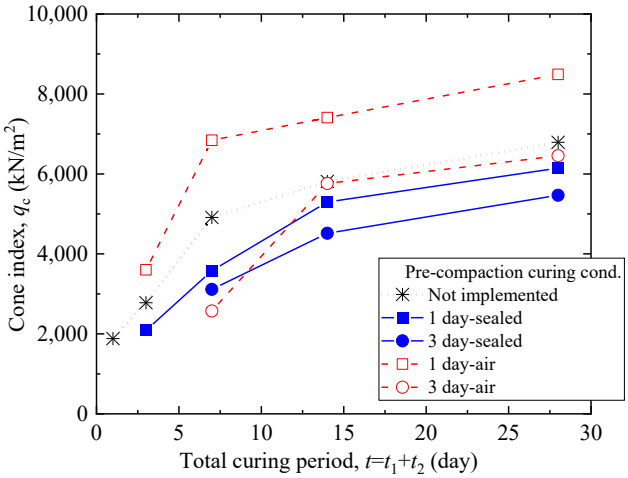

(c) BFCB-treated-samples

Figure 4.15 Relationships between (q_c) and (t)

As shown in Fig. 4.15, regardless of the difference in the pre-compaction curing conditions, q_c increases with t; however, for the PSAS-R-treated samples, the q_c values of the samples with pre-compaction curing in the sealed environment are significantly lower than those of the samples without pre-compaction curing. For the PSAS-N-treated samples, the difference in q_c between pre-compaction curing under sealed and non-pre-compaction curing conditions is small. As described previously, there was no significant difference in w at compaction between the samples with sealed pre-compaction curing and those without pre-compaction curing (Fig. 4.9). Therefore, the degree of difference in q_c of each type of treated sample between the two conditions could be attributed to the difference in the strength reduction caused by crumbling. As mentioned earlier, the PSAS-N-treated samples had a relatively low strength in the early stage and gradually increased in strength. Therefore, the strength reduction caused by crumbling could be insignificant relative to that of the PSAS-R-treated samples.

Focusing on the q_c values of the samples with air pre-compaction curing, Fig. 4.15 shows that the strength development differs depending on the type of stabilizer and primary curing period. For the PSAS-N-treated samples, the q_c values of the samples with air pre-compaction curing, where the period is either 1 or 3 days, are higher than those of the samples without pre-compaction curing, except for one result. However, for the PSAS-R-treated samples, the q_c values of the samples with air pre-computation curing are lower than those of the samples without pre-compaction curing. For the BFCB-treated samples, the q_c values of the samples with air pre-compaction curing are higher than those of the samples without pre-compaction curing when the pre-compaction curing period is 1 day. The reason for the different trends in the strength development appears to be related to the water content during compaction. This will be discussed in detail in the last section of this chapter.

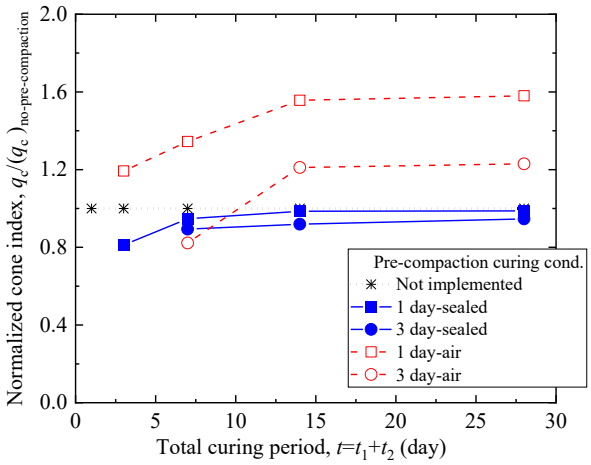

(a) PSAS-N-treated samples

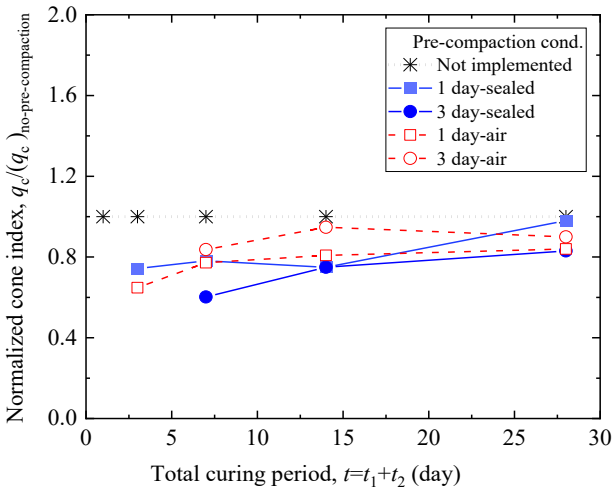

(b) PSAS-R-treated samples

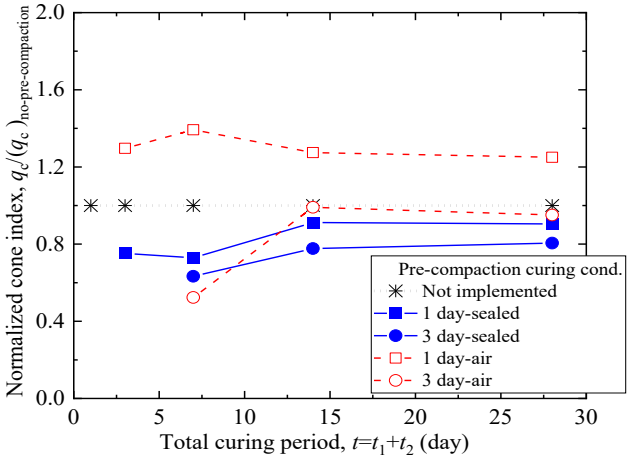

(c) BFCB-treated samples

Figure 4.16 Relationships between the normalized cone index ($q_c/(q_c)_{no\text{-}pre\text{-}compaction}$) and ($t$)

Figures 4.16(a), (b), and (c) show the relationships between the normalized cone index $q_c/(q_c)_{no\text{-}pre\text{-}compaction}$ and t for the PSAS-N, PSAS-R, and BFCB-treated samples, respectively. Normalization was performed by dividing the q_c value of the sample by the $(q_c)_{no\text{-}pre\text{-}compaction}$ value of the sample with the same t and no pre-compaction curing. The q_c values of the sealed pre-compaction-cured samples are lower than those of the samples without precomputation curing, but the degree of reduction varies depending on the initial strength development of the stabilizer. We also confirm that the q_c values of the air pre-compacted samples can be higher or lower than those of the samples without pre-compaction curing, depending on the initial strength development of PSAS treated soil and the pre-compaction curing period. Notably, the q_c values of the PSAS-treated samples pre-compacted in a sealed environment tend to decrease with an increase in t_1 for the same t. This is also true for the BFCB-treated samples.

4.5.2 Relationship between Water Content (w) and Cone Index Result (ρ_d)

In the previous section, It was addressed whether the q_c values of the PSAS-treated samples with pre-compaction curing were greater or lower than those without pre-compaction curing depending on the pre-compaction curing environment, the number of curing days, and the initial strength of PSAS-treated soil. In this part, we will look into the mechanism(s) by which the pre-compaction curing conditions and subsequent crumbling affect the strength of PSAS-treated samples. Pre-compaction curing refers to the curing process that occurs before a specimen is crumbled.

Figures 4.17(a), (b), and (c) show the relationships between the water content w and q_c values obtained from the PSAS-N, PSAS-R, and BFCB-treated samples, respectively. As mentioned previously, regardless of the type of stabilizer, the w values of the samples without pre-compaction curing and those the samples with sealed pre-compaction curing are relatively close (Fig. 4.9), and the q_c values of the latter samples are lower than those of the former samples (Fig. 4.15). However, there is a slight difference in q_c between the two conditions of the PSAS-N-treated samples compared with those of the PSAS-R-treated samples. This was because the strength development of the PSAS-N-treated samples slows with time; therefore, the strength reduction by crumbling can be smaller than that of the PSAS-R-treated samples.

For the PSAS-N treated samples shown in Fig. 4.17(a), at t = 7, 14, and 28 days, the q_c values of the 3-day sealed-cured sample decreased by 10.7%, 8.1%, and 5.4%, respectively, relative to the q_c of the sample without pre-compaction curing. Meanwhile, for the PSAS-R treated cases shown in Fig. 4.17(b), at t = 7, 14, and 28 days, the q_c values of the 3-day sealed-cured sample decreased by 39.8%, 25.1%, and 16.3%, respectively, relative to the q_c of the sample without pre-compaction curing. The strength reduction owing to the crumbling of the PSAS-R-treated samples is much higher than that of the PSAS-N-treated samples.

In fact, in the PSAS-N-treated case shown in Fig. 4.17(a), a comparison of q_c between the sealed and air-cured samples shows an increase in q_c of 42.0–60.0% for a decrease in w of approximately 10%. Meanwhile, in the PSAS-R-treated samples shown in Fig. 4.17(b), a comparison of q_c between the sealed and air-cured samples indicates an increase in q_c of 7.7–39.0% for a decrease in w of approximately 10%.

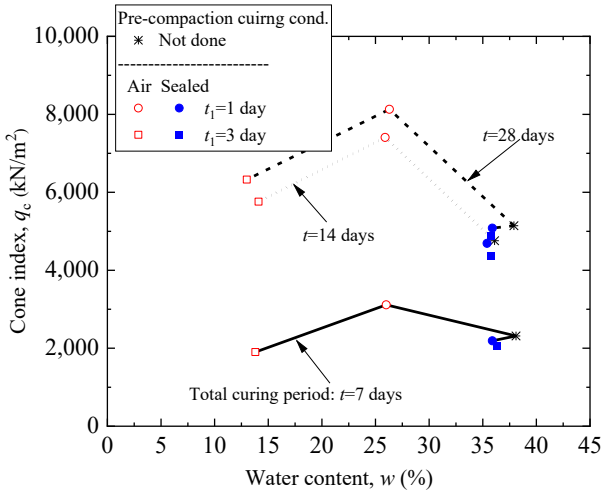

(a) PSAS-N-treated samples

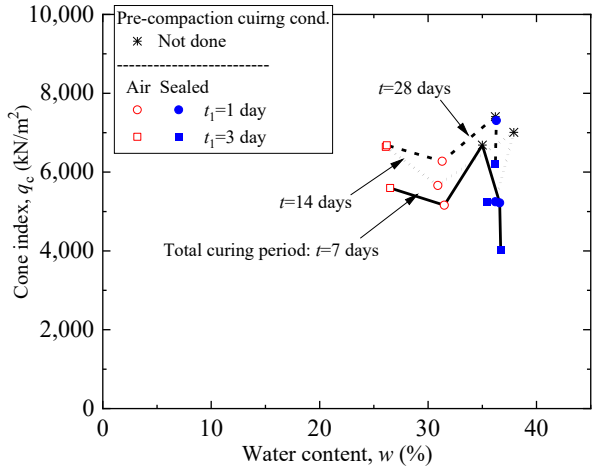

(b) PSAS-R-treated samples

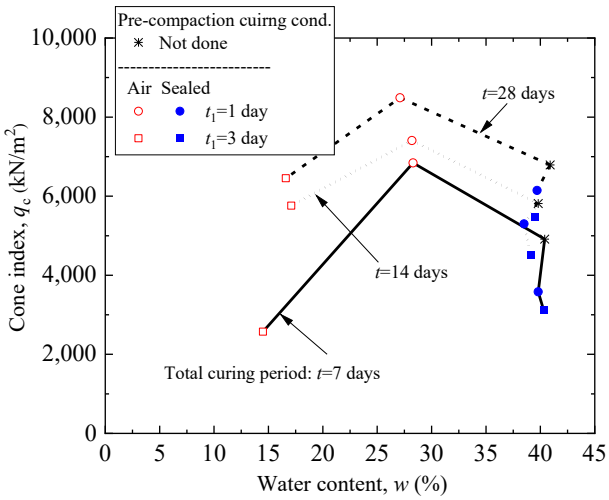

(c) BFCB-treated samples

Figure 4.17 Relationships between (w) and (q_c)

4.6 REPEATABILITY CHECK FOR STRENGTH DEVELOPMENT (Kasaoka clay)

4.6.1 Sample Preparation

In the study to assess the repeatability of strength development characteristics due to initial strength (higher or lower), Kasaoka Clay is employed in conjunction with two different types of chemical stabilizers: PSAS-N and PSAS-R. These stabilizers are mixed with Kasaoka Clay at varying dry mass ratios to investigate their effects on the strength properties of the treated samples. Table 4.5 provides an overview of the mixture ratios used in the experiment. For the PSAS-R samples, two different dry mass ratios of Kasaoka Clay are utilized: 20% and 50%. On the other hand, for the PSAS-N samples, only one dry mass ratio of Kasaoka Clay is considered, which is 20%.

Table 4.5 Mixture ratios for PSAS-treated samples with Kasaoka clay

Sample type	The water content of Kasaoka clay, w (%)	Addition ratio of PSAS-N A_{PS} (%)	Addition ratio of PSAS-R A_{PS} (%)
PSAS-N-treated samples	60.4 ($w = w_L$)	20	0
PSAS-R-treated samples		0	20 &50

The sample preparation process is the same as samples prepared with Ao clay. Similar to the Ao clay treated sample, samples were prepared with no pre-compaction curing, sealed curing and air curing. Table 4.6 shows the test scenario name with curing conditions for PSAS-N & PSAS-R treated samples. In Table 4.6, the titles of the test cases show the kind of stabilizer and amount of stabilizer used, the type of pre-compaction curing, the duration of pre-compaction curing (or zero if there is no pre-compaction curing), and the duration of post-compaction curing. For instance, N-0-7 is a PSAS-N treated sample with no pre-compaction curing and a post-compaction curing length of 7 days, whereas RS-S3-11 is a PSAS-R treated sample where 20% PSAS-R is used with 3 days of sealed pre-compaction curing and a post-compaction curing period of 11 days. Further, RH-S3-11 is a PSAS-R treated sample where 50% PSAS-R is used with 3 days of sealed pre-compaction curing and a post-compaction curing period of 11 days.

4.6.2 Relationship between Water Content (w) and Pre-compaction Curing Period (t_1)

During the process of compaction for each of the test scenarios, the amount of water that was present in each sample was measured and shown in Fig. 4.18. Fig. 4.18 depicts the water content (w) of each sample plotted against the pre-curing period(t_1). In the figures, the value of t_1 for the samples that did not undergo pre-compaction curing (also known as uncrumbled samples) has been set to zero. The water content (w) of all PSAS-N-treated, and PSAS-R-treated stays almost unchanged after pre-compaction curing in a sealed environment, but it drops after pre-compaction curing in an air environment. In addition, the water content (w) of the samples treated with PSAS-R where a 50% additional ratio was used does not decrease to the same substantial degree as the water content (w) of the samples treated with the other stabilizers. This is due to the fact that the

samples that were treated with PSAS-R (50% additional ratio) harden more quickly after being mixed.

Table 4.6 Curing conditions for PSAS-N-treated, PSAS-R-treated, and BFCB-treated samples

Test scenario name			Pre- compaction curing period (t_1) and environment	Post-compaction curing period (t_2) under the soaked environment	Total curing period ($t=t_1+t_2$)
PSAS-N-treated samples	PSAS-R-treated samples (20%)	PSAS-R-treated samples (50%)			
N-0-1	RS-0-1	RH-0-1	Not Implemented	1	1
N-0-3	RS-0-3	RH-0-3		3	3
N-0-7	RS-0-7	RH-0-7		7	7
N-0-28	RS-0-28	RH-0-28		28	28
N-S1-2	RS-S1-2	RH-S1-2	1-day sealed curing	2	3
N-S1-6	RS-S1-6	RH-S1-6		6	7
N-S1-13	RS-S1-13	RH-S1-13		13	14
N-S3-4	RS-S3-4	RH-S3-4	3-day sealed curing	4	7
N-S3-11	RS-S3-11	RH-S3-11		11	14
N-A1-2	RS-A1-2	RH-A1-2	1-day air curing	2	3
N-A1-6	RS-A1-6	RH-A1-6		6	7
N-A1-13	RS-A1-13	RH-A1-13		13	14
N-A3-4	RS-A3-4	RH-A3-4	3-day air curing	4	7
N-A3-11	RS-A3-11	RH-A3-11		11	14

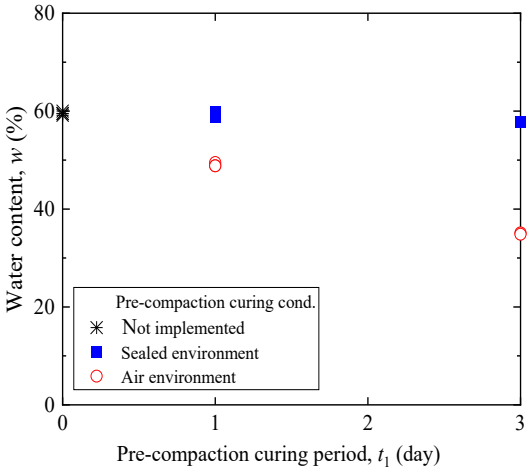

(a) PSAS-N treated sample

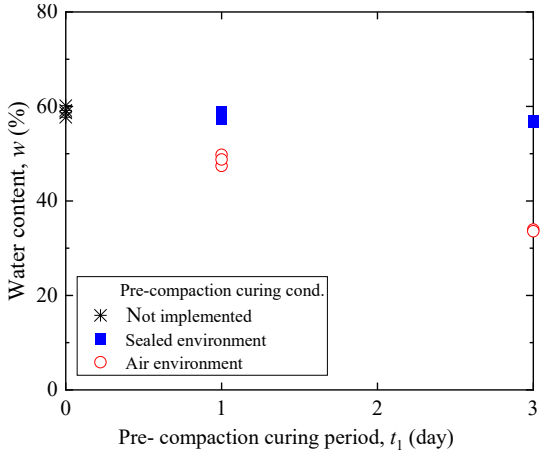

(b) PSAS-R treated sample (20%)

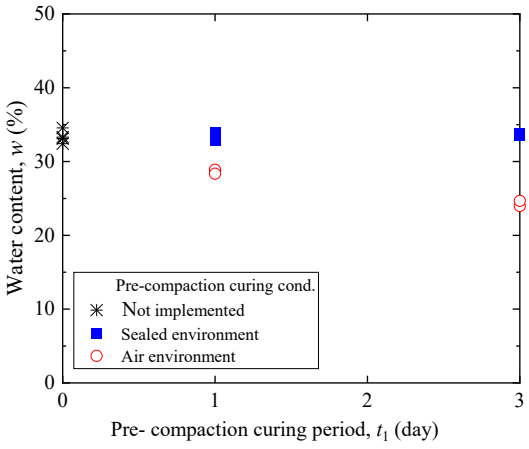

(c) PSAS-R treated sample (50%)

Figure 4.18 Relationships between the water content (w) and primary curing period (t_1)

4.6.3 Cone Index Test Result

Figure 4.19 (a), (b) &(c) depict the test results acquired from the PSAS-N and PSAS-R-treated specimens, respectively. Irrespective of the disparities in pre-compaction curing conditions, the cone index strength exhibits a progressive increase over time. In PSAS-N & PSAS-R treated case where 20% stabilizer was added, the strength, q_c values of the specimens that went through air pre-compaction curing, with curing periods of either 1 or 3 days, are higher than the q_c values of the samples with no pre-compaction curing. Also, in these two cases, samples with 1-day air pre-compaction curing show higher strength compared with samples with 3-day air pre-compaction curing. On the other hand, the case where the addition ratio of PSAS-R is 50% showed a different trend. All samples with sealed or air pre-compaction curing show lower strength compared with samples with no pre-compaction curing. (similar to PSAS-R treated with Ao clay). It is because, with the increment in the addition ratio of PSAS-R, the strength development in the initial stage is higher. So, the strength reduction due to crumbling is significant.

The relationships between the normalized cone index and t for the PSASs-treated cases with Kasoka clay are shown in Fig. 4.20 (a), (b) & (c).

4.6.4 Relationship between Water Content (w) and Pre-compaction Curing Period (t_1)

Figure 4.21(a), (b) and (c) show the correlations between the water content w and q_c values obtained from the PSAS-N and PSAS-R (20% and 50% addition ratio) treated samples with Kasoka clay. When the initial strength development is not high, similar types of behaviour are observed (PSAS-N & 20% PSAS-R treated case). For, PSAS-N treated case (Fig. 4.21(a)), At t = 7 and 14 days, the q_c values of the 3-day sealed-cured sample decreased by 29% and 19%, respectively, in comparison to the q_c of the sample where pre-compaction curing was not implemented. At t = 7 and 14 days, for PSAS-R (20%) treated specimen, the q_c values of the 3-day sealed-cured sample (Fig. 4.21(b)) decreased by 28% and 27%, respectively, in comparison to the q_c of the sample where pre-compaction curing was not implemented. On the other hand, comparing the 3-day q_c of the sealed and air-cured samples in the PSAS-N-treated example (Fig. 4.21(a)) reveals an increase in q_c of 12.0-22.0% for a reduction in w during air curing. Meanwhile, comparing the 3-day q_c of the sealed and air-cured samples in the PSAS-R (20%) treated example (Fig. 4.21(b)) reveals an increase in q_c of 40.0-73.0% for a reduction in w during air curing.

On the other hand, when the initial strength development is high, for the PSAS-R (50%) treated cases shown in Fig. 4.21(c), at t = 7, 14 days, the q_c values of the 3-day sealed-cured sample decreased by 42%, 23%, respectively, relative to the q_c of the sample without pre-compaction curing. The strength reduction owing to the crumbling of these samples is much higher than that of the samples where the initial strength development is not that high. A comparison of q_c between the sealed and air-cured samples indicates an increase in q_c of 7–30% for a decrease in w of approximately 6%.

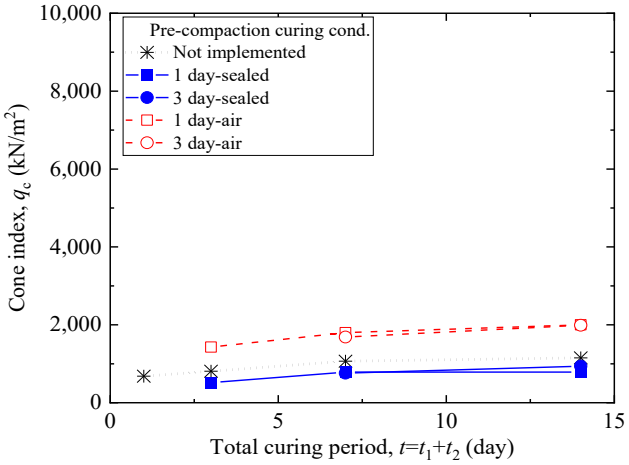

(a) PSAS-N treated sample

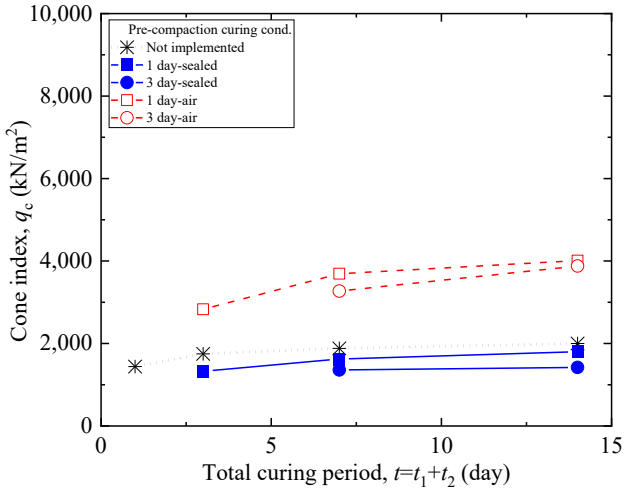

(b) PSAS-R treated sample (20%)

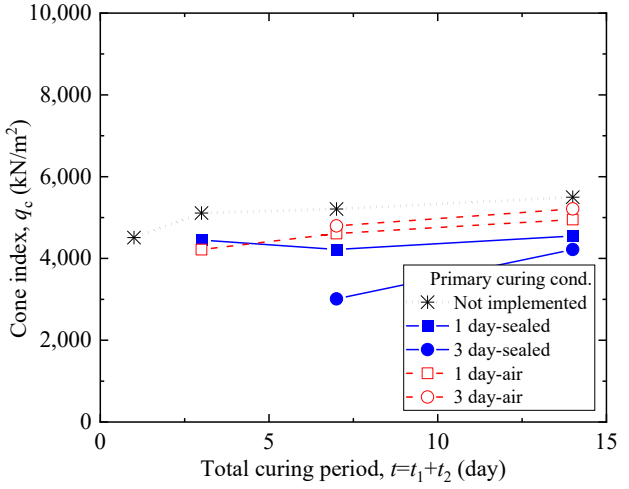

(c) PSAS-R treated sample (50%)

Figure 4.19 Relationships between (q_c) and (t)

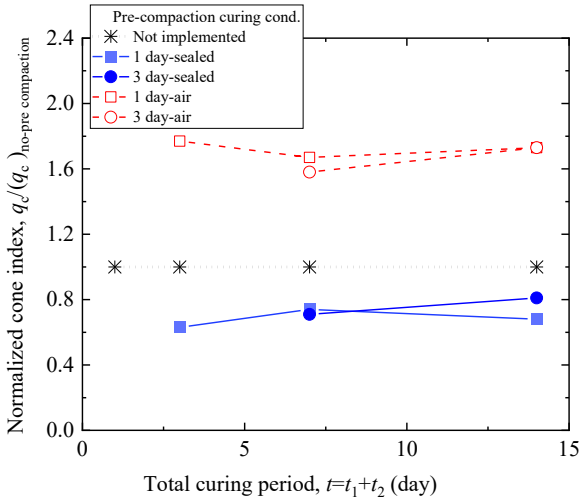

(a) PSAS-N treated sample

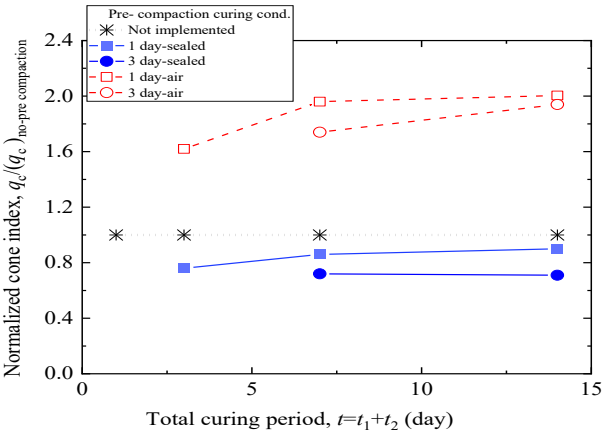

(b) PSAS-R treated sample (20%)

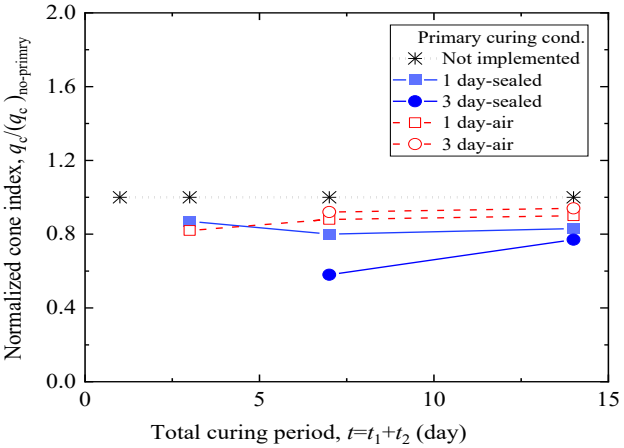

(c) PSAS-R treated sample (50%)

Figure 4.20 Relationships between the normalized cone index $(q_c/(q_c)_{\text{no-pre compaction}})$ and (t)

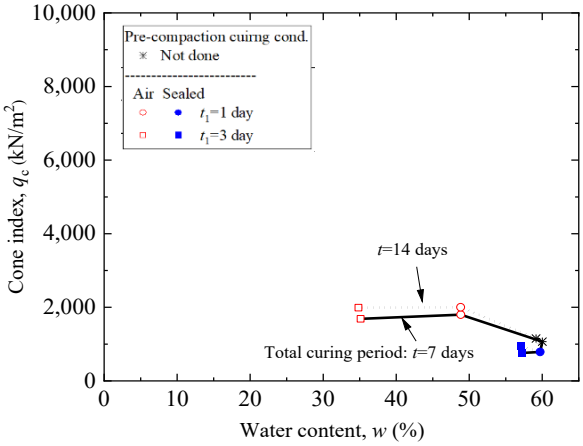

(a) PSAS-N treated sample

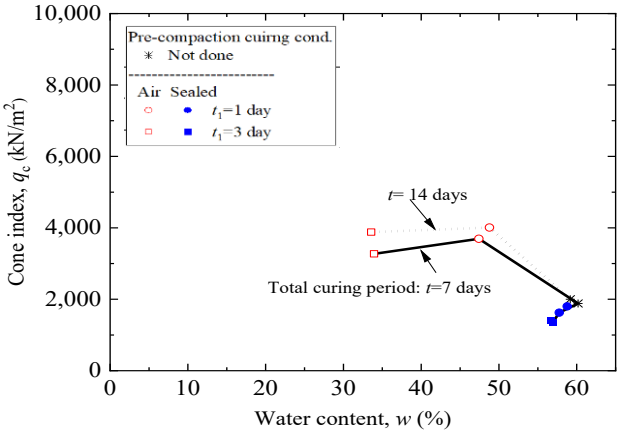

(b) PSAS-R treated sample (20%)

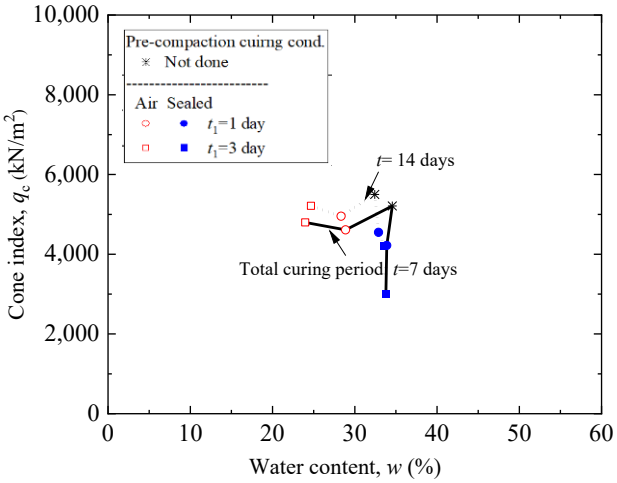

(c) PSAS-R treated sample (50%)

Figure 4.21 Relationships between (w) and (q_c)

4.7 MECHANISM OF STRENGTH DEVELOPMENT

In the context of PSAS-treated soil with different types of clay, two distinct cases are observed. In the first case, the initial strength development of the PSAS-treated soil exhibits slow progress (Ao clay treated with PSAS-N; Kasaoka clay treated with PSAS-N; Kasaoka clay treated with 20% PSAS-R) On the other hand, in the second case, the initial strength development of the PSAS-treated soil shows rapid development (Ao clay treated with PSAS-R; Kasaoka clay treated with 50% PSAS-R). Figure 4.22 (a) schematically illustrates the first case, while Figure 4.22 (b) represents the second case.

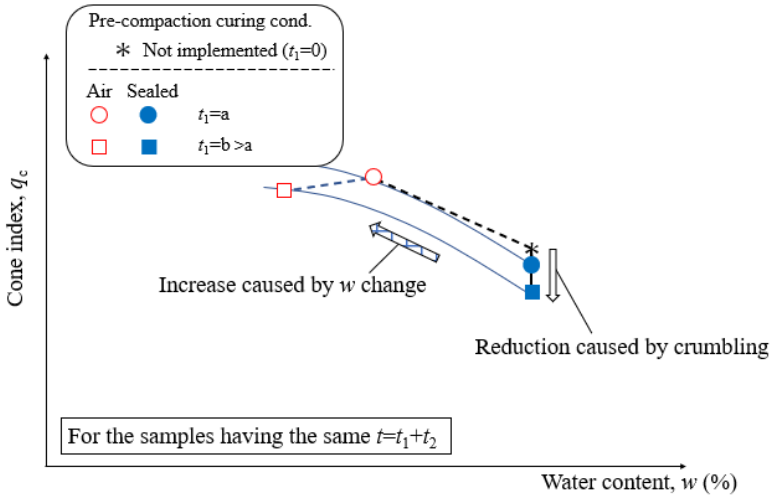

(a) Scenario with initial strength development of the PSAS-treated soil exhibits slow progress

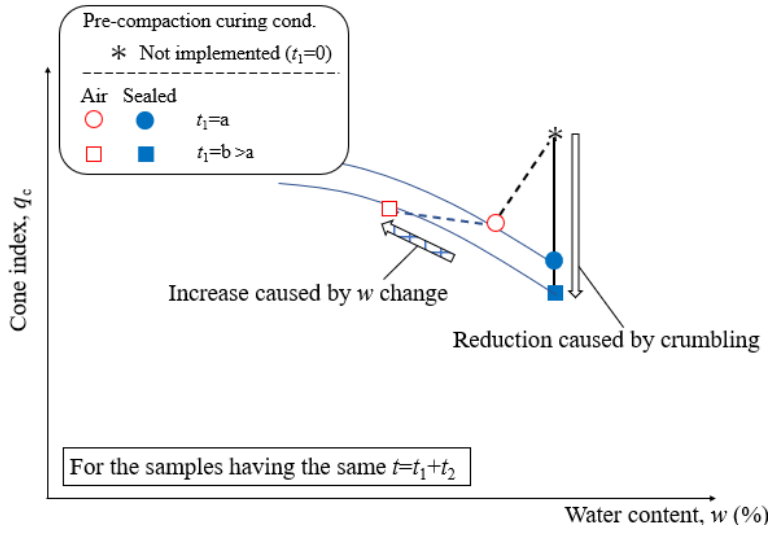

(b) Scenario with the initial strength development of the PSAS-treated soil shows rapid development.

Figure 4.22 Schematic image of the mechanism for the change in cone index of PSAS-treated samples owing to crumbling and change in water content

Based on the test results shown in Fig. 4.17 (PSASs treated with Ao clay) and Fig. 4.21 (PSASs treated with Kasaoka clay), Figs. 4.22 (a) and (b) demonstrate that the q_c values of samples with sealed pre-compaction curing are lower than that of a sample without pre-compaction curing. The water content at compaction (w) was set to be the same for the samples without pre-compaction curing and those with sealed pre-compaction curing. Figures 4.22(a) and (b) also demonstrate that with an increase in t_1, the q_c values of the samples with sealed primary curing decrease. Figure 4.22(a) shows a scenario in which initial strength development is small which means hydrate generation is low in the initial stage. So the strength reduction owing to crumbling is small. Fig. 4.22 (b) shows a scenario in which initial strength development is rapid which means hydrate generation is high in the initial stage. So the strength reduction owing to crumbling is large.

Figures 4.22(a) and (b) schematically depict the effect of w on q_c. In many scenarios, the strength of the treated soil immediately after compaction is maximized when it is compacted at a water content slightly less than w_{opt}. Meanwhile, when immersed in water, the strength of the soil compacted at or near w_{opt}, or slightly higher than w_{opt}, is often at the maximum. When the w of the PSAS-N-treated samples or PSAS-R-treated samples after air pre-compaction curing approaches w_{opt} at compaction, the q_c of the soaked samples is expected to be maximized. After the soil reach at optimum water content, with further air curing, the water content of the soil is less than the optimum water content. In this state, the soil particles have less lubrication and do not adhere as well to each other. As a result, the interparticle friction and cohesion are reduced, leading to a decrease in soil strength.

Due to air pre-compaction curing, the water content of treated soil is reduced as well as degree of saturation is also reduced. When the soil reaches its optimum water content due to air pre-compaction curing, it has the maximum amount of moisture required for optimal particle packing and inter-particle bonding. If further air pre-compaction curing is conducted, the water content decreases, and the soil particles lose some of their ability to stick together, reducing cohesion and strength.

Therefore, as shown in Fig. 4.22(a), when the strength reduction owing to crumbling is small and the strength increases owing to the reduction in water content, the q_c values of the air-cured samples can be higher than those of the samples without pre-compaction curing. This condition was applied to the samples when initial strength development is slow. However, as shown in Fig. 4.22(b), when the strength reduction owing to crumbling is significant and the strength increase owing to the reduction in water content is moderate, the q_c values of the air-cured samples can be lower those that of the samples without pre-compaction curing, although the q_c values increase from those of the samples with sealed pre-compaction curing. This condition was applied to samples where strength development is rapid.

4.8 KEY FINDINGS

4.8.1 Crumbling Effects

To determine the effects of crumbling on PSAS-treated clay, sealed pre-compression curing was performed. Here, Ao clay and Kasaoka clay were chosen based on their respective liquid limits. In addition, two distinct PSAS types, PSAS-N and PSAS-R, were utilized in this study due to their distinct water absorption and retention mechanisms, particulate size distributions, and chemical compositions.

In PSAS-treated soil, if PSAS particles get less water (the water absorption rate of PSAS is low or the mixture ratio of PSAS is less & initial water content of clay is high) (PSAS-N and Ao clay; PSAS-N and Kasaoka clay; PSAS-R (20%) and Kasaoka clay), hydrate formation in PSAS particles is negligible because all the water is initially absorbed by the pores of PSAS. The existence of fewer hydrates causes the initial strength development in the treated soil to lower and so crumbling doesn't have an effect on it.

On the other hand, In PASA-treated soil, If PSAS particles get more water (the water absorption rate of PSAS is high or the mixture ratio of PSAS is high & initial water content of clay is high) (PSAS-R & Ao clay; PSAS-R (50%) & Kasaoka clay) initially water is absorbed by the pores of the particles. After that hydrate formation occurs. It causes rapid hydrate formation in the initial stage. That's why the strength development in the treated soil in the initial stage is much high. Due to crumbling, the hydrates disappear causing a reduction in strength. Figure 4.23 describes this entire mechanism.

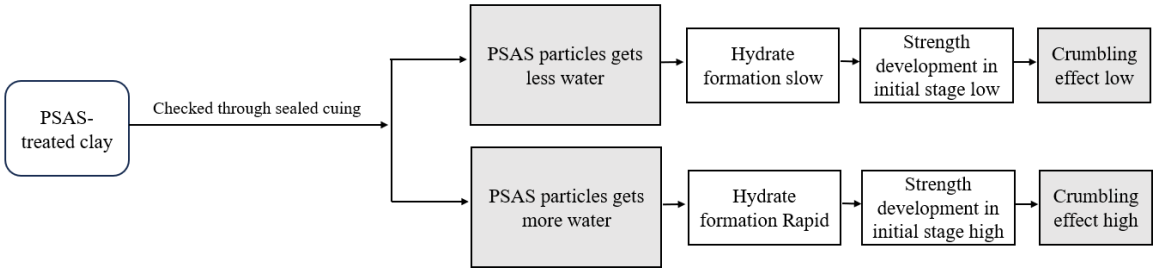

Figure 4.23 Crumbling Effects

4.8.2 Pre-compaction Curing Effect

Pre-compaction curing effect (Fig. 4.24) in PSAS-treated soil is very much related to the effect of crumbling. With air pre-compaction curing, the water content, w approaches w_{opt} at compaction. So q_c of the soaked samples is expected to be maximized. If the crumbling effect in PSAS is small, strength development in PSAS-treated soil is higher compared with samples where no pre-compaction curing is applied. On the other hand, if the crumbling effect in PSAS is high, strength development in PSAS-treated soil is lower compared with samples where no pre-compaction curing is applied. Destruction of hydrates during crumbling causes strength reduction.

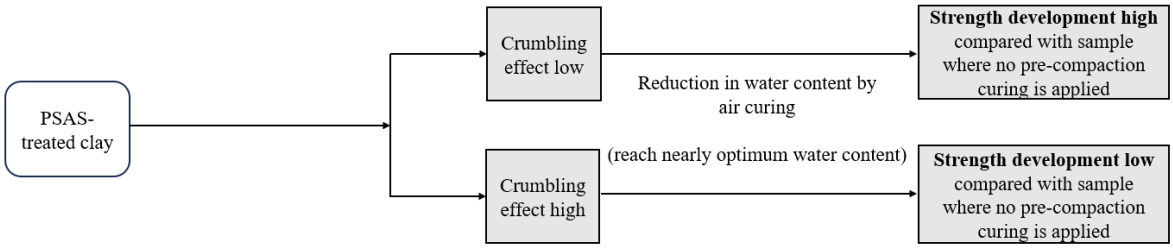

Figure 4.24 Pre-compaction curing effects

4.9 INCREASE EFFECTIVENESS OF PRE-COMPACTION CURING

The investigation revealed that in the absence of crumbling effects in PSAS, air curing for a specific duration (samples prepared for this research, it was one day) allows the soil to achieve its optimum water content, which, in turn, results in the highest strength when compacted. To expedite the pre-compaction curing process, it was bifurcated into two stages: primary and secondary curing, as depicted in Fig.4.25. The primary stage occurs before crumbling and then secondary curing accelerated water content reduction due to reduced particle size. However, the negligible impact of this crumbling on soil strength remains unaffected. This innovative approach showed potential for efficiently achieving desired soil properties

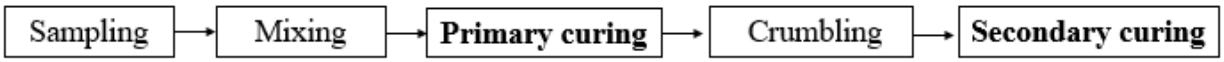

Figure 4.25 Pre-compaction curing stages

At first sample was prepared by mixing Ao clay and PSAS-N, following the conditions specified in table 4.1. Subsequently, primary curing (air) was carried out for a duration of 3 hours. Following this, the samples were subjected to the crumbling process. After crumbling, secondary curing (air) was conducted for an additional 2 hours. Through this approach, the samples achieved nearly optimum water content within 5 hours (Fig.4.26), significantly reducing the time required compared to the previous duration of 1 day (Fig.4.9(a)).

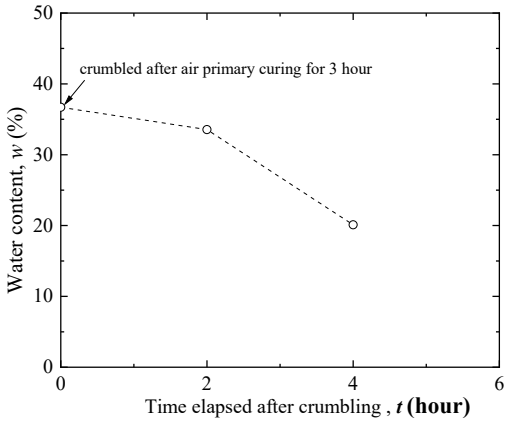

Figure 4.26 water content reduction due to two-stage pre-compaction curing

4.10 SUMMARY

This chapter examined the effects of primary curing and crumbling on the physical, compaction, and strength of PSAS-treated soils using two types of PSASs with varied water absorption and retention. Whether sealed or air primary-cured, PSAS-treated samples disintegrated into particles resembling sand and gravel. It is also discovered that samples with a lower water content were more fragile. For samples treated with BFCB, the same observation was made. At first, construction generated soil was made with Ao clay. It was discovered that the oven-dried samples of each treated sample did not match the combined PSDs, which were calculated by adding the PSDs of each material. This demonstrates that particles treated with PSAS and BFCB are chemically bonded. According to the results of the compaction test, the dry densities of PSAS-treated samples with sealed primary curing were almost identical to those without primary curing for one type of PSAS. The same pattern was observed in samples treated with BFCB. For the other types of PSAS, the PSAS-treated samples with sealed primary curing had lower dry densities than those without primary curing. Depending on the initial strength development, the degree of disturbance caused by the disintegration may vary. The rapid formation of hydrates in one type of PSAS may have substantially disturbed the treated samples, resulting in a decrease in dry density, due to their crumbling. The cone index tests performed after post-compaction curing in a soaked environment indicated that the cone indexes of the PSAS-treated samples with pre-compaction curing were either higher or lower than those of the PSAS-treated samples without pre-compaction curing, depending on the pre-compaction curing environment, number of curing days, and type of PSAS. The difference was attributed to the combined effects of "strength loss due to crumbling" and "strength gain due to water content reduction during compaction." For PSAS-treated soils with early strength development, the mechanism suggests that the strength reduction induced by crumbling should be considered. However, for PSAS-treated soils with delayed strength development, adjusting the water content of the treated soils during pre-compaction curing prior to compaction is effective. The repeatability of the test is checked by making construction-generated soil with Kasaoka clay. Finally, it is suggested for PSAS-treated soil without any crumbling effects, the precompaction curing can be divided into two stages. It accelerate strength within shortest possible time. These newfound understandings are essential for applications of PSAS-treated soils in which compaction is a necessary step. When considering PSAS-treated soils that gain early strength, it is important to take into account the strength fall that is produced by crumbling. However, for PSAS-treated soils that have a gradual development of strength, it is helpful to modify the water content of the treated soils correctly during pre-compaction curing before compaction. This is done in order to prepare the soil for compacting. In addition, it is necessary to adjust the curing conditions in the laboratory mixture design so that they are reflective of the conditions found in the field. This is carried out to ensure that there is no disparity between the observations made in the field and those made in the laboratory. It is important to note that the cone index was used to evaluate the mixture design strategy presented in this work for PSAS-treated soils. This is due to the fact that in Japan, the classification and application of construction-generated soils are frequently judged by the cone index q_c. On the other hand, the treated soils can be required to reach a particular level of performance with regard to aspects such as strength, stiffness, permeability, and so on. After estimating the mixing condition using the proposed

method, it is required in these situations to confirm the performance by carrying out mechanical tests or testing of the hydraulic conductivity. Additionally, research on the impact of environmental changes, such as recurrent wetting and drying, on the longevity of treated soils will be required, and this topic is going to be covered in the following chapter.

References

Dong, P.H., Hayano, K., Kikuchi, Y., Takahashi, H., Morikawa, Y., 2011. Deformation and crushing of particles of cement treat granulate soil. Soils and Foundations. 51(4), 611–624.

H. Takahashi, Y. Morikawa, E. Ichikawa, K. Hayano, Y. Okusa Model tests on compressibility and bearing capacity of lean-mixed granular cement treated soil JSCE Journal of Geotechnical and Geoenviromental Engineering, 66 (2) (2010), pp. 236-249

Hayano, K., Fujishima, K., 2013. Effects of paper sludge ash and fly ash on mixture design of cement-treated granulated soils. Geotechnics for Sustainable Development (Phan, DL ed.), 375–378.

Hayano, K., Yamauchi, H., Wakuri, N., Tomiyoshi, S., 2016. A new granulation method with the process of crumbling partially-cemented liquid muds and its application to a motocross track. Procedia Engineering. 143, 98–103.

Japanese Geotechnical Society. Standards. JGS, 0716, 2009: Test method for cone index of compacted soils. JGS, Tokyo, Japan.

Japanese Geotechnical Society. Standards. JGS 0122–2009: Test method for water content of soils by the microwave oven. JGS, Tokyo, Japan.

Japanese Geotechnical Society. Standards. JGS 0131–2009: Test method for particle size distribution of soils. JGS, Tokyo, Japan.

Japanese Geotechnical Society. Standards. JGS 0141–2009: Test method for liquid limit and plastic limit of soils. JGS, Tokyo, Japan.

CHAPTER 5

DURABILITY ASSESSMENT THROUGH POST-COMPACTION CURING

5.1 INTRODUCTION

In Chapter 4, we examined the influence of pre-compaction curing and crumbling on the conventional flow diagram for the laboratory mixture design test. It has an effect on pre-compaction curing and subsequent crumbling which is a little different from cement-treated soil depending on the initial strength of PSAS-treated soil. It is therefore anticipated that post-compaction curing will also affect PSAS-treated specimens. For instance, when PSAS-treated soil is used to construct irrigation earth dams, the soil may be subjected to dry and wet cycles, which may cause a change in the soil's strength. This is possible when soil is used to construct irrigation earth barriers. These cycles have an effect on the soil's durability when treated with PSAS. Commonly, the durability of cement-treated soil is evaluated using unconfined compressive strength, which is inapplicable to PSAS-treated soil due to their dissimilar water absorption mechanisms. This chapter will introduce a novel concept for assessing the durability of PSAS-treated soil.

5.2 ASSESSMENT OF DURABILITY

There has not been a thorough investigation of how post-compaction curing conditions affect the development of strength in the material. For instance, when PSAS-treated soil is used to construct irrigation earth dams (Watanabe et al., 2021), the soil may be subjected to dry and wet cycles, which may result in a change in the strength of PSAS-treated soils. This can occur when the soil is used to build irrigation earth dams. Previous research conducted on soils treated with lime or cement demonstrated that dry and wet cycles affect the development of the soil's strength (Khoury and Zaman 2002, 2007; Zhang and Tao 2006; Beriha et al., 2018). Additionally, previous research demonstrated that the soil's strength varies as a result of continual drying and wetting, depending on the conditions (Beriha et al., 2018, Ye et al., 2018). As a result, conducting proper evaluation tests to determine the durability of soils that have been treated with cement or lime is frequently necessary. However, the durability of PSAS-treated soils subjected to repeated drying and wetting and the evaluation of their durability are currently unknown.

In light of the information presented above, the purpose of this study was to conduct a series of evaluations in order to evaluate the durability of PSAS-treated clays that were placed in environments that alternated between dry and wet conditions. First, clays that had been subjected to a variety of pretreatments were analyzed with regard to their particle sizes. Unconfined compression tests using demolded specimens were carried out on treated clays that had been subjected to several cycles of drying and wetting. Unconfined compression strength is the most common test for evaluating the stability of cement or lime-treated soil. Discussions on the durability assessment of PSAS-treated clays are presented, considering the characteristics of each evaluation test while comparing the test results with those of cement-treated clays.

5.2.1 Assessment with Particle Size Analyses

Sieve analyses were performed on PSAS-N-, PSAS-R-, and BFCB-treated samples to investigate the differences in the PSDs due to differences in the pretreatment conditions. Table 5.1 summarizes the mixture conditions for the treated samples. As shown in the table, to make the initial water content of Ao clay equal to the liquid limit, w_L, it was modified to w = 40.7%. Afterwards, to prepare PSAS-N- and PSAS-R-treated samples at a dry mass ratio of 20%, we combined PSAS-N or PSAS-R with Ao clay, whereas for samples treated with BFCB, the stabilizer was mixed with Ao clay at a dry mass ratio of 6 %. A compact kitchen mixer was used to combine the samples for 10 min. Consequently, pre-compaction curing was conducted on each treated sample for one day under exposure to air (hereafter referred to as air pre-compaction curing). After air-pre-compaction curing, each sample was crumbled for 2 min using the same compact kitchen mixer.

Table 5.1 Mixture conditions for PSAS-N-treated, PSAS-R-treated and BFCB-treated samples

Type of sample	Water content of Ao clay, w (%)	Additional ratio of PSAS-N or PSAS-R, A_{PS} (%)	Additional ratio of BFCB, A_{BFCB} (%)
PSAS-N-treated samples, PSAS-R-treated samples	40.7 ($w = w_L$)	20	0
BFCB-treated samples		0	6

After that, sieves ranging from 0.075 to 75 mm were employed to conduct the analysis on each sample. The JGS 0131 method was followed when doing sieve analyses. This protocol specifies that soil samples be rinsed with water while being stirred by hand, and then dried in the oven before sifting. This process can be thought of as giving the samples with a combination of a dry and wet environment. In contrast, for the purpose of this investigation, sieve analyses were initially carried out on each treated sample while it was still in its unprocessed state, which means that neither washing nor drying was carried out in advance of the analyses. After that, the sieve analyses were carried out on the dried samples that had previously been washed with water for three minutes before being dried in an oven at 110° C. In the end, dry samples were subjected to another cycle of sieve analysis. These samples had previously been washed for 15 minutes and then dried in an oven at 110° C.

The PSDs of samples treated with PSAS-N, PSAS-R, and BFCB, respectively, are displayed in Figure 5.1 (a), (b), and (c), depending on which of the above three pretreatment conditions they were subjected to. In addition, the figures present the integrated PSDs, which were calculated by taking into account the PSD of each individual material (Chapter 3) and the mixture ratio (Table 5.1) respectively. According to the figures, the samples that were treated with PSAS-N or PSAS-R consisted of particles that were the size of sand and gravel when they were in their natural state. This was the case even though the samples had not been washed or dried before to the sieve examinations. There was no evidence of fine content found. This was similarly the case for the samples that were treated with BFCB. In the meantime, the oven-dried samples had fine contents, despite the different types of stabilizers. On the other hand, the PSDs of the samples that were

dried in an oven did not correspond to those of the combined PSDs. This suggests that the particles within the treated samples must form chemical bonds with one another at some point. In addition to the particle disintegration caused by rinsing, furnace drying was thought to cause the loss of some hydrates such as ettringite (Bannai and Nakagawa, 1968, Nozawa et al. 2017, Harashima and Ito, 2015), which resulted in the particle disintegration and produced fines. As shown in Fig. 5.1, the appearance of finer contents was related to the length of the washing period. This was due to the fact that increasing the length of time spent washing increased the possibility of particle wear and fragmentation. As a result of these observations, there is a growing concern that the PSAS-treated clays and the BFCB-treated clays may turn out to be muddy. On the other hand, it is quite doubtful that the treated clays, once the structure is complete, will be subjected to a condition in which they will be washed with water while being agitated.

5.2.2 Assessment with Unconfined Compression Tests

In the second part of the process, unconfined compression tests were carried out on samples that had been treated with PSAS-N, PSAS-R, and BFCB in order to study the change in strength that was associated with dry-wet curing. In accordance with the mixing conditions detailed in Table 5.1, samples treated with PSAS-N, PSAS-R, and BFCB were created. After layering each mixture three times in a steel mold with internal dimensions of 50 mm in diameter and 100 mm in height, each layer was then compressed 12 times with a 1.5 kg rammer at a drop height of 20 cm. The final product had dimensions of 10 mm in diameter and 100 mm in height. After that, the specimens that had been compacted together with the molds , and were allowed to cure for three days at a temperature of 20 ±1 ℃ indoors (Figure 5.2). After that, we removed the molds from the specimens. A small number of samples from each treated group went through a series of dry-wet curing cycles (Figure 5.2), while the remaining samples were continually soaked in water. During each dry-wet curing cycle, the samples were dried in an oven at a temperature of 40 ℃ for two days, and then wet for one day by being submerged in water. The specimens were subjected to unconfined compression testing in accordance with JGS 0511 after undergoing either repetitive drying-wetting curing cycles or continuous soaked curing. The unconfined compression test described above was conducted three times for the samples prepared under the same conditions.

Figure 5.3 shows the change in the unconfined compressive strength q_u of the specimens associated with the wetting curing or soaked curing. The figure shows the mean value of qu and the range of variation of the three test results for each case. For the BFCB-treated samples, the mean value of q_u increased with increasing curing period, regardless of the curing conditions. . The average value of qu was slightly higher for the dry-wet curing than for the soaked curing. This could be due to the accelerated hydration reaction of the cement at higher curing temperatures (Babasaki, et al., 1996). However, the mean value of q_u increased for the PSAS-N- and PSAS-R-treated samples in the case of soaked curing; however, the mean value of q_u decreased in the case of dry-wet curing after several dry-wet curing cycles. The mean value of q_u decreased earlier in the dry-wet curing for the PSAS-R-treated samples than for the PSAS-N-treated samples. The reason behind this decrease is due to loss of hydration. In PSAS-N, initially, hydrate generation is slow as described in the previous chapter. At first, by drying hydrate generation is accelerated upto 3rd cycle. Then after that the hydrates started decreasing due to repeated drying. In PSAS-R, initial water

absorption was very high which cause this strength increase in 1st cycle. But this water is absorbed by pores of PSAS particles. During drying they disappear & cause complete failure of sample in this second cycle. As shown in Fig. 5.4, the repeated dry-wet-curing-induced cracks in the PSAS-R-treated specimen, resulting in the loss of the integrity of the specimen. Based on these results, it is reasonable to conclude that the samples treated with PSAS-N and PSAS-R have a durability that is lower than that of the samples treated with BFCB when subjected to dry-wet curing cycles. However, there is still the question of whether the evaluation carried out using unconfined compression test specimens is suitable for the PSAS-treated samples. This is because water absorption and retention are both physically driven by the pores that are present in the PSAS particles. On the other hand, water absorption and retention in BFCB-treated soil is completely occurs through a chemical reaction. The decrease in q_u in the PSAS-treated sample could be partially due to the loss of cementation; however, without restraint, the PSAS-treated specimens should easily fail in their dry states even though water absorption and retention are physically induced by the pores of the particles. As with the BFCB-treated samples, the hydration reaction in the PSAS-treated samples may be accelerated at higher temperatures, resulting in a higher q_u as observed in the early stages of dry-wet curing of PSAS-N-treated samples. However, if the contribution of physical water absorption and retention by the particles' pores to the strength development is significant, the PSAS-treated samples without restraint should easily fail in their dry states, although the pores were not lost in the drying process. In Fig.8, the PSAS-R-treated samples failed earlier in the dry-wet curing process than the PSAS-N-treated samples, suggesting that the contribution of physical water absorption and retention to the strength development was higher for the PSAS-R-treated samples. This was consistent with the higher initial W_{ab} of PSAS-R than PSAS-N in Fig. 3.3, because physical water absorption and retention was expected to occur immediately after the PSASs contact with water.

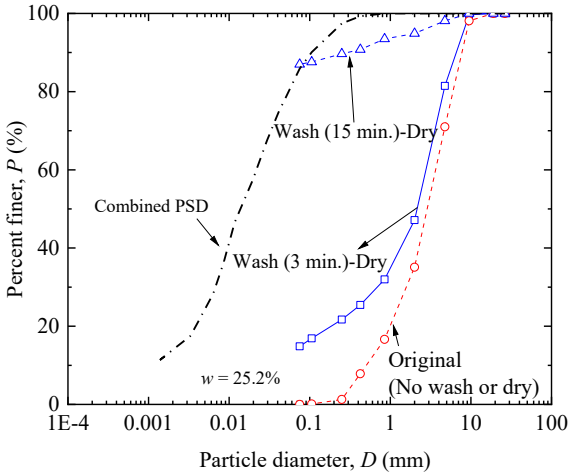

(a) PSAS-N-treated samples

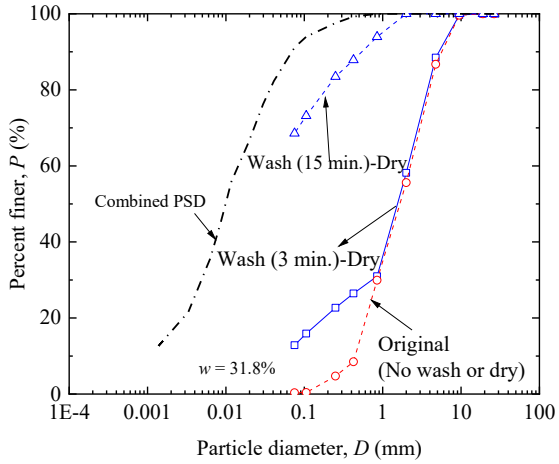

(b) PSAS-R-treated samples

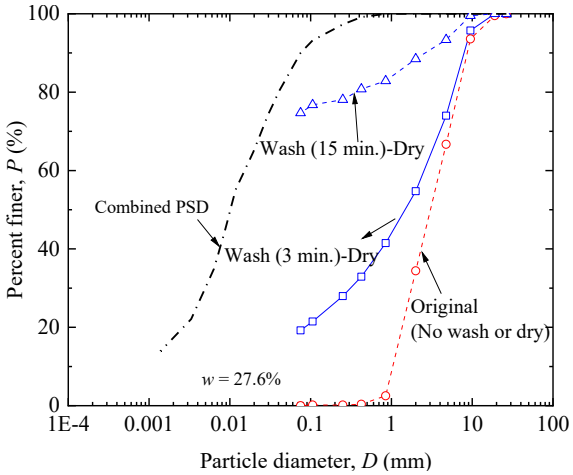

(c) BFCB-treated samples

Figure 5.1 PSDs of each treated sample with three pretreatment conditions

(a) Sample kept 20 ±1 ℃ for 3 days

Dry curing

Wet curing

Figure 5.2 Unconfined Compression test specimen preparation

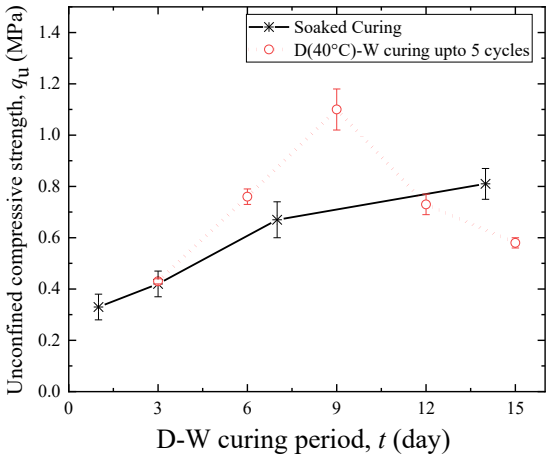

(a) PSAS-N

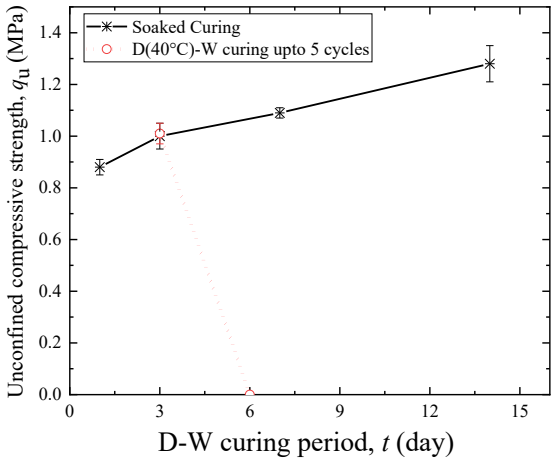

(b) PSAS-R

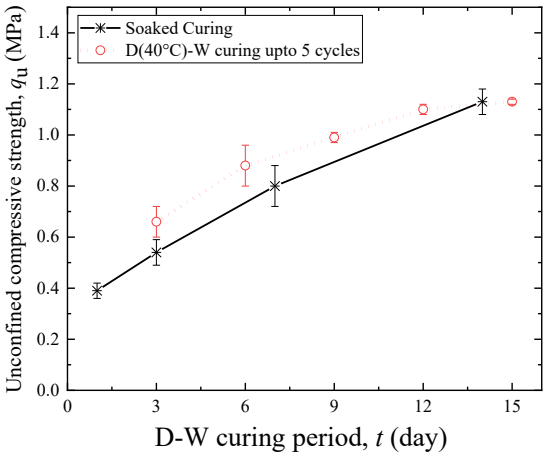

(c) BFCB

Figure 5.3 Change in unconfined compressive strength associated with dry-wet curing and soaked curing



(a) PSAS-N after 5 cycles (b) PSAS-R after 2 cycles (c) BFCB after 5 cycles

Figure 5.4 Specimen after the dry-wet curing cycles

5.3 ASSESSMENT OF DURABILITY FROM CONE INDEX TEST

In contrast to BFCB, which gains strength through the process of solidification brought on by hydration, PSASs develop a certain amount of strength by the physical absorption and retention of water, as was covered in Section 6.2. In light of this, it is possible that the results of the evaluation of the treated clay's durability will differ depending on whether or not the PSAS-treated sample was restrained. In light of the information presented above, a series of cone index tests were carried out in molds using materials that had been treated with PSAS-N, PSAS-R, and BFCB in order to study the change in strength that is related to dry-wet curing.

5.3.1 Specimen Preparation and Curing Conditions

The preparation of the samples that were treated with PSAS-N, PSAS-R, and BFCB was carried out in accordance with the mixture conditions detailed in Table 5.1. The process for preparing the sample was precisely the same as the one detailed in section 5.2.2.

Compaction was carried out in molds in accordance with the JGS standard JGS 0711 immediately following the preparation of the samples in order to prepare the specimens. Before being poured into a mold with a diameter of 10 cm, each sample was first divided into three equal layers. After carefully setting up each successive layer, the mold was subjected to a series of 25 blows from a hammer weighing 2.5 kg and fell from the distance of 30 cm. After molds were made by compacting the treated materials as specimens, the specimens were cured using a variety of processes. Some specimens were cured in an atmosphere that was continually soaked, while others were cured using a dry-wet process. The specific conditions required for soaking curing and wet curing are outlined in Table 5.2.

For soaked curing, every mold containing the treated samples was submerged in water. The entire mold was cured while submerged in water such that the top of the specimen was below the surface. Various total curing periods, t=1, 3, 7, 14, 28, and 45 days, were used, as listed in Table 5.2. After the appropriate soaked curing period, cone index tests were performed according to JGS 0716. It should be noted that Ca leaching occurs over a long period when cement-treated soil is soaked in water. For example, Hashimoto et al. (2008) have pointed out that the water to solid ratio during

soaking affects the amount of Ca leached. The same is likely to occur with PSAS-treated soils. However, the strength degradation associated with Ca leaching occurs slowly over a long period. The Ca leaching starts from the exposed surface and gradually progresses to the interior of treated soils. Laboratory and field test results summarized by Takahashi et al. 2018 shows that the depth of strength degradation due to Ca leaching is only about 10 mm or less in one year. In this study, the maximum period of immersion of treated soils was 45 days, and in this case, the degradation may be only about 1 mm from the top surface for a specimen height of 127 mm. In addition, the cone index is evaluated based on penetration resistance at penetrations of 50, 75, and 100 mm from the top surface. Thereby, the strength changes associated with the Ca leaching were considered negligible. Based on the above, we did not control the value of the water to solid ratio during immersion of treated clays.

Whereas, for the cases of dry-wet curing, specimens were dried at temperatures of T=40 ºC or 80 ºC. There is no test method available to study the effect of dry and wet (D-W) cycles on the durability of sustainable materials. The standard procedure (ASTM D559 2015- Standard Test Methods for Wetting and Drying Compacted Soil-Cement Mixtures) was slightly modified for this study. That's why, in the drying process, a high temperature, 80 °C was used in this study. Also, in PSAS, existence of ettringite was found. Previous studies shows at 80 °C hydrates like ettringite disappear (Kawai et al. 2018). To check that effect, 80 °C was used in this research. After drying for the required period, as shown in Table 6.2, the specimens were soaked in water in the same manner as mentioned before. For all cases, the wet (soaked) curing period was one day. The duration of drying and wetting were determined based on the respective dry and wetting periods (42hrs and 5hrs) specified in ASTM D 559, considering the ease of working on a 24hrs basis. The specimens were subjected to the dry-wet curing process for several cycles, as shown in Table 5.2. Figure 6.5 shows the specimens under dry- and wet-curing conditions. In the case of a single dry-wet cycle curing, the effects of different drying periods on the treated specimens were investigated. The temperature was set at 40 ºC to prevent the loss of ettringite during drying. The two-day drying at 40 °C and one-day wetting curing was repeated for 1, 2, 3, 4, 5, 6, 7, 8, and 15 cycles. The two-day drying at 80 °C and one-day wetting curing was repeated for one, two, three, and four cycles. The 5-, 8-, and 14-day drying at 40 °C and one-day wetting curing were cycled only once. After completing dry-wet curing for the required number of cycles, cone index tests were conducted.

Table 5.2 Conditions for curing for PSAS-N-treated, PSAS-R-treated, and BFCB-treated specimens

Curing type	Dry at 40º C (days)	Dry at 80 ºC (days)	Wet (Soaked) (days)	Number of D-W cycles
Soaked curing	N/A	N/A	1, 3, 7, 14, 28, 45	N/A
Dry-Wet curing	2	N/A	1	1, 2, 3, 4, 5, 6, 7, 8, 15
	N/A	2		1, 2, 3, 4
	2, 5, 8, 14	N/A		1

(a) Dry curing (b) Wet curing

Figure 5.5 Specimens subjected to dry-wet curing

In addition to those for the cone index tests described above, specimens (molded samples) were prepared in the same way to verify the internal drying and wetting conditions. The cone index specimen was 100 mm in diameter and 127 mm high, larger than the unconfined compression test specimen (50 mm in diameter and 100 m high). In addition, because the specimen was contained in a mold, water cannot enter or exit from the sides of the specimen, but only from the top. Therefore, it was checked whether the specimens dried or wetted uniformly during dry-wet curing. Specially, after drying and wetting, the samples were removed from the mold and the water content, w, was measured based on JGS 0122. Figure 5.6 (a) shows the profiles of w along the specimen height after drying at 40 º C and Fig. 5.6 (b) shows those after wetting. Although there was some variation, w was distributed almost homogeneously throughout the specimens under both dry and wet conditions.. Figure 5.6 (c) shows the difference in the w between drying and wetting processes. The difference in w between the PSAS-treated specimens was higher compared with that between the BFCB-treated specimens. Based on the results in Fig.5.6 (c), we investigated in more detail whether different types of stabilizers retained different amounts of moisture during dry-wet curing cycles.

Figure 5.7 shows examples of the change in w and the degree of saturation, S_r due to the dry-wet curing cycles for the PSAS-N-, PSAS-R-, and BFCB-treated specimens. In all cases, higher temperatures resulted in specimens with lower w as well as S_r at the drying state. Notably, S_r decreased in PSAS-treated specimens than in BFCB-treated specimens during drying, although the additional amount of PSASs was higher than that of BFCB. This may be because the water absorbed and retained by the pores of the particles evaporated more easily during drying than the water bound in the hydrates. However, the S_r of the PSAS-treated specimens during drying increased gradually with the number of dry-wet curing cycles, indicating that the hydration progressed in the pores with the cycles so that the contribution of the physically absorbed and retained water decreased. More detailed confirmation of the above assumed phenomenon will be necessary in the future study, e.g., by microscopic structural and crystallographic investigations, as in Yoobanpot et al. 2020a, 2020b; Jamsawang, et al. 2021.

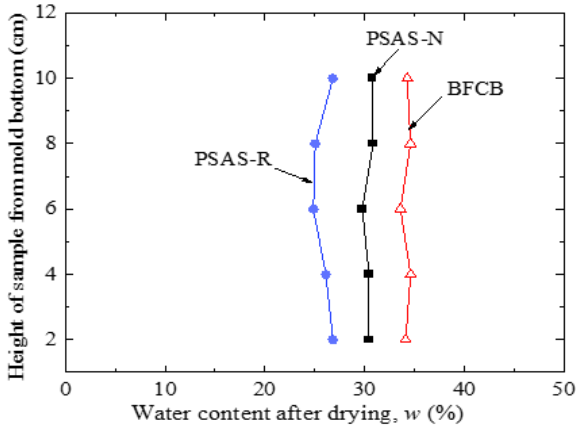

(a) Water content after drying

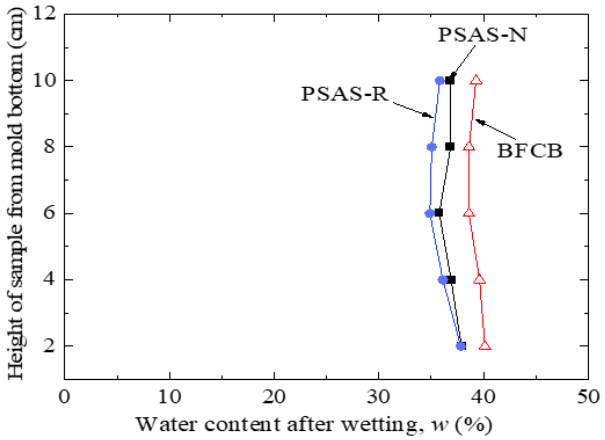

(b) Water content after wetting

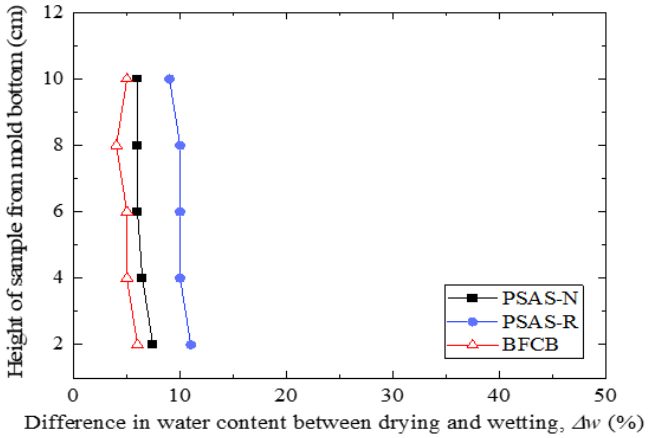

(c) Difference in water content between drying and wetting conditions

Figure 5.6 Water content profiles of the specimens subjected to two days of drying at 40 ºC and one-day wetting (D: dry, W: wet)

Finally, the effect of different drying periods on the water retention of each treated clay was examined. Figure 5.8 shows the changes in w and S_r for different drying periods at 40º C for the PSAS-N-, PSAS-R-, and BFCB-treated specimens. In all observations, the longer the drying period, the lower the w as well as the S_r. It was again observed that S_r was lower in PSAS-treated specimens than in BFCB-treated specimens during drying.

5.3.2 Strength Development Associated with Dry-Wet Curing

Figure 5.9 shows the correlation between the cone index, q_c, and curing period, t, of the treated specimens that were continuously soaked in water. The PSAS-R-treated specimens exhibited a significant increase in strength in the early stage, whereas the PSAS-N-treated specimens exhibited a comparatively low strength in the early stage, and a gradual increase in strength was observed. The difference observed in q_c in Fig. 5.9 is partially consistent with the difference in W_{ab} between PSAS-N and PSAS-R as described in Chapter 4. However, as shown in Chapter 4, the W_{ab} of both PSAS-N and PSAS-R hardly increased after 24 h, whereas as shown in Fig. 5.9, q_c of the treated specimens increased after 24 h. Although the details of the reason for this gap require further study, it is assumed that the reaction between the PSASs and Ao clay might contribute to the strength increase. Additionally, Fig. 5.9 shows that the BFCB-treated samples exhibited strengths that were intermediate to those of the PSAS-R-treated and PSAS-N-treated samples. However, the addition ratios of BFCB and PSASs were different.

Figure 5.10 shows the relationships between q_c and t of the PSAS-N-, PSAS-R-, and BFCB-treated specimens subjected to dry-wet curing. The relationships between the specimens that were continuously soaked in water are also shown in the figure. As shown in Fig. 5.10, the q_c of the BFCB-treated specimens subjected to the cycles of two days drying at 40 ℃ and one-day wetting curing increased with the t. This was also true for PSAS-N- and PSAS-R-treated specimens. This observation is different from that obtained from the unconfined compression test results shown in Fig. 5.3. As described in Section 5.2.2, q_u of the PSAS-N- and PSAS-R-treated specimens decreased in the case of dry-wet curing after several dry-wet curing cycles. The difference observed between the cone index and unconfined compression test results suggested that care should be taken when testing methods to evaluate the durability of PSAS-treated soils subjected to dry-wet curing.

In Figs. 5.10 (a) and (b), the q_c values of the PSAS-treated specimens subjected to the cycles of two-day drying and one-day wetting curing were higher than those of the specimens continuously soaked in water. As described in Section 5.1, not only the water absorption and retention by the pores of the particles but also hydration might have occurred in the PSAS. In this scenario, the strength development of the PSAS-treated specimens during the curing period could be accelerated by high temperatures during drying. The results shown in Fig. 5.10 (c) also suggest that the hydration in the BFCB-treated specimens could be accelerated by high temperatures during drying. Nevertheless, it is interesting to note that the q_c of the specimens subjected to 8- or 14-day drying curing tended to be lower than that of the specimens subjected to the two-day drying. This was also true for each type of treated specimen. This trend may be attributed to the free water in the

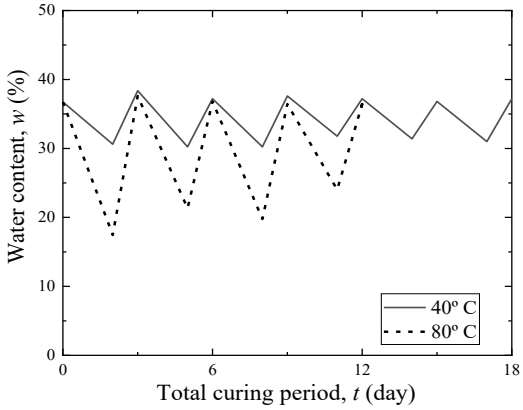

(a-1) w (PSAS-N)

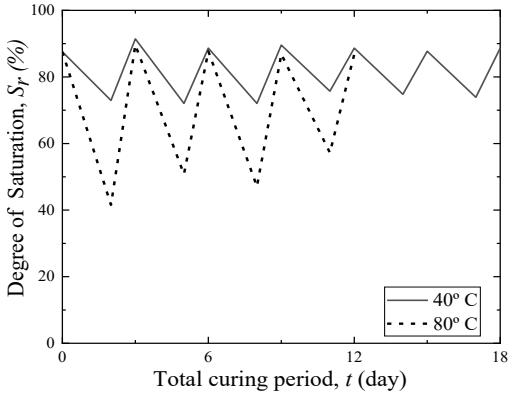

(a-2) S_r (PSAS-N)

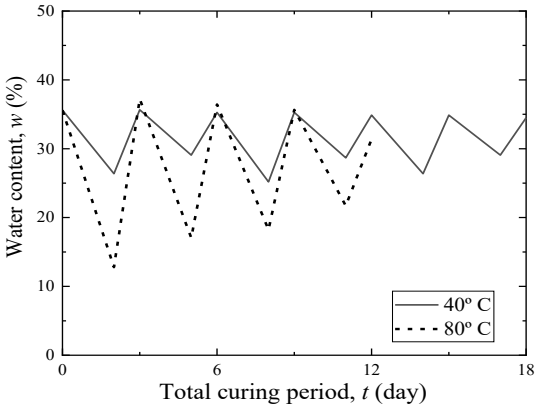

(b-1) w (PSAS-R)

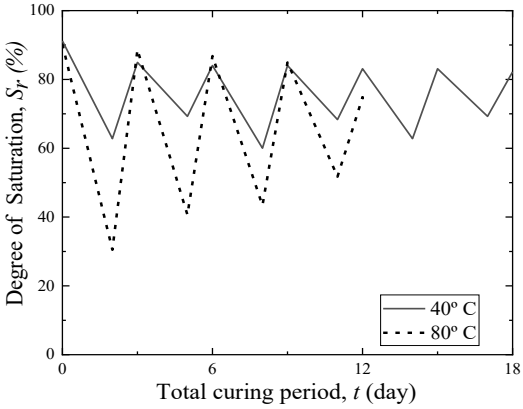

(b-2) S_r (PSAS-R)

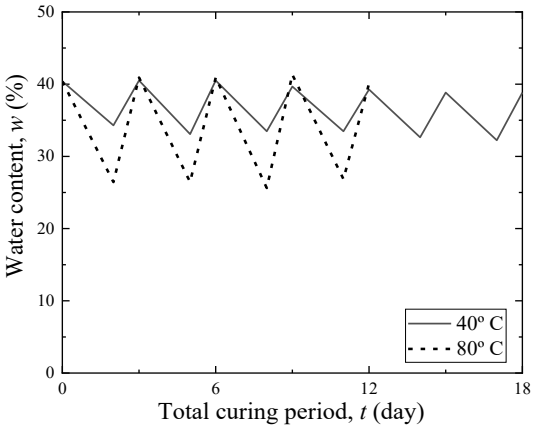

(c-1) w (BFCB)

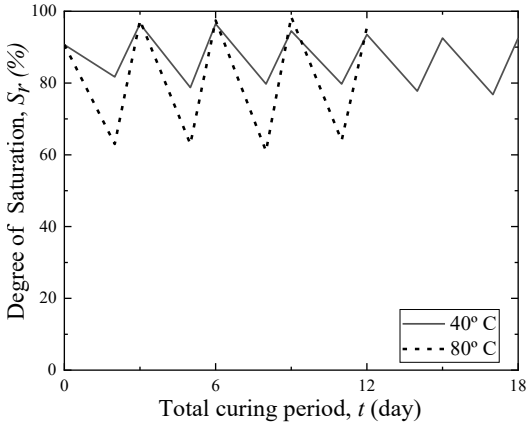

(c-2) S_r (BFCB)

Figure 5.7 Examples of change in w and S_r due to repeated dry-wet curing cycles

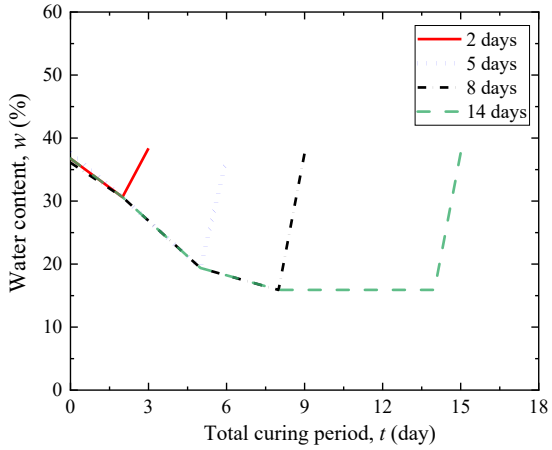

(a-1) w (PSAS-N)

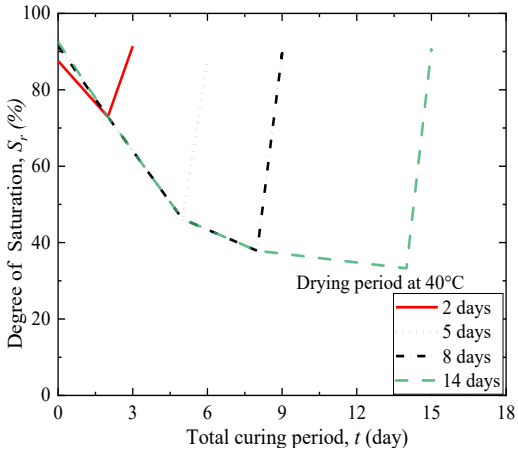

(a-2) S_r (PSAS-N)

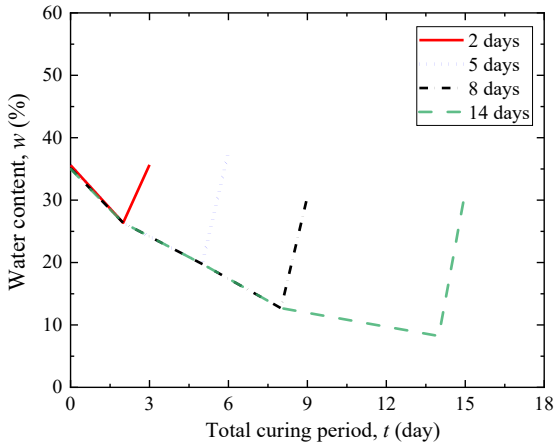

(b-1) w (PSAS-R)

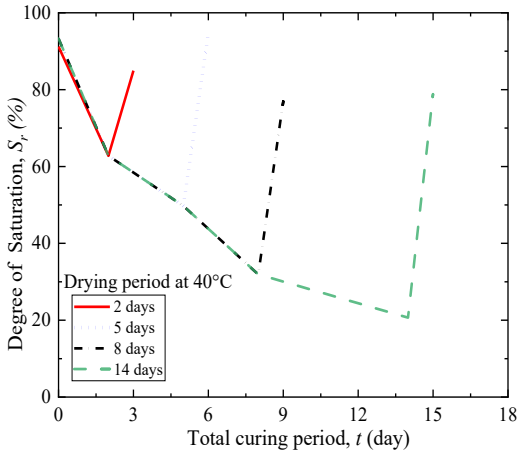

(b-2) S_r (PSAS-R)

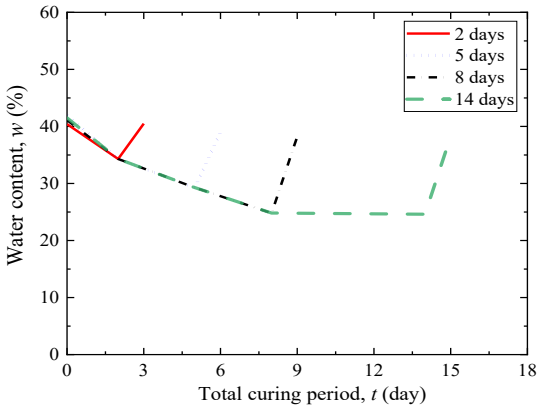

(c-1) w (BFCB)

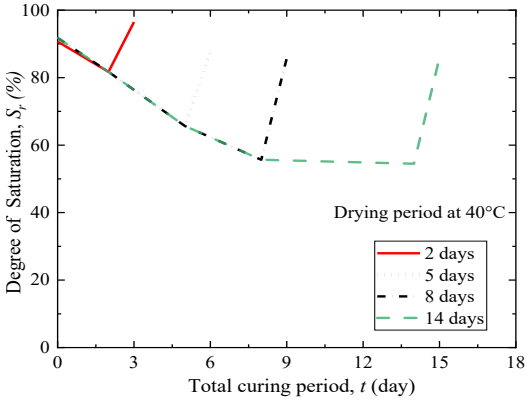

(c-2) S_r (BFCB)

Figure 5.8 Change in w and S_r due to dry-wet curing (drying at 40 ºC)

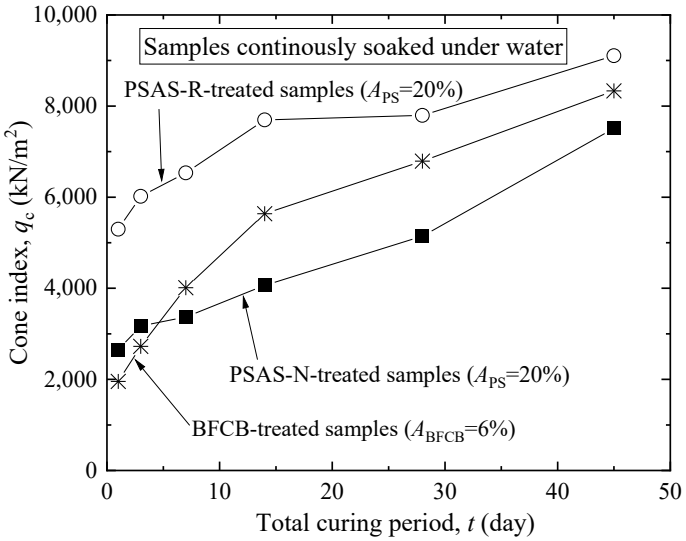

Figure 5.9 Connections between the cone index, q_c and the curing period, t for the soaked curing condition

treated specimens becoming insufficient through long-term drying for further hydration development.

The maturity index M has often been used to predict q_u of cement-treated soils with various curing temperatures and curing periods. The maturity is the concept to combine the effects of curing time and temperature. In this study, attempts were made to apply the concept of maturity to evaluate q_c of PSAS-treated specimens. In his keynote lecture, Kitazume, 2020 summarized equations proposed by previous studies to define different M denoted as M_1, M_2, M_3 and M_4 for cement-concrete or cement-treated soils. Among the M_1, M_2, M_3 and M_4, the following M_2 and M_4, which are relatively commonly used for cement treated soils in Japan, were selected in this study to apply the concept of maturity to q_c of the PSAS-treated specimens.

$$M_2 = \Delta t * (2.1)^{(T-T_0)/10} \quad (1)$$

$$M_4 = 2 * \exp\left(\frac{T-T_0}{10}\right) * \Delta t \quad (2)$$

where M (M_2 and M_4) the maturity index, T is the curing temperature (°C), T_0 is the reference temperature (-10°C), and Δt is the curing period (days).

Figures 5.11 and 5.12 show the relationships between q_c and M_2 or M_4, respectively. Figures (a), (b), and (c) show the relationships between PSAS-N-, PSAS-R-, and BFCB-treated soil specimens. Irrespective of the stabilizer type, q_c increased with an increase in M_2 or M_4. In addition, the differences in q_c between the continuously soaked curing samples and the dry-wet curing specimens were small, except for specimens with S_r reduced below a certain level during drying. Specifically, when S_r was lower than 50% for PSAS-N, 45% for PSAS-R, and 65% for BFCB, q_c

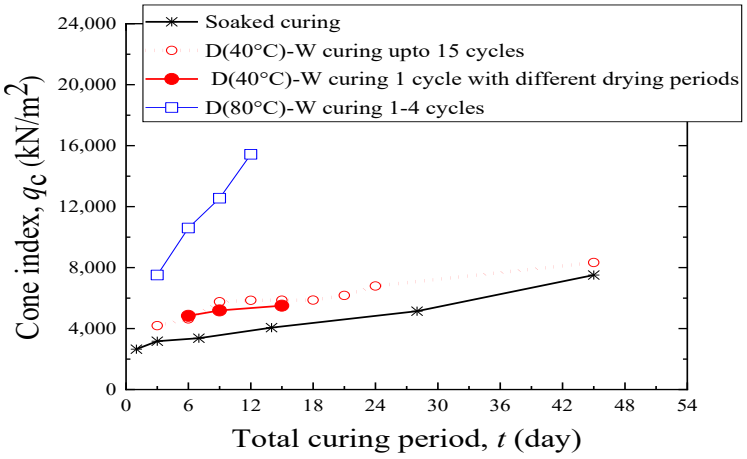

(a) PSAS-N

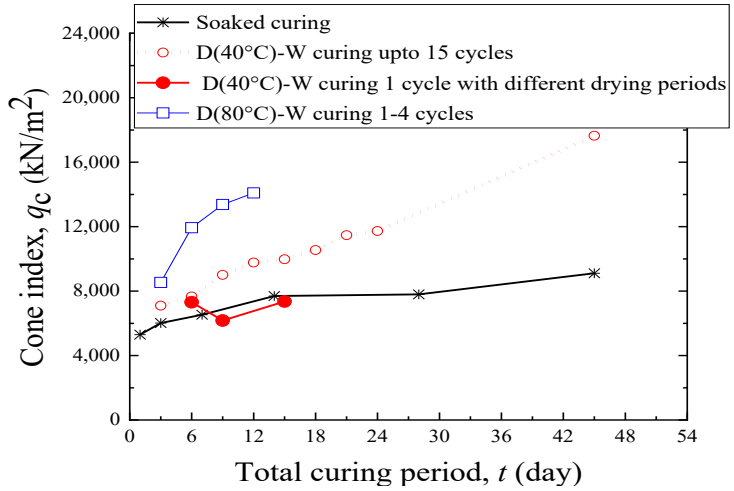

(b) PSAS-R

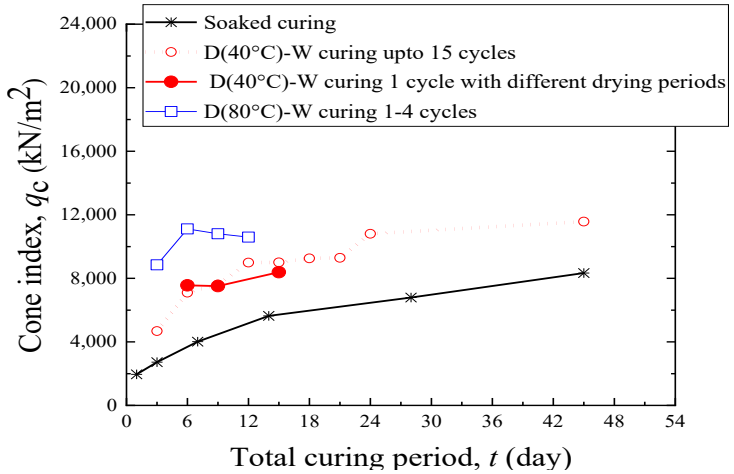

(c) BFCB

Figure 5.10 Relationships between q_c and t (D: dry, W: wet)

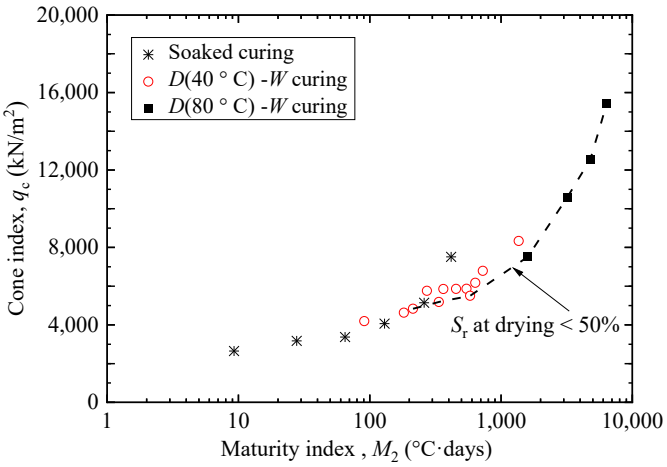

(a) PSAS-N

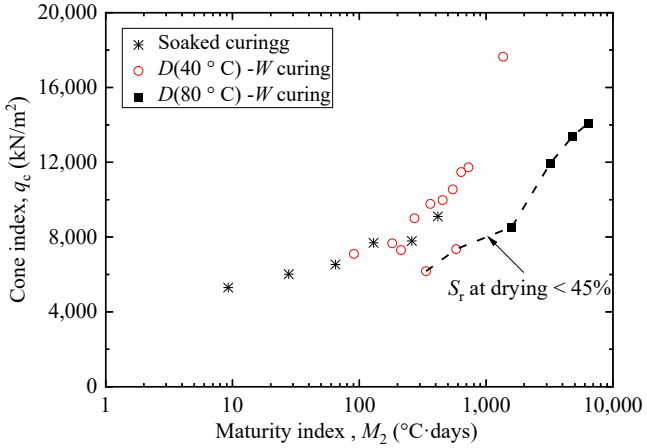

(b) PSAS-R

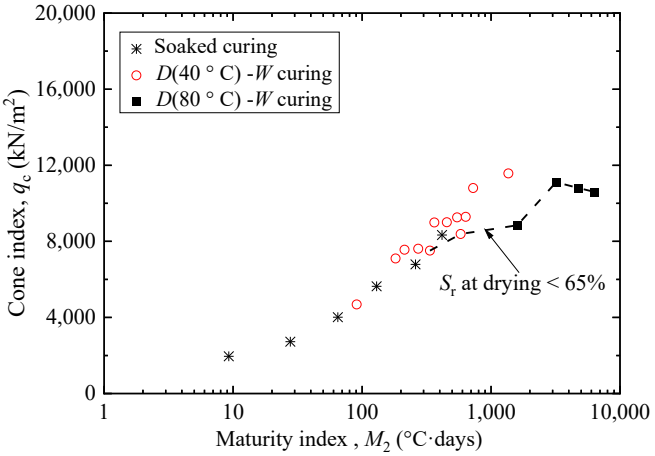

(c) BFCB

Figure 5.11 Relationships between q_c and M_2 (D: dry, W: wet)

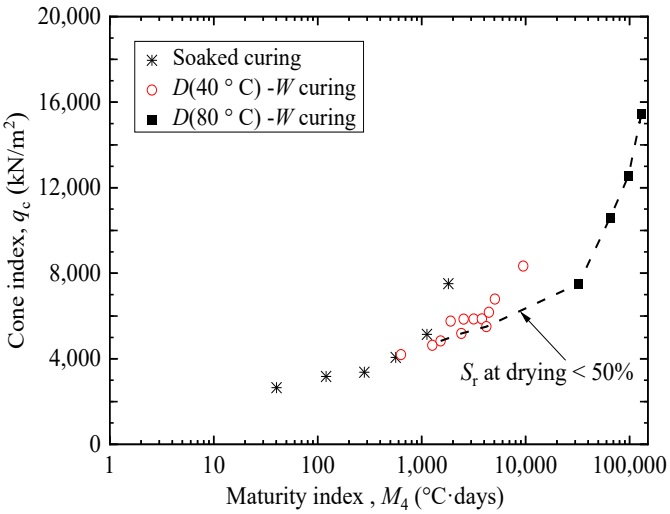

(a) PSAS-N

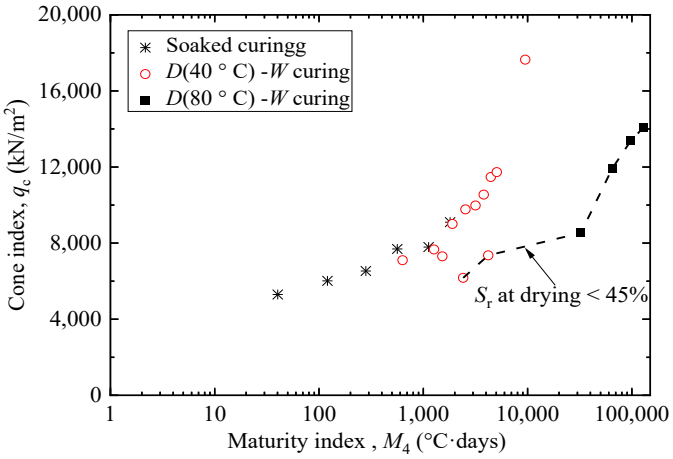

(b) PSAS-R

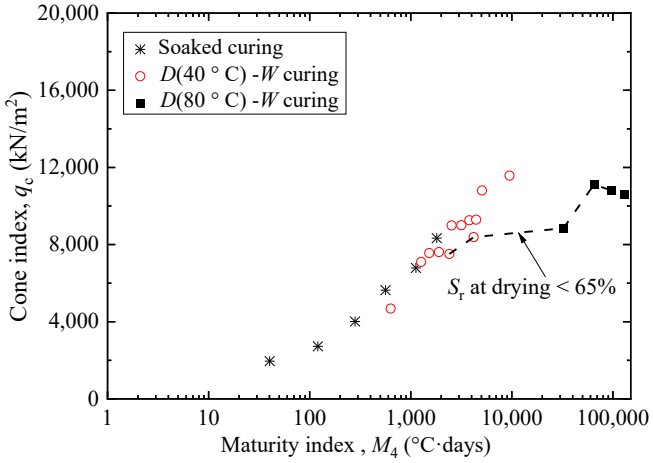

(c) BFCB

Figure 5.12 Relationships between q_c and M_4 (D: dry, W: wet)

was lower than that of specimens with S_r above these values at the same M_2 or M_4. This might have been caused by an insufficient amount of free water for hydration, as mentioned earlier. These observations suggest that the concept of maturity may be applicable to PSAS-treated soils to some extent, as it is for cement-treated soils. However, the following conditions must be satisfied for the concept of maturity to be applicable:1. The treated soil was subjected to repeated dry and wet cycles under restraint, and 2. The treated soil must not be excessively dry. These findings suggest that it is important to evaluate the durabilities of PSAS-treated soils in laboratory tests by incorporating curing conditions that reflect the site environment. In addition, future studies are expected to investigate the long-term deterioration of PSAS-treate soils due to Ca leaching, etc.

5.4 XRD ANALYSIS

The concept of maturity index is applicable to PSAS-treated soil under specific conditions. The process involves drying and wetting the soil samples, and XRD (X-ray Diffraction) analysis was conducted on PSAS-N, PSAS-R, and BFCB samples. XRD analysis was conducted in PSAS-N, PSAS-R & BFCB when only stabilizers were hydrated and kept 2-days at oven at 40 °C for drying and 1-day for wetting. The formation of hydrates supports the concept of maturity index application in PSAS-treated soil, similar to cement-treated soil.

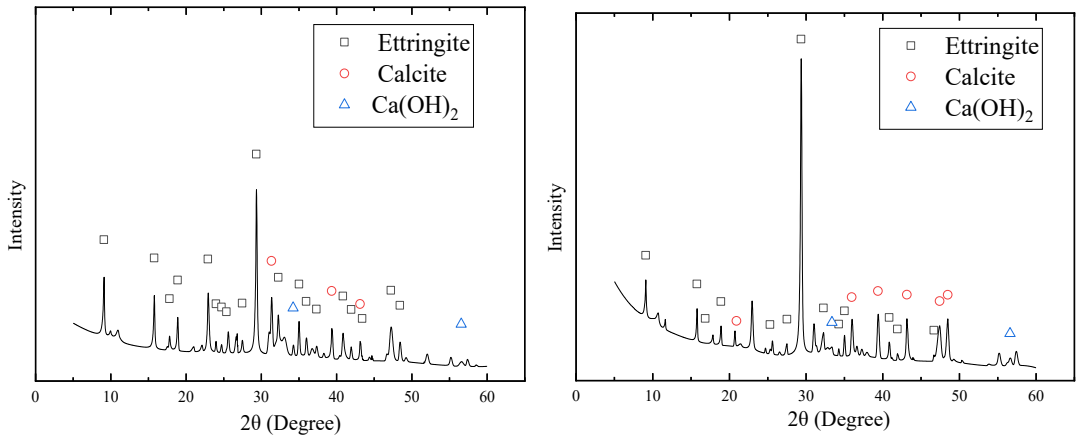

(PSAS-N) (PSAS-R)

Figure 5.13 XRD analysis of stabilizers after drying at 40 °C for 2day & soaked for 1day

5.5 SUMMARY

In this study, various tests were conducted to assess the durability of PSAS-treated clays subjected to wet-dry or dry-wet environments via different types of evaluation tests. The durability obtained was discussed based on the characteristics of the evaluation tests. Sieve analyses were conducted on PSAS- and BFCB-treated samples to investigate the difference in the PSDs owing to the difference in pretreatment conditions. As the washing period of samples prior to sieving increased, finer contents appeared in the obtained PSDs. These observations raised the concern that the PSAS-treated clays, as well as the BFCB-treated clays, may become muddy. However, it is

unlikely that the treated clays after the construction will be exposed to washing with water while being agitated. Unconfined compression tests were conducted on the PSAS- and BFCB-treated samples to investigate the change in strength associated with dry-wet curing. For the BFCB-treated samples, q_u increased with curing time. On the other hand, q_u decreased for the PSAS-treated samples after several dry–wet curing cycles. These observations indicate that the durability of PSAS-treated samples to dry-wet curing cycles is lower than that of BFCB-treated samples. However, the question remains as to whether the evaluation using unconfined compression test specimens was appropriate for the PSAS-treated samples, where water absorption and retention were physically induced by the pores of the PSAS particles. A series of cone index tests were conducted on PSAS- and BFCB-treated samples to investigate the change in the strength associated with dry-wet curing. The samples were subjected to dry-wet curing in molds. The q_c of the BFCB-treated samples subjected to the cycles of two days drying at 40 ℃ and one-day wetting curing increased with the *t*. This was also true for the PSAS-treated samples. This observation differs from that obtained from the unconfined compression test results, suggesting that the confinement of the samples in the evaluation tests is essential for evaluating the durability of PSAS-treated soils subjected to dry-wet curing. The concept of maturity can be applied to PSAS-treated soils with various curing temperatures and curing periods, similar to cement-treated soils. However, the following conditions must be satisfied for the concept of maturity to be applicable:1. The treated soil must be subjected to repeated dry and wet cycles under restraint, and 2. Treated soil must not be excessively dry.

References

Babasaki, R, Terashi, M., Suzuki, T., Maekawa, A., Kawamura, M., Fukazawa, E., 1996. Japanese Geotechnical Society Technical Committee Reports: Factors influencing the strength of improved soil. Proc. of the 2nd International Conference on Ground Improvement Geosystems. Vol. 2. pp. 913-918.

Bannai, H. and Nakagawa, K., 1968, Thermal properties of ettringite, Gypsum & Lime, 97, pp. 11–17 (in Japanese).

Beriha, B., Biswal, D. R., Sahoo, U. C., 2018. Effect of wet-dry cycles on mechanical strength properties of cement stabilized granular lateritic soil. In: Springer, Cham, International Congress and Exhibition" Sustainable Civil Infrastructures: Innovative Infrastructure Geotechnology." pp. 112-121.

Hashimito, K., Otsuki N., Nishida, T., 2008. Long term prediction of strength deterioration considering Cl^- due to Ca leaching from cement-treated soil. Journal of JSCE (C Geotech. 64(2), pp. 226–237 (in Japanese)).

Jamsawang, P., Charoensil, S., Namjan, T., Jongpradist, P., Likitlersuang, S., 2021. Mechanical and microstructural properties of dredged sediments treated with cement and fly ash for use as road materials. Road Materials and Pavement Design, 22(11), pp. 2498-2522.

Japanese Geotechnical Society Standards, JGS 0131–2009: Test method for particle size distribution of soils. JGS, Tokyo, Japan.

Japanese Geotechnical Society. Standards. JGS 0511–2009: Test method for unconfined compression test of soils. JGS, Tokyo, Japan.

Japanese Geotechnical Society Standards JGS 0711-2009 Test method for soil compaction using a rammer. JGS, Tokyo, Japan.

Japanese Geotechnical Society Standards. JGS, 0716, 2009: Test method for cone index of compacted soils. JGS, Tokyo, Japan.

Japanese Geotechnical Society Standards. JGS 0122–2009: Test method for water content of soils by the microwave oven. JGS, Tokyo, Japan.

Kawai, S., Hayano, K., Yamauchi, H., 2018. Fundamental study on curing effect and its factor on the strength deformation characteristics of PS ash-based improved soil. Journal of JSCE (C Geotech. 74, pp. 306–317 (in Japanese)).

Khoury, N. N., & Zaman, M. M., 2002. Effect of wet-dry cycles on resilient modulus of class C coal fly ash-stabilized aggregate base. Transportation research record. 1787(1), pp. 13-21.

Khoury, N. N., & Zaman, M. M., 2007. Durability of stabilized base courses subjected to wet–dry cycles. International Journal of Pavement Engineering. 8(4), pp. 265-276.

Kitazume, M., 2020. Keynote Lecture: Recent development of quality control and assurance of deep mixing method. In book: Geotechnics for Sustainable Infrastructure Development.

Nozawa, R., Saito, T., Sato, K., and Saeki, T., 2017, Effect of drying condition and temperature history on water contents of ettringite structure, Cement Science and Concrete Technology, 70, pp. 1–8 (in Japanese).

Takahashi, H., Morikawa, Y., Fujii, N., Kitazume, M., 2018. Thirty-seven-year investigation of quicklime-treated soil produced by deep mixing method. Proceedings of the Institution of Civil Engineers-Ground Improvement, 171(3), pp. 135-147.

Watanabe, Y., Nguyen Binh, P., Hayano, K., Yamauchi, H., 2021. New mixture design approach to paper sludge ash-based stabilizers for treatment of potential irrigation earth dam materials with high water contents. Soils and Foundations. 61(11), pp. 1370–1385.

Ye, H., Chu, C., Xu, L., Guo, K., Li, D., 2018. Experimental studies on drying-wetting cycle characteristics of expansive soils improved by industrial wastes, Advances in Civil Engineering 2018(3), pp. 1-9.

Yoobanpot, N., Jamsawang, P., Poorahong, H., Jongpradist, P., Likitlersuang, S., 2020a. Multiscale laboratory investigation of the mechanical and microstructural properties of dredged sediments stabilized with cement and fly ash. Engineering geology, 267, pp. 105491.

Yoobanpot, N., Jamsawang, P., Simarat, P., Jongpradist, P., Likitlersuang, S., 2020b. Sustainable reuse of dredged sediments as pavement materials by cement and fly ash stabilization. Journal of Soils and Sediments, 20, pp.3807-3823.

Zhang, Z., Tao, M., 2006. Durability of cement stabilized low plastic soils. In: Transportation Research Board 2006 Annual Meeting, CD-ROM Publication, Transportation Research Board, National Research Council, Washington DC. 06-1255.Z.

CHAPTER 6

PROPOSED LABORATORY MIXTURE DESIGN FLOW

6.1 INTRODUCTION

In Chapter 5, we have extensively examined the consequences of pre-compaction curing and the subsequent crumbling process on construction-generated soil treated with PSAS-based stabilizers. Furthermore, Chapter 5 delves into the effects of post-compaction curing and its impact on the durability of PSAS-treated soil, like cement-treated soil. Drawing upon these valuable findings, this chapter aims to propose a revised laboratory mixture design flow specifically adopted for treating construction-generated soil using PSAS-based stabilizers. The optimized mixture design will be designed to enhance the overall performance and long-term stability of the PSAS-treated soil. Additionally, we will showcase practical applications of this research in real-world field scenarios, demonstrating the tangible benefits and effectiveness of employing PSAS-based stabilizers for sustainable soil improvement in construction projects

6.2 EFFECTS OF PRE & POST COMPACTION CURING WITH CRUMBLING

Sealed curing experiments, as detailed in Chapter 4, were carried out to assess the impact of crumbling on the treated soil. When comparing the strength development with and without pre-compaction curing, if the difference is minimal, it indicates a low generation of hydrates during the sealed curing process. Consequently, during crumbling, there is a reduced likelihood of hydrates being destroyed, leading to negligible effects on the treated soil's strength development in such instances. However, certain scenarios exhibit significant crumbling effects due to the rapid and substantial formation of hydrates. In such cases, conducting crumbling would destroy these hydrates, leading to a sudden reduction in strength.

The influence of pre-compaction curing on PSAS-treated soil is closely intertwined with the effects of crumbling. Air pre-compaction curing drives the water content towards the optimum water content (w_{opt}) during compaction. Consequently, the cone index strength (q_c) of soaked samples is expected to be maximized. When the crumbling effect in PSAS is minimal, the strength development in PSAS-treated soil surpasses that of samples without pre-compaction curing. Conversely, in cases where the crumbling effect in PSAS is pronounced, the strength development in PSAS-treated soil is lower than in samples without pre-compaction curing. The reduction in strength is attributed to the destruction of hydrates during the crumbling process. In scenarios where the crumbling effects are minimal, achieving the optimum water content (w_{opt}) leads to the attainment of the highest strength in PSAS-treated soil. To expedite the process of reaching wopt, the pre-compaction curing period can be divided into two stages: primary and secondary curing. Chapter 4 demonstrates that this division significantly reduces the time required from 1 day to less than 5 hours to reach the desired wopt. Consequently, the two-stage pre-compaction curing method proves to be a more efficient approach for accelerating the achievement of optimal water content and, subsequently, enhancing the strength development in PSAS-treated soil.

Chapter 5 the cone index test results indicated the confinement of the samples in the evaluation tests is essential for evaluating the durability of PSAS-treated soils subjected to dry-wet curing which differs from unconfined compression test results. In geotechnical engineering, the maturity index and durability of cement-treated soil are connected in a manner that relates to the strength development and long-term performance of the stabilized soil. The maturity index in cement-treated soil is used to estimate the progress of cement hydration, which influences the strength gain and durability of the treated soil. The concept of maturity can be applied to PSAS-treated soils like cement-treated soils with conditions; one is treated soil with repeated dry and wet cycles should be under restraints and another is treated soil must not be excessively dry.

To understand the effects of pre-compaction curing, subsequent crumbling and post-compaction curing on PSAS-treated soil, a modified laboratory mixture design flow was proposed for treating the soil with PSAS-based stabilizers which was the ultimate goal of this research.

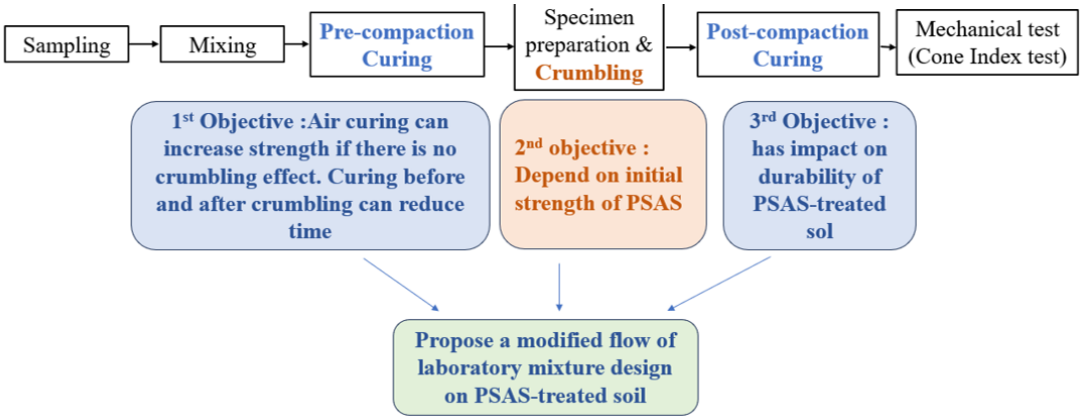

Figure 6.1 Goal of the research

6.3 PROPOSED FLOW

Figure 6.2 shows the proposed laboratory mixture design flow based on the current findings. Based on the concept explained in 6.2, pre-compaction curing was divided into primary & secondary curing. In between them, crumbling was conducted.

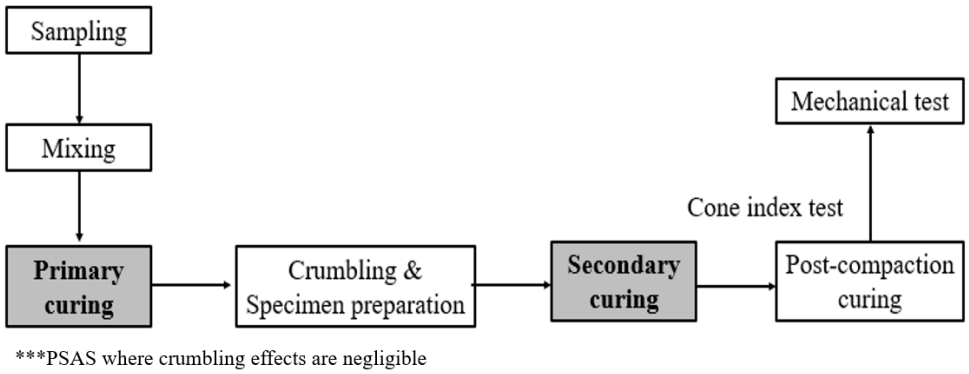

Figure 6.2 Proposed laboratory mixture design flow

The proposed flow can reduce working time in the actual field.

6.4 PRACTICAL IMPLEMENTATION OF THIS RESEARCH

Previously much research has been conducted on construction generated soil with PSAS. The ultimate focus of those research was to reduce the initial water content of construction generated soil. Thats why those research only focuses on the instantaneous water absorption capacity of PSAS (Mochizuki et al., 2003; Shigematsu et al., 2010; Elias, 2015). But this research focuses on the water content reduction due to crumbling and curing treatment instead of instantaneous treatment.

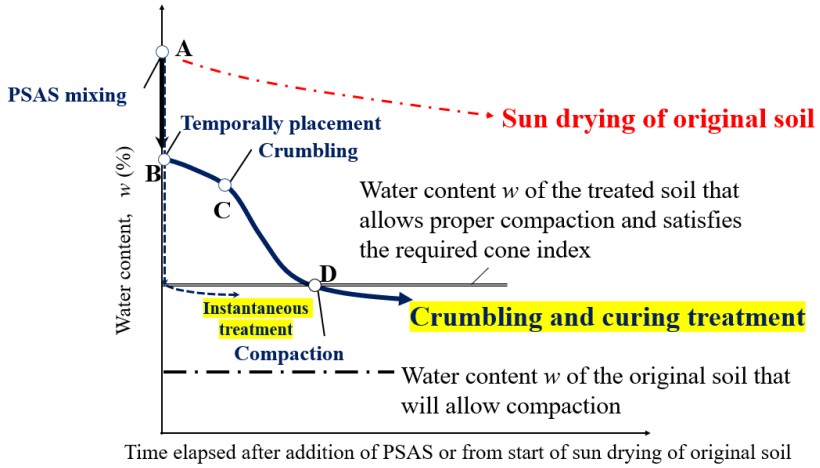

Figure 6.3 Benefits of the proposed flow

Figure 6.3 illustrates the practical advantages of the proposed flow in real-field applications. Sun-drying construction-generated soil is time-consuming and challenging to achieve the specific water content necessary for maximum compaction strength. Therefore, incorporating PSAS with construction-generated soil facilitates the process. Instantaneous treatment to reach the optimum water content would demand a high volume of PSAS to absorb the untreated soil's water content. As an alternative, the proposed flow suggests mixing PSAS-treated soil, placing it nearby the construction site, and subjecting it to air curing for a specific duration. Subsequent crumbling and additional air curing further promote water evaporation, enabling the soil to attain the desired water content for optimal compaction strength. Notably, this approach requires a lower amount of PSAS compared to the instantaneous treatment, making it a more efficient and practical solution for soil improvement.

6.5 SUMMARY

The findings from Chapters 4 and 5 have provided valuable insights into the impacts of pre-compaction curing, crumbling, and post-compaction curing on PSAS-treated soil. Summarizing these results, this chapter presents a modified laboratory mixture design flow for treating construction-generated soil. The proposed flow optimizes the treatment process by considering the effects of crumbling and curing, which collectively contribute to reducing the required amount of

PSAS for soil stabilization. Implementing the proposed flow in real-world applications offers several significant contributions. Firstly, it allows for more efficient and effective treatment of construction-generated soil, as it takes into account the specific water content required for optimal compaction strength. Secondly, by incorporating the effects of crumbling and curing, the proposed flow helps to mitigate the quantity of PSAS needed for soil treatment, thereby reducing material costs and enhancing the overall sustainability of the process. Consequently, this research can lead to practical and resource-efficient solutions for improving soil conditions in construction projects, with potential applications in various field settings where construction-generated soil requires stabilization and enhancement.

References

Mochizuki, Y., Yoshino, H., Saito, E. and Ogata, T., 2003. Effects of soil improvement due to mixing with paper sludge ash. In Proceeding of China-Japan Geotechnical Symposium (pp. 1-8).

Shigematsu, H., Demura, Y., Fujiwara, Y., 2010. Stabilization of poor soil by paper mill sludge mixing. Doboku Gakkai Ronbunshuu C. 66(4), 695–705 (in Japanese).

Elias, N., 2015. Strength development of soft soil stabilized with waste paper sludge. International Journal of Advanced Technology in Engineering and Science, 141–149.

CHAPTER 7

CONCLUSIONS AND FUTURE RECOMMENDATION

7.1 CONCLUSIONS

For making an eco-friendly society, efforts have been made the use sustainable materials produced by industrial processes for treating construction-generated soil. One result of such research efforts was the development of paper sludge ash-based stabilizers (PSASs) for soil stabilization. PSASs utilize paper sludge (PS) ash, which is produced by burning the PS discharged from paper mills. Soil combined with PSASs exhibits improved stability. Other studies have also reported that the strength of soils treated with PSASs increases with curing because a PSAS is expected to create a hydration reaction when combined with water, although the reaction is not as strong as that of cement. Chapter 2 gives us a clear idea about the conventional flow of the laboratory mixture design for treating construction-generated soil with cement-based stabilizers. Previous studies have reported that the strength characteristics of construction-generated soils treated with cement or lime are strongly affected by the primary and secondary curing conditions. These findings suggest that the strengths of PSAS-treated soils are affected by these conditions. However, this problem has not been investigated in detail. Like construction-generated soils treated with cement or lime, the strength of PSAS-treated soils is expected to be affected by pre- and post-compaction curing conditions as well. However, this issue has not been investigated in detail. Moreover, the effects of the crumbling on the strength development of PSAS-treated soil like cement-treated soil has not also been investigated. Further, the effects of repeated dry and wet (D-W) cycle during post-compaction curing on the strength development of PSAS-treated soil, has not been investigated in detail. In an attempt to overcome those limitations, this study has been conducted to understand the effect of pre-compaction curing, subsequent crumbling and post-compaction curing on the strength development of PSAS-treated soil and based on that a modified flow is proposed for treating construction-generated soil with PSAS.

For understanding the effect of pre-compaction curing, subsequent crumbling and post-compaction curing on the progress of strength of PSAS-treated soil, two types of clay based on their liquid limit, two types of PSAS: PSAS-N and PSAS-R have been taken. The properties of PSAS vary depending on their sources, chemical compositions, water absorption capacity and particle size distributions. Chapter 4, investigated the effects of the pre-compaction curing conditions and subsequent crumbling on the physical, compaction, and strength characteristics of PSAS-treated soils using two types of PSASs with different water absorption and retention performances. For comparison, the same investigation was conducted on soils treated with blast furnace cement type B (BFCB). Moreover, the mechanisms by which the pre-compaction curing conditions and subsequent crumbling affected the strength of PSAS-treated soils were discussed based on the test results.

Chapter 5 aimed to assess the durability of PSAS-treated clays subjected to wet-dry, or dry-wet environments via different evaluation tests. First, particle size analyses were conducted on clays treated with different pretreatments. Treated clays underwent unconfined compression tests subjected to repeated dry-wet cycles with demolded specimens. Cone index tests were also

conducted on the treated clays subjected to repeated dry and wet cycles, while the specimens were restrained in molds. Discussions on the durability assessment of PSAS-treated clays are presented, considering the characteristics of each evaluation test while comparing the test results with those of cement-treated clays.

The research accomplishments have validated the originality of the study and demonstrated that like cement-treated soil, the conventional flow diagram has an effect also on PSAS-treated soil.

a. The effects of the pre-compaction curing conditions and subsequent crumbling on the physical, compaction, and strength characteristics of PSAS-treated soils

- The experimental results revealed that after crumbling, the PSAS-treated samples produced sand and gravel-like granules, regardless of the sealed or air pre-compaction curing conditions. In addition, we observed that the lower the water content at crumbling, the smaller the particle size of the wet samples. This was also true for the BFCB-treated samples. We also observed that the PSDs of the oven-dried samples (of any treated sample) did not match the combined PSDs, which were calculated by considering the PSD of each material constituting the treated samples. This suggests that chemical bonding occurred among the particles of the PSAS-treated and BFCB-treated samples.
- The compaction test results indicated that for one type of PSAS, the dry densities of the PSAS-treated samples with sealed pre-compaction curing were almost the same as those without pre-compaction curing. The same trend was observed for the BFCB-treated samples. However, for the other types of PSAS, the dry densities of the PSAS-treated samples with sealed pre-compaction curing were lower than those without pre-compaction curing. This could be attributed to the variation in the degree of disturbance caused by the crumbling depending on the type of PSAS. The rapid formation of hydrates in one type of PSAS might have significantly disturbed the treated samples owing to the crumbling, resulting in a decrease in ρ_d.
- The cone index tests conducted after post-compaction curing in a soaked environment suggested that the cone indexes of the PSAS-treated samples with pre-compaction curing were higher or lower than those of the samples without pre-compaction curing depending on the pre-compaction curing environment, the number of curing days, and initial strength development of PSAS. The difference was considered to be caused by the combined effects of the "strength reduction owing to crumbling," and "strength increase owing to water content reduction at compaction." The mechanism suggests that for PSAS-treated soils with rapid strength development, the strength reduction caused by crumbling should be considered. However, for PSAS-treated soils with slow strength development, it is effective to appropriately adjust the water content of the treated soils during pre-compaction curing before compaction. Moreover, we suggest setting the curing conditions in the laboratory mixture design to reflect the field conditions and to minimize the discrepancies between field and laboratory observations.
- In cases, where crumbling effects were negligible dividing pre-compaction curing into two stages: primary curing and secondary curing could accelerate water evaporation. It helped the treated soil sample to reach a certain water content at which compaction can provide the highest strength.

b. various tests were conducted to assess the durability of PSAS-treated clays subjected to wet-dry or dry-wet environments via different types of evaluation tests

- Sieve analyses were performed on PSAS- and BFCB-treated samples to determine the difference in PSDs resulting from the pretreatment conditions. As the washing time of samples prior to sieving increased, finer particles were obtained in the PSDs. These findings raised the possibility that PSAS-treated clays and BFCB-treated clays may become muddy. However, it is improbable that the treated clays will be washed with water while being agitated after construction.
- The PSAS- and BFCB-treated samples were subjected to unconfined compression experiments to determine the strength change associated with dry-wet curing. For samples treated with BFCB, q_u increased over time. In contrast, q_u decreased in samples treated with PSAS after multiple dry–wet curing cycles. Findings from this study suggest that the resistance of PSAS-treated samples to dry-wet curing cycles is inferior to that of BFCB-treated samples. The question persists, however, as to whether the evaluation using unconfined compression test specimens was suitable for PSAS-treated samples, where water absorption and retention were physically induced by the PSAS particles' pores.
- A series of cone index experiments were performed on PSAS- and BFCB-treated samples in order to determine the strength change resulting from dry-wet curing. In molds, the samples were subjected to dry-wet curing. The quality of samples treated with BFCB and subjected to cycles of two days of drying at 40 °C and one day of wetting curing increased with time. This also held true for samples treated with PSAS. This observation contradicts the results of the unconfined compression tests, indicating that the confinement of the samples in the evaluation tests is essential for determining the durability of PSAS-treated soils subjected to dry-wet curing.
- Similar to cement-treated soils, the concept of maturity index can be applied to PSAS-treated soils with varying curing temperatures and curing times. However, the following conditions must be satisfied for the concept of maturity to be applicable:1. The treated soil must be subjected to repeated dry and wet cycles under restraint, and 2. Treated soil must not be excessively dry.

c. proposed laboratory mixture design flow for treating construction generated soil with PSAS-based stabilizers

- Based on the results obtained a modified laboratory mixture design flow is proposed for treating construction-generated soil with PSAS which is slightly different from cement treated case. It is because PSAS has different water absorption properties compared with cement.
- Modified laboratory mixture design flow will help to reduce the amount of PSAS used for treating construction generated soil in the actual field.

7.2 RECOMMENDATIONS FOR FURTHER STUDY

- In this research strength properties of PSAS-treated soil was checked. Other geotechnical properties like permeability of the compacted PSAS-treated soil needs further investigation.
- Future studies are expected to investigate the long-term deterioration of PSAS-treated soils due to Ca leaching, etc.
- In addition to PSASs, the use of sustainable materials, such as bio ash from various industries, has increased for the treatment of construction-generated soil. However, they may have properties distinct from cement. Like, PSAS-treated soil, the conventional flow of laboratory mixture design may influence soil treated with biomass, according to the findings of this study. This aspect of construction-generated soil that has been treated with biomass requires additional research.